Dissertation
Submitted to the
Combined Faculties for the Natural Sciences and for Mathematics
of the Ruperto-Carola University of Heidelberg, Germany
for the degree of
Doctor of Natural Sciences

Presented by

Pharmacist **Fozia Noor**, MPhil, DEA
Born in Karachi, Pakistan

Date of oral exam: 26th January 2006

Solid Phase Synthesis and Biological Studies on Metal Conjugates of Bioactive Peptides for Targeted Delivery

Referees : Prof. Dr. Nils Metzler-Nolte
Prof. Dr. Ralf Kinscherf

To
my Parents
Noor M. Khan and Nargis Bano

Acknowledgments

Foremost, I am indebted to Prof. Dr. Nils Metzler-Nolte, my supervisor, for his support and guidance during this research work. I thank him not only for providing me with the lab facilities but also for his confidence and trust in me and for the multitude of little advices he has given me during the course of this work.

I would like to thank Prof. Dr. A. Jäschke, the director of the Institute for Pharmacy and Molecular Biotechnology, for his support and understanding especially during the practical courses with the Pharmacy students. I cordially thank Prof. Dr. A. Jäschke, Prof. Dr. Fricker and Prof. Dr. R. Kinscherf for their participation as members of the examination committee. I am obliged to Dr. Ralf Kinscherf for additionally accepting to be the thesis examiner.

Acknowledgments are due to my collaborators also, without whom the present work would not have been accomplished with success. I am grateful to Prof. Dr. Wölfl, Department of Biology, IPMB, in whose labs the yeast assay for cytotoxicity was carried out. My gratitude to yet another collaborator Prof. Dr. Bläuenstein of the Centre for Radiopharmaceutical Science, Paul Scherrer Institute, Villingen, Switzerland for providing the facilities for the receptor binding studies. My sincere thanks to Dr. E. Garcia-Garayoa for actually carrying out these assays and for her advices.

I would like to express my gratitude to Prof. Dr. Ralf Kinscherf, Institute for Anatomy and Cell biology III, Heidelberg, for providing me with the lab facilities to carry out most of the biological studies presented in this thesis. I thank him for his remarkable willingness to help whenever needed, his countless advices and for his valuable time.

I express my thanks to Mrs. Ulrike Traut and all other members of the Prof. Metz's lab at the Institute for Anatomy and Cell biology III, for their support. My special thanks to Dr. Gabriel Bonaterra for his valuable advices on numerous occasions and for teaching me Spanish!

I am grateful to Mrs. Karin Weiß and Mrs. Viola Funk for their support. Thank you Karin, for your concerns and for the numerous publications that helped me in my work. Thank you Viola, for your friendly kindness and your advices. I would like to thank the technical staff, Mr. Rudy Heiko of IPMB and the former technicians Mr. P. Weyrich and Mr. D. Holzman for their help regarding the maintenance and repair of various instruments. I thankfully acknowledge Mrs. Flock, Mrs. Seith, and Dr. Gross of the Mass spectrometry lab for the mass spectra and Mrs. Fisher and Mrs. Termine for the NMR spectroscopy.

I appreciate the assistance of my two students Mr. Jakub Novotny and Ms. Monika Seidel who successfully completed diploma work and Wahlpflichtpraktikum, respectively, last year.

My sincere thanks are due to a friend and colleague, Mrs. Dina Pavlovic-Rossman for her friendly support and sympathy. I would like to specially thank Dr. Annette Wüstholz for her friendship and help. I thank my colleagues, Dr. Andrea Maurer, Ms. Merja Neukamm, Dr. S. Kirin, Dr. T. Kresbohm, Dr. U. Schatzschneider, Mr. Xavier de Hatten and my former colleagues for their support. Special thanks to the visiting scientist Dr. Stephanie Cronje from South Africa and former visiting scientist Prof. Dr. H. B. Kraatz from Canada.

My friends of near and far…Shamoona, Farah, Nathalie, Ghislaine, Helene, Christine, Steffi, Stephane, Hendrick…thank you all for your support.

My profound gratitude to Mr. and Mrs. Sauer for their love and help. They have been like a family to me supporting me when I missed my family on so many occasions. Affectionate thanks to Mr. and Mrs. Hertle for their loving kindness.

My best friend, Dr. Nousheen Mushtaq who supported me over so many years with her friendship and goodwill. I thank you for your love and your confidence in me.

Special thanks to Prof. Dr. Z. S. Saify, former Dean of the Department of Pharmaceutical Chemistry and Vice chancellor of Karachi University, for his support and kindness. Thank you for giving me this virus of research!

Finally, it is the support of my loved ones that has enabled me to accomplish this work. I am grateful to Jean-Christophe Gallet, who stood by me over all these years, for his jovial brightness that gave me motivation, good humour that lightened the dark days and affection that gave me courage. My brothers, Mustafa and Mujtaba who supported me so earnestly and Khalid, though youngest but with a big heart and optimism. My sisters, Aliya and Uzma…little ones of the family as you'll always be, for your big understanding. I cannot ask for a better family. Thank you all for your help. Thank you all for your love. My parents…without whom I would not be what I am today. My father…many years ago you encouraged me to take the first step into the unknown, to aspire such a bold endeavour. My mother…It's your love that encouraged me and your optimism that gave me hope. I am blessed to have the love and prayers of you both. It is only your support that gave me the courage and perseverance to achieve this milestone in my life…

Fozia Noor, 21st December 2005, Heidelberg.

The submitted research work was accomplished between January 2002 and August 2005 at the University of Heidelberg. The chemical synthesis work was carried out at the Chemistry department, Institute of Pharmacy and Molecular Biotechnology. The major part of biological studies was carried out at the Institute of Anatomy and Cell biology III in collaboration with Dr. R. Kinscherf. The yeast cytotoxicity test was performed by Stephan Walczak in collaboration with Prof. Dr. Wölfl of the Biology department of the Institute of Pharmacy and Molecular Biotechnology, University of Heidelberg. The receptor binding studies were carried out by Dr. E. Garcia-Garayoa in collaboration with Prof. Dr. P. Bläuenstein of the Centre for Radiopharmaceutical Science, Paul Scherrer Institute, Villingen, Switzerland.

Part of this work has been published as follows:

A cobaltocenium-peptide bioconjugate shows enhanced cellular uptake and directed nuclear delivery

Fozia Noor, Annette Wüstholz, Ralf Kinscherf, N. Metzler-Nolte, *Angew. Chem. Int. Ed*. **2005** 44(16), 2429-2432.

Contents

Summary

Peptide-based drug delivery systems and therapeutics have gained an enormous attention during the last ten years. Progress in this field will lead to site specific delivery, improved receptor affinities, efficient cellular uptake and/or nuclear targeting. Thus, in this research project, metal conjugates of some bioactive peptides were synthesized and biologically tested in order to evaluate the effects of these metal moieties on the biological activities such as the cellular uptake, nuclear targeting and binding affinity, of these selected peptides.

In this study, the two redox active metallocenes, ferrocene and cobaltocenium and in addition the cytotoxic platinum were chosen as metal labels. The investigated peptides were the Simian Virus 40 nuclear localisation signal (NLS), the HIV transactivator of transcription (TAT) peptide and the small regulatory peptide, the neurotensin (NT). Metal conjugates of these bioactive peptides were successfully synthesized by solid phase peptide synthesis (SPPS) which was used not only for the covalent bonding of the metallocenes to the peptides but also for the complexation of platinum to the peptides and fluorescence labelling with FITC. Comprehensive characterisation of the synthesized bioconjugates was carried out by various techniques such as NMR, RP-HPLC, MS and electrochemistry.

The cellular uptake and nuclear localisation of the metallocene-NLS and -TAT bioconjugates was monitored by fluorescence microscopy in living liver cancer cells (Hep G2). The metallocene-NLS conjugates were efficiently internalized by the cells and were localised in the nuclei of the Hep G2 cells. The metallocene moiety is responsible for the enhanced cellular uptake of these bioconjugates and the NLS transports the organometallic species into the nuclei. This is the first example of the directed nuclear delivery of ferrocene and the cobaltocenium cation, by conjugation to the NLS peptide. The use of the scrambled NLS sequence (NLS_{scr}) abolishes the nuclear targeting property of the conjugates. All metallocene-NLS bioconjugates were found to be non-toxic in concentrations up to 1mM in the WST-1 proliferation assay.

In case of the metallocene-TAT bioconjugates, the ferrocene moiety plays a role in the escape of the conjugate from the endosomes, which is an advantage because the utility of TAT peptide as a vector for cellular delivery is limited by its inability to escape from the endosomes. Moreover, these peptides are toxic in higher concentration due to cell membrane perturbation. This was also demonstrated in the present study using the WST-1 proliferation assay.

In the last part of the project, metal conjugates of wild type NT(8-13) and the modified Pseudoneurotensin (pNT) were synthesized and tested for their binding affinity to the NTR1 receptors in the HT 29 adenocarcinoma cell line. Replacement of Arg^8-Arg^9 with Lysines in pNT led to a significant decrease in the binding affinity. The metal-NT bioconjugates showed good receptor affinity especially the cobaltocenium-NT conjugate (IC_{50}=2.3nM). In this case, the lipophilicity of the metallocene bioconjugate may facilitate the crossing of the blood brain barrier which is a limiting factor in any centrally intended therapy. The Pt-NT bioconjugate also showed good affinity (IC_{50}=6.8nM) for the receptors. Thus, such bioconjugates may be specifically and selectively delivered to the tumour tissues that overexpress the neurotensin receptors.

In conclusion, the optimised synthesis procedures for the studied metals and the peptides were established. The biological studies demonstrate a great potential of these metals for the improvement of the biological functions of the tested peptides especially for use as vectors for cellular uptake and targeted nuclear delivery. This represents a novel application of bioorganometallic chemistry in biological systems.

Zusammenfassung

Peptid-basierten Wirkstoff-Transportsystemen und Therapeutika wurde in den letzten zehn Jahren große Aufmerksamkeit gewidmet. Fortschritte auf diesem Gebiet versprechen gezielten Transport, erhöhte Rezeptor-Affinitäten, effiziente zelluläre Aufnahme und/oder Aufnahme in den Zellkern. Dementsprechend wurden in dieser Arbeit Metallkonjugate einiger biologisch aktiver Peptide synthetisiert und auf ihre biologische Wirksamkeit getestet. Ziel war es, die Effekte der Metall-Struktureinheiten auf die biologische Aktivität wie Aufnahme in die Zelle bzw. den Zellkern sowie die Bindungsaffinität der Peptide zu untersuchen.

In dieser Arbeit wurden die redox-aktiven Metallocene Ferrocen und Cobaltocen sowie das cytotoxische Platin als Metall-Komponenten ausgewählt. Untersuchte Peptide waren das Kernlokalisierungssignal (NLS) des viralen Antigens SV 40 T, das HIV-TAT-Peptid (transactivator of transcpition) und das kleine regulatorische Peptid Neurotensin (NT). Metallkonjugate dieser biologisch aktiven Peptide wurden mit Hilfe der Festphasen-Peptidsynthese (SPPS) erhalten. Diese Methode wurde nicht nur Knüpfung der kovalenten Bindung zwischen Peptid und Metallocen verwendet, sondern auch zur Komplexierung des Platins durch die Peptide und zur Fluoreszenz-Markierung mittels FITC. Die synthetisierten Biokonjugate wurden mit unterschiedlichen Techniken wie NMR, RP-HPLC, MS und elektrochemischen Verfahren umfassend charakterisiert.

Die Aufnahme der Metallocen-NLS- und –TAT-Biokonjugate in die Zelle und den Zellkern wurde durch Fluoreszenzmikroskopie in lebenden Leberkrebszellen (Hep G2) verfolgt. Die Metallocen-NLS-Konjugate wurden effizient in die Zellen aufgenommen und waren in den Zellkernen der Hep G2-Zellen lokalisiert. Die Metallocen-Struktureinheit ist verantwortlich für die erhöhte Aufnahme dieser Biokonjugate in die Zelle wohingegen die NLS-Einheit den Transport der organometallischen Spezies in den Zellkern ermöglicht. Dies ist das erste Beispiel eines gezielten Transportes von Ferrocen und des Cobaltocenium-Kations in den Zellkern durch Konjugation mit dem NLS-Peptid. Die Verwendung einer intern vertauschten NLS-Sequenz (NLS_{scr}) unterbindet die zielgerichtete Aufnahme in den Zellkern. Alle NLS-Biokonjugate waren im WST-1 Proliferations-Assay nicht toxisch.

Im Fall der Metall-TAT-Biokonjugate spielt die Ferrocen-Einheit eine Rolle beim Verlassen der Endosome durch Konjugate, was insofern vorteilhaft ist, als daß die Wirksamkeit von TAT als Vektor für den zellulären Transport durch seine Unfähigkeit, die Endosomen zu verlassen, eingeschränkt ist. Darüberhinaus sind diese Peptide in höherer Konzentration toxisch aufgrund einer Störung der Struktur der Zellmembran. Auch dies wurde in der vorliegenden Arbeit mit Hilfe des WST-1 Proliferations-Assay nachgewiesen.

Im letzten Teil des Projektes wurden Metall-Konjugate vom Wildtyp NT(8-13) sowie vom modifizierten Pseudoneurotensin (pNT) synthetisiert und bezüglich ihrer Bindungsaffinität zu NTR1-Rezeptoren in der HT 29 Ardenokarzinomzelllinie getestet. Substitution in pNT von Arg^8-Arg^9 durch Lysine führte zu einer signifikanten Erniedrigung der Bindungsaffinität. Die Metall-NT-Biokonjugate zeigten eine hohe Rezeptoraffinität, insbesondere das Cobaltocenium-NT-Konjugat (IC_{50}=2.3nM). In diesem Fall könnte die Lipophilie der Metallocen-Biokonjugate eine Überwindung der Blut-Hirn-Schranke ermöglichen, die einen limitierenden Faktor in jeder auf das ZNS zielenden Therapie darstellt. Das Pt-NT-Biokonjugat zeigte ebenso eine hohe Affinität (IC_{50}=6.8nM) für die Rezeptoren. Dementsprechend könnten solche Biokonjugate insbesondere und selektiv in Tumorgewebe transportiert werden, in denen Neurotensin-Rezeptoren überexprimiert sind.

In dieser Arbeit wurden die optimierte Synthesemethoden für die Konjugate der untersuchten Metalle und Peptide etabliert. Die biologischen Untersuchungen zeigen das große Potential dieser Metalle für die Verbesserung der biologischen Wirkungen der untersuchten Peptide insbesondere für die Verwendung als Vektoren für die zelluläre und die gerichtete Aufnahme in den Zellkern. Dies stellt eine neue Anwendung der Bioorganometallchemie in biologischen Systemen dar.

List of abbreviations

BB	Backbone (aminoethylglycine)
Boc	*t*-Butoxycarbonyl
Cc	Cobaltocene
CcC(O)	Cobaltocenium carboxylic acid
CH_2Cl_2	Dichloromethane
CPP	Cell penetrating peptides
Cv	Cystal violet
CV	Cyclic Voltammetry/Cyclic voltammogram
d	Doublet (NMR)
dd	Doublet of doublet (NMR)
DAP	Diaminopropionic acid
DIPEA	Diisopropylethylamine
DMF	Dimethylformamide
DMSO	Dimethylsulfoxide
DNA	Deoxyribonucleic acid
E	Potential
ESI	Electron ionization spray
Fc	Ferrocene
FcC(O)	Ferrocene carboxylic acid
Fer	Ferrocenylalanine
FITC	Fluorescein isothiocyanate
Fmoc	9-Fluorenylmethoxycarbonyl
Hep G2	Human hepatic cancer cell line
HOBt	1-Hydroxybenzotriazole
Hz	Hertz
IR	Infra red
J	Coupling constant (NMR)
m	Multiplet (NMR)
M	Molar
mca	Methoxycoumarin
MeCN	Acetonitrile
MeOH	Methanol
mM	Millimolar
Mtt	4-Methyltrityl
m/z	Mass per charge ratio
NLS	Nuclear localisation signal (PKKKRKV)
NLS_{src}	Scrambled nuclear localisation signal (KKVKPKR)
NMR	Nuclar magnetic resonance
NT	Neurotensin (RRPWIL)
pNT	Pseudoneurotensin (KKPWIL)
PBS	Phosphate buffered saline
ppm	Parts per million
Pt	Platinum
RT	Room temperature
R_t	Retention time (HPLC)
Pbf	2,2,4,6,7-Pentamethyldihydrobenzofurane-5-sulfonyl
RP-HPLC	Reverse phase high performance liquid chromatography
s	Singlet (NMR)
SPPS	Solid phase peptide synthesis
SWV	Square wave voltammetry/square wave voltammogram
t	Triplet (NMR)
TAT	Transactivator of Transcription (GRKKRRQRRR)
TBTU	2-(1H-benzotriazole-1-yl)-1,3,3-tetramethyluronium tetrafluoroborate
TFA	Trifluoroacetic acid
TIS	Triisopropylsilane
vs.	Versus
WST-1	(4-[3-(4-iodopheny)-2-(4-nitrophenyl)-2*H*-5-tetrazolio]-1,3-benzene disulfonate)
δ	Chemical shift (NMR)

Introduction

Drug discovery nowadays is a multidisciplinary effort linking various fields of science together. Fields like Inorganic and organometallic chemistry that were once thought to be incompatible with biology have found evergrowing relevance in biological systems. This has resulted in certain hybrid fields of science such as the Bioorganometallic chemistry.

Last 50 years have seen Bioorganometallic chemistry emerging as an established field of science[1-5] and in very simple terms it deals with biologically significant organometallic species with at least one direct metal-carbon (M-C) bond. Bioorganometallic chemistry has integrated the classical organometallic chemistry to biology, biochemistry, medicine and biotechnology to a remarkable extent.[1, 2, 7-10] Recent advances in fields such as human genetics especially the discovery of genetic basis of various pathological conditions,[11-14] the 3-D structural analysis by X-ray crystallography[15] and other sophisticated spectroscopic techniques have, no doubt, brought the implication of metals in biological systems to the forefront of drug discovery for diagnostic as well as therapeutic purposes. This has in turn fuelled the enthusiasm of the bioorganometallic scientists to apply their expertise to the field of biology. In this regard, the development and improvement of synthetic methods, the efficiency of synthesis achieved by combinatorial synthesis and the possibility to synthesize biological material artificially have played very important roles. Inorganic and organometallic moieties can now be easily incorporated in a variety of biomolecules thereby allowing diverse structural and functional studies under physiological conditions.[10, 16-23] Bioorganometallic derivatives of amino acids and peptides have been comprehensively reviewed.[16, 24] One elegant way to incorporate an organometallic moiety in biomolecules such as amino acids and peptides is through covalent bonding.[24-32] This usually involves the most reactive nucleophilic functions of peptides or proteins such as the free *N*-termini of peptides, the primary amino groups of lysine residues and the thiol groups of cysteine residues.[33] The lysine residues are particularly interesting since they are generally abundant and due to their hydrophilic character are usually located on the surface of proteins.[34]

Many organometallic compounds exhibit high stability in aerobic aqueous media and therefore, can be applied as novel applications in biology and medicine. The unique properties of the organometallic moiety bound to biomolecules can be exploited in a number

of ways such as the sensitive detection of the biomolecule,[35] biomolecular sensing and switching devices,[36, 37] other detection techniques such as atomic absorption spectroscopy[38, 39] and electrochemistry,[40, 41] various diagnostic tools,[19, 20, 42-44] nuclear medicine and radiopharmaceuticals.[45]

To review all the organometallic moieties and their applications in biological systems is beyond the scope of this thesis. The discovery and elucidation of the structure of ferrocene,[46] a metallocene, is considered as the starting point for modern organometallic chemistry.[47] Therefore later descriptions are limited to the metallocenes specially ferrocene and cobaltocenium derivatives and in addition, to platinum analogues which are also a subject of research presented in this thesis.

Metallocenes

In simple terms, metallocenes are a class of compounds in which a transition metal ion in the +2 valence state is sandwiched between two cyclopentadienyl rings (scheme 1.1). They are electrically neutral compounds soluble in organic solvents and insoluble in water. It is important to mention here the metallocene dihalides that contain the transition metal ion in the +4 valence state with two cyclopentadienyl ligands and two halide or pseudohalide ligands. The metallocene dihalides slowly undergo hydrolysis in water with the release of one or both halide ions.

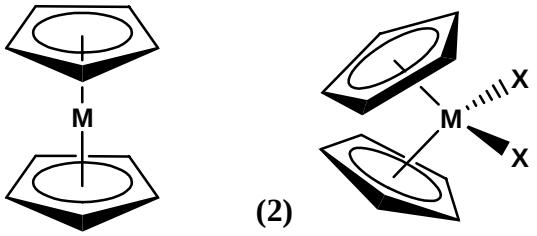

(1) **(2)**

Scheme 1.1: Structure of Metallocene (**1**) and Metallocene dihalide (**2**), where M indicates the metal.

Metallocenes are small, rigid and hydrophobic molecules that, in principle, can easily cross cellular membranes. Even when derivatized with polar substituents, the metallocenes can still cross the cell membrane.[48] The cyclopentadienyl rings, though resembling simple aromatic rings, are rather thick being as thick as they are wide.[48] In this way they may mimic the binding of aromatic compounds but can block the active site due to their bulk. However the most remarkable characterising feature of the metallocenes is the fact that the

metal atom is so tightly bound to the cyclopentadienyl rings that it cannot be dislodged without destroying the whole structure of the metallocene. Metallocenes of transition metals have been extensively studied especially in the field of catalysis.[49, 50] One special area of interest is the study of the electronic properties of the metallocenes and their derivatives.[51, 52] The metallocenes have also found interesting applications in physical and material chemistry.

However, as remarked earlier, the biggest challenge and special interest of the bioorganometallic chemist is to exploit the potential of these unique compounds in the domain of biology. This field is still in its infancy where not all the molecular mechanisms are well understood. This has resulted in a diversity of biological applications in order to assess the true potential in each field of study. A great deal of research is still required to properly understand the various activities and their mechanisms at molecular and cellular level.

Applications of Metallocenes in Biological Systems

This will be a brief account of the most documented and exploited applications of the metallocenes and their derivatives in biology. We can broadly divide these applications into following major themes:

1. Radiopharmaceuticals and Nuclear Medicine

A recent review by Schubiger and Schibli[45] has very well outlined the current use and the future potential of organometallic radiopharmaceuticals. Radioactive metallocenes have found diagnostic and therapeutic applications in nuclear medicine.

The synthesis and use of Ruthenocene derivatives containing ^{97}Ru or ^{103}Ru that even impart organ specificity has been described as early as the late 1970s.[53-55] Examples of half sandwiched complexes with a radioactive metal centre coordinated with carbonyl ligands are already available in the literature. The cyclopentadienyl metal core is highly lipophilic and has a great potential for functionalisation to incorporate certain therapeutics that require passage through the blood brain barrier such as the steroids and analogues of the neuropeptides. Wenzel et al. reported for the first time the synthesis of cyclopentadienyl derivative of ^{99m}Tc.[56] Recently, Alberto et al. reported a unique aqueous based synthesis of this compound[57] and thus enabled the handling of such compounds in aqueous media at a

physiological pH for the functionalisation of biomolecules.

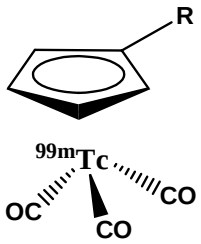

Scheme 1.2: Half sandwich compound with ^{99m}Tc as reported by Wenzel and Alberto.

The labelling of small receptor targeting molecules such as those for neuroreceptors, with ^{99m}Tc has been the focus of research.[58] Some of these compounds have been used for dopamine receptor imaging.[59, 60] Katzenellenbogen et al. have recently reported the potential of η^5-cyclopentadienyltricarbonyl rhenium and technetium derivatives of tropane for Dopamine transporter (DAT) imaging.[61] Other classes of targeted receptors include the serotonergic receptors[62] and the steroid receptors for progestrone and oestrogen.[63-71] In addition, the potential of ^{103}Ru-ruthenocene-glycine derivatives as surrogate for ^{123}I-hippuran has been described.[72]

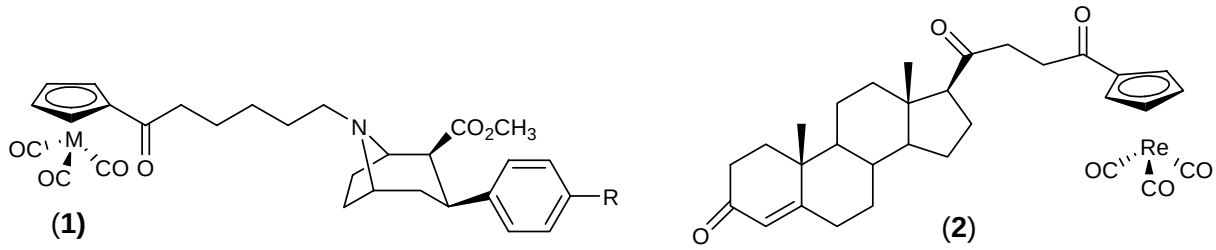

Scheme 1.3: Organometallic derivative of tropane for DAT (**1**) and of progesterone (**2**).

2. Detectors and Biosensors

Metallocenes exhibit characteristic physicochemical properties that can be used as detection and analytical tools by the use of various techniques like spectroscopy such as IR and electrochemistry.

In this regard, ferrocene can be definitely singled out due to its stability and reversible redox activity.

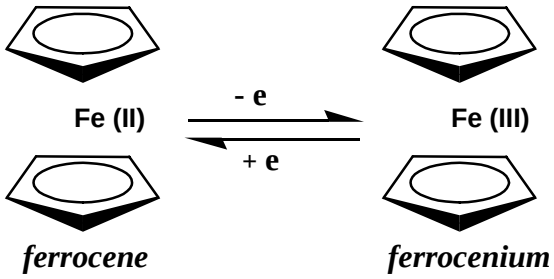

Scheme 1.3: Redox behaviour of ferrocene.

It is used as a chemical sensor for cations and anions.[73-75] Ferrocene mediated electron transfer in glucose oxidase has led to its use in the monitoring of the glucose levels in the blood.[23, 42, 76, 77] Ferrocene has also been employed for selective recognition of nucleotides and DNA for use in DNA sensors[78-82] on the basis of its electrochemical properties. Various applications of ferrocene labelled DNA oligomers as gene sensors have been reviewed in detail.[47]

Using the IR spectroscopy, Jaouen's group has developed the technique of carbonylmetalloimmunoassay (CMIA) for the quantification of antiepileptic drugs.[83, 84] It is a nonradioactive immunoanalytical method in which a metal carbonyl probe is chemically attached to the hapten to form a tracer. This tracer competes with the analyte for specific antibody binding in a liquid phase immunoassay. The remaining free tracer is extracted and quantified with FTIR spectroscopy on the basis of the strong absorption bands of the carbonyl ligands. Recently, an improved version of the CMIA which is solvent free, biocompatible and more sensitive has been reported.[85]

3. Anticancer therapy

The metallocenes are considered as a new class of antitumour organometallic compounds since they are structurally and chemically unrelated to the well known platinum based anticancer drugs. The antitumour metallocenes can be, in a very broad sense, further divided into metallocene dihalides and metallocene derivatives of ferrocene.

Metallocene dihalides (see scheme 1.1 (**2**), where M= Ti, V, Mo, Nb) have exhibited a wide spectrum of activity against a range of tumours in experimental models.[86-89] Titanocene dichloride has been most extensively studied and is the only metallocene dihalide to have entered clinical trials.[90-92] Unfortunately, the efficacy of Cp_2TiCl_2 in

advanced renal cell carcinoma or metastatic breast cancer was too low to be pursued further.[93] Although, interactions with DNA are postulated mechanism of action for these compounds,[94-98] the different chemical stabilities at physiological pH[97, 99] and the different coordination chemistries[95, 98, 100, 101] of these metallocenes indicate significantly different modes of action for each metallocene.[101] Recent studies on these compounds with proteins such as transferrin,[102, 103] human serum albumin,[104] protein kinase C,[88] topoisomerase II[88, 105] and glutathione[106] have confirmed that the interaction with proteins and amino acids play a role in the anticancer activity of the metallocene dihalides. Active research is still going on in this area.

Conflicting reports exist in literature about the cytotoxicity of ferrocene compounds. Köpf-Maier, in 1984,[107] demonstrated for the first time the antitumour activity of some ferrocenium complexes. Although much speculation exists, until now, the mechanism of action remains an ambiguity. In this regard, the chemistry of ferrocene/ferrocenium complexes should not be overlooked.

The early reports on the antineoplastic activity of ferrocene[108-110] describe ferrocene derivatives with organic moieties that themselves are most probably responsible for the effects observed. It is interesting to note that nitrogen mustard ferrocenes had a stimulatory effect on tumour growth.[109]Other studies suggesting specified targets such as DNA cleavage[111] and Topoisomerase inhibition[112] are *ex-vivo* studies. Polymeric ferrocene conjugates with antiproliferative activity have also been reported.[113]

It was shown that the antitumour effects of ferrocene were dependent on the unstability of the ferrocenium cation[114] and that stabilizing substituents lead to a decrease in the antitumour activity. More recently, Osella et al., have demonstrated that only the ferrocenium species (FeIII) are able to inhibit the growth of Ehrlich ascites tumour cells *in-vivo*. This inhibitory activity is independent of the redox potentials of the tested compounds. This report confirmed the early reports that Fe(II) bearing ferrocenes are unable to inhibit cell growth.[115-117] The ferrocenium salts induce DNA damage. However the cytotoxicity of ferrocenium salts is not due to direct linkage to DNA but their ability to generate oxygen active species which induce oxidative DNA damage. The possibility of intercalation is ruled out. Osella showed that ferrocenium salts in physiological solutions generate $OH^{\cdot}$ radicals. A direct relation between generation of $OH^{\cdot}$ radicals and DNA damage could not be

established by these independent tests. The *in-vivo* cytotoxicity could be caused by an immediate attack on the cell membranes carried out by $OH^{\cdot}$ radicals generated in extracellular fluid by ferrocenium salts. The same group has recently reported the generation of hydroxy radicals upon degradation of the ferrocenium derivative ($DEMFc^{+}$) (scheme 1.4) in cells. The iron ions liberated during this decomposition had a synergistic effect on the activity of bleomycin.[118]

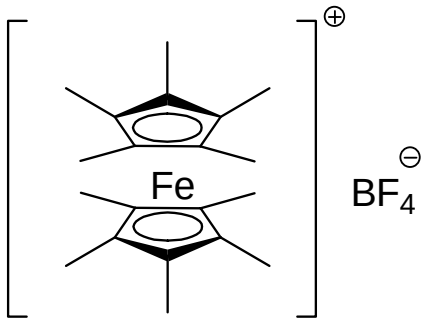

Scheme 1.4: Decamethylferrocenium tetrafluoroborate.

A recent study has indicated a non-apoptotic pathway for the action of ferrocene derivatives.[119] Another study has attributed the antitumour activity of ferrocene to its immune-stimulatory effect that is mediated by redox active signalling.[120] Indeed a very recent observation by Kraatz shows that as the redox potential increased, the toxicity of ferrocene pyrazole conjugates decreased.[121]

All these diverse studies lead to the conclusion that complex mechanisms are involved in the antitumour activity of ferrocene derivatives and which are highly dependent on the chemical properties of the conjugates. The neutral ferrocene has to undergo some kind of activation before an antitumour effect is elicited.

4. Functional and Structural mimetics of proteins

The earliest amino acid derivatives of ferrocene were reported by Schlögel et al.[122] Since then attempts have been made not only to make different derivatives from chemical point of view but also in order to employ the unusual characteristics of the metallocenes to mimic the structural features of peptides.[30, 31] One of the first examples was the substitution of the phenylalanine residue with either ferrocenylalanine or with cymantrenylalanine moieties (scheme 1.5) in peptides such as enkephalin,[123, 124] substance P,[125] bradykinin[125] and

angiotensin.[126, 127] However in most cases this substitution resulted in decreased activities or lower affinity indicating that although ferrocene does resemble the aromatic system but interacts poorly with the receptors.

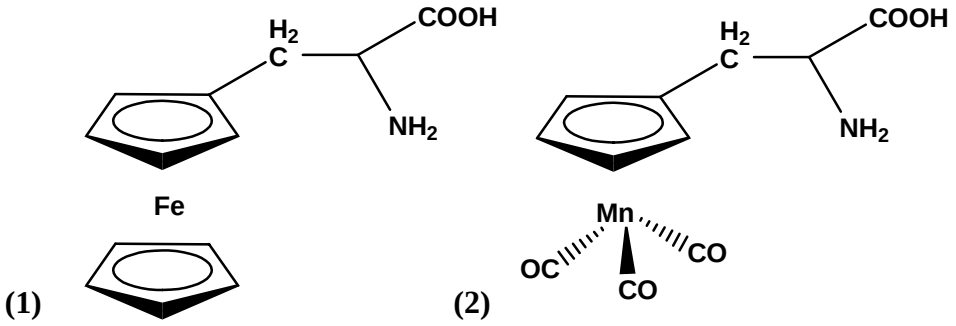

Scheme 1.5: Ferrocenylalanine (Fer) **1** and Cymantrenylalanine (Cym) **2**.

Many enzymatic reactions involve oxidation or reduction of bound substrates and are dependent on electron transfer processes. Modified metalloproteins have been used to get a better understanding of these processes.[128, 129] The electron transfer is dependent upon the structure of the proteins. The β-sheets allow easier electron transfer than the α-helical peptides.[130] The secondary and tertiary structure of the protein as well as the hydrogen bonding[131] influences the rate of electron transfer. Ferrocene can be used as a sensitive electrochemical probe to detect small structural changes.[132] An extensive description on the redox behaviour of ferrocenoylpeptides has been reported by Kraatz.[133]

Protein scaffolds play an important role in the biological function[134] and are usually involved in the recognition of the protein by its receptor and subsequent conformational changes that enable the binding and elicitation of a physiological response. These scaffolds include the α-helices, β-turns and β-sheets which constitute the secondary structural elements of the peptide.[135] Structural features of ferrocene amino acids and peptides has been extensively studied.[31, 136-138] Ferrocenes are recognized as organometallic scaffolds[139] for molecular receptors. Hirao et al. have reported dipeptide podand derivatives of ferrocene that exhibited helical molecular arrangement in the crystal packing of those molecules with intramolecular hydrogen bonds.[137, 140-142] Oligoproline derivatives of ferrocene that have a helical structure have also been reported and their redox behaviour studied.[138]

β-turns are responsible for the proper folding of the protein which in turn is essential for the biological function. β-turns align the β-strands in either parallel manner (usually called the α/β barrel arrangement) for example in Triosephosphate isomerase or in the antiparallel manner such as in staphylococcal nuclease. Pyruvate kinase has both parallel and antiparallel β-sheet arrangement.

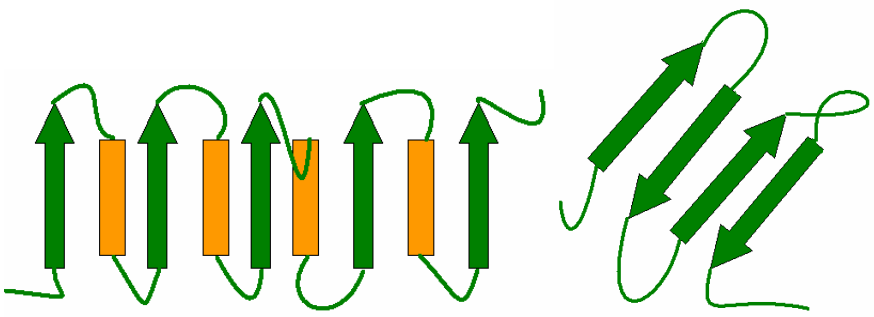

Scheme 1.6: Parallel (A) and antiparallel (B) arrangement of β-sheets. The β-strands are indicated by green arrows and the orange rectangles indicate the α-helices.

Due to their important structural function, the β-turns have been extensively studied. Artificial β-turn mimetics have been reported.[139, 143, 144] In this regard the metallocenes are very good candidates since the two Cp rings could be functionalised and the whole metallocene structure could then serve as a turn mimetic.

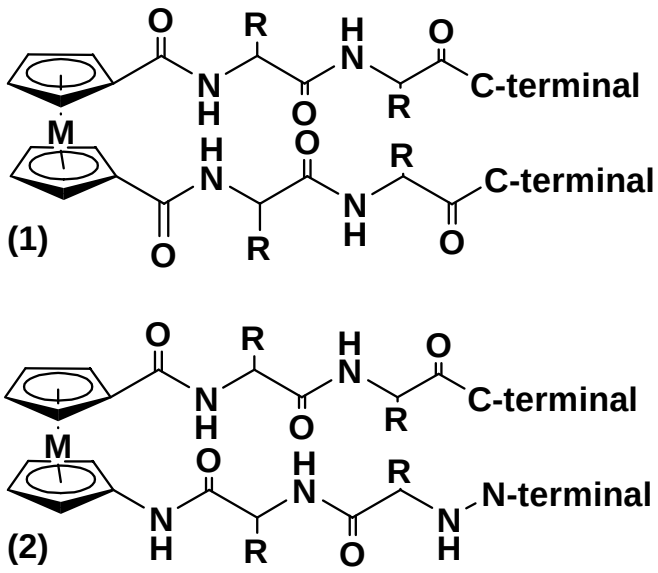

Scheme 1.7: Metallocene β-turn mimetics.

Bioorganometallic chemists have realised this potential of metallocenes and some reports of β-turn mimetics appeared in the literature recently.[145-147] This may allow not only an understanding of the folding of peptides but may ultimately be used as peptidic sensors e.g. based on the redox behaviour of ferrocene.

5. Miscellaneous applications in Biochemistry, Microbiology and Medicine

Metallocenes especially ferrocene have been tested *in-vivo* in man and other species.[148-150] Due to their lipophilicity they have been valuable tools in the study of absorption, distribution and utilization of iron. Compounds have been reported[151, 152] which upon oral administration are metabolized and the Fe^{+2} is stored in the liver.

Metallocene derivatives have been shown to inhibit certain metabolizing enzymes and thus they may allow the study of the enzyme active site as well as the receptor site. β-Ferrocenylalanine is an inhibitor of phenylalanine hydroxylase and phenylalanine decarboxylase.[153, 154] Another derivative, ferrocenylcholine inhibits the hydrolysis of butyrylcholine by horse serum butyrylcholinestrase.[155]

Another unusual application of metallocenes has been their use for histochemical and immunological analyses. A dextran derivative of ferrocene has been employed in the indirect identification of lectin receptors via electron microscopy.[156] Cais and co-workers have developed the non-isotopic metalloimmunoassays for the quantification of antigens and antibodies.[157, 158]

Metallocenes can be used to modify antibiotics in order to address the problem of resistance. A series of ferrocenylpenicillins and ferrocenyl cephalosporins have been reported.[159, 160] In addition a ferrocene derivative bearing both penicillin and cephalosporin rings has also exhibited antibiotic activity. Various other ferrocene derivatives have shown antimicrobial activity against some bacteria, yeasts and fungi. More recently, the antibacterial activity of some ferrocenyl and cobaltocenium peptide bioconjugates has been studied.[161]

Cobaltocenium derivatives

Though much research had been consecrated to ferrocene and its derivatives as well as the radioactive metallocenes and the antitumour metallocene dihalides, not many reports about the cobaltocenium derivatives and their application in biological systems could be found in literature. Cobaltocenium derivatives are isostructural with ferrocene although naturally bearing a positive charge.[162]

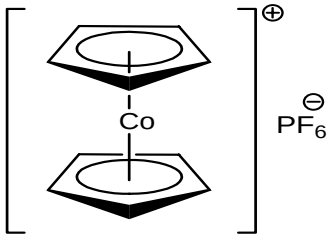

Scheme 1.8: Cobaltocene usually isolated as hexafluorophosphate salt.

Incorporation of metals in dendritic structures has led to new compounds with novel magnetic, electronic, photophysical or catalytic properties.[163-166] Ferrocene is the most widely used redox active moiety incorporated in dendrimeric structures.[165, 167, 168] These dendrimeric structures can be employed as electrode surface modifiers,[169] as electrochemical biosensors,[170] as multisite guests for supramolecular assemblies[171] and as sensors for anions.[172] Cobaltocenium is a good candidate for incorporation or functionalization of dendritic structures by the virtue of its excellent stability and reversible one electron reduction to give the neutral cobaltocene. In fact, the synthesis and the redox properties of cobaltocenium dendrimers have been reported.[169, 173]

Cobaltocenium salts are highly resistant to oxidation even in the presence of strong oxidizing agents like fuming nitric acid, potassium permanganate and ozone.[174] Due to their stability and robustness the cobaltocenium salts could be used as models for the synthesis and application of derivatives of other metallocenes especially those of ferrocene. As noted earlier, ferrocene derivatives act as potent haptens[175] but they undergo enzymatic degradation. Therefore, the use of stable cobaltocenium salts has been proposed. In addition, the cobaltocenium derivatives could also be used in biological systems as electron dense markers in electron microscopy and X-ray crystallography and as carriers of ^{60}Co in radiotherapy. Recently some cobaltocenium derivatives have been reported as anion

sensors.[176] Cobaltocenium has also been used for reference potential calibration in microdisk electrodes.[177]

Platinum derivatives

The antitumour properties of Cisplatin were reported by Rosenberg and co-workers in 1969.[178, 179] Cisplatin is one of the rare curative drugs. Other analogues of platinum that are now in use for the treatment of various solid tumours are carboplatin and oxaliplatin.

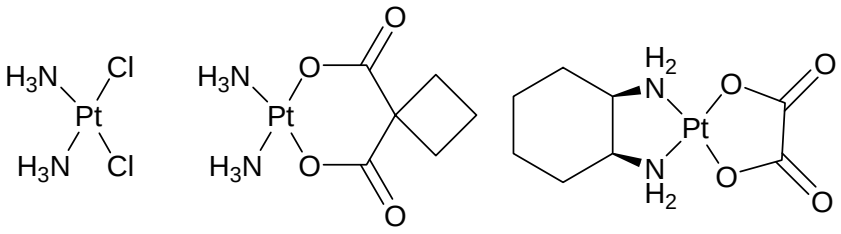

(1) **(2)** **(3)**

Scheme 1.9: Clinically used platinum drugs, Cisplatin (**1**), Carboplatin (**2**) and Oxaliplatin (**3**).

These platinum compounds exert their anticancer activity by covalently modifying cellular DNA.[180, 181] Cisplatin and carboplatin form similar adducts with DNA covalently coordinating with two adjacent guanines on the same strand forming an intrastrand cross link.[182] This in turn bends the DNA resulting in local distortion that triggers a chain of cellular events that ultimately cause the death of the cell.[183] The severe side effects of these drugs include nephrotoxicity, ototoxicity, neurotoxicity and myelosuppression. In addition, poor solubility also limits the effectiveness of cisplatin. As such, some lipophilic Pt (IV) complexes have been reported as prodrugs yielding Pt (II) on reduction *in-vivo* by endogenous biomolecules such as glutathione and ascorbate.[184]

One more major problem encountered in therapy with cisplatin is the resistance of the cancer cells to the drug due to reduced cellular accumulation, increased production of intracellular platinophiles such as glutathione and metalothionein as detoxifiers, enhanced DNA repair and increased tolerance of DNA to platination.[185-187]

One interesting approach has been recently reported in which carboplatin analogues were conjugated through a polyethyleneglycol linker to the nuclear localisation signal in order to facilitate nuclear targeting.[188] Though nuclearly localised, the conjugates were less active

than the free drug forming less Pt-DNA adducts. The study supported the hypothesis that carboplatin, unlike cisplatin, require cytosolic activation prior to its binding to DNA. An excellent review by Lippard explains the cellular processing of the platinum anticancer drugs.[189]

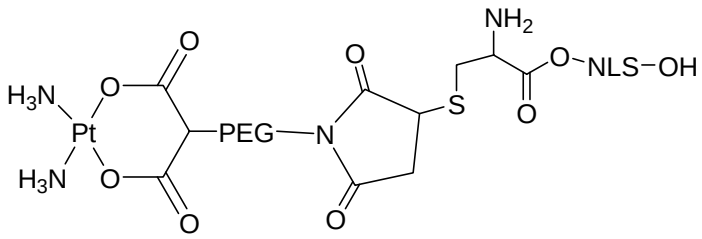

Scheme 1.10: An NLS-PEG analogue of carboplatin.[189]

Recently, peptide conjugates of platinum (II) complexes have been synthesized on the solid support and characterized.[190-193] Some platinum-PNA bioconjugates have also been reported[194] as potential antisense agents.

From the above description the biological potential of organometallic compounds is evident. To incorporate various organometallics in bioactive peptides for either discovery of novel bioactivity or modulation of a biological activity is an extremely tempting objective. However, for targeted drug design, the understanding of the mechanisms by which the organometallics exert their effects is fundamentally important. Many of the underlying mechanisms of activity for most organometallics are far from being fully understood, emphasizing the need for an effort at a molecular and cellular level. Although the site of action of most of the antitumour organometallics especially those of ferrocene derivatives has been suggested to be intranuclear, the passage of these compounds through various biological membranes such as the cell membrane and the nuclear membrane has not been thoroughly investigated. Passage through these biomembranes in intact cells is a prerequisite for any non-receptor mediated biological action. Similarly, bioselectivity is highly desired especially in case of anticancer agents. Lack of selectivity is often a limiting factor in the use of chemotherapeutics.

Following description shall concentrate on the peptides that play a role in cellular uptake and nuclear localisation such as the TAT and NLS peptides. Finally a brief account of small regulatory peptides especially neurotensin shall be presented. All these peptides i.e. nuclear

localisation signal (NLS), transactivator of transcription (TAT) and neurotensin (NT) are the project of research presented in this thesis.

Transport across biological membranes

Biological membranes are natural barriers and they ensure compartmentalisation in living systems. They control the influx and efflux of solutes from cells and from cell organelles. The basic structural unit of these biological membranes is the phospholipid bilayer.

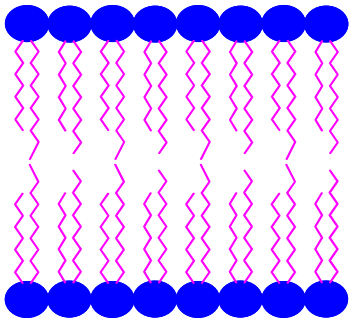

Scheme 1.11: Lipid bilayer cell membrane showing polar heads and non-polar tails.

The delivery of any compound across a given membrane is a challenge. The passage of drugs and gene therapy agents (DNAs or plasmids) through various biological barriers such as the cell or nuclear membrane still poses a problem, especially when a large population of cells is targeted. To effect cellular entry, various transfection agents like PEI (polyethyleneimine) or cell permeablising agents like digitonin or direct injections into the cytoplasm are commonly used. Low molecular weight compounds, including many drugs, may enter cells by passive diffusion. However, P-glycoproteins usually pump them out of the cells before they gain access to the nucleus. Enhanced cellular, but not nuclear, uptake of radio-metals has been achieved by conjugation to peptides for receptor-mediated uptake.[195-198] In gene therapy, the transport of the therapeutic DNA from cytoplasm to the nucleus is an additional complication because it is inefficient in most cases and it is considered as major limiting step in non-dividing cells. Physical methods that facilitate transport into the nuclei include microinjection, liposome fusion or electroporation of conjugates containing an NLS and a drug.[199-202]

Transport across the cell membrane

One of the main constraints in the design of drugs whose interaction targets are located within the host cells is cell membrane permeability. Only compounds with a narrow range of molecular size, net charge and polarity are able to diffuse through the lipid bilayers of the cell membranes and thus reach their pharmacological target.[203]

There are two major pathways by which macromolecules gain cellular entry namely endocytosis (scheme 1.12) and direct translocation through the membrane by a mechanism described as penetration.[204]

Scheme 1.12: The process of endocytosis with self sealing property of the cell membrane.

Endocytosis is an energy dependent mechanism that involves the adsorption of the macromolecule on the surface of the membrane or membrane associated receptors followed by vesicle formation. The vesicular machinery then directs the internalised molecules to appropriate compartments for either destruction or recycling. Delivery of molecules via the endocytosis pathway is often limited by insufficient endosomal escape, restricted diffusion, degradation or lack of nuclear entry. The second mode of entry into the cells is not well understood but appears to occur through an energy independent mechanism. Both endocytic and non-endocytic modes of uptake have been observed.[205]

Short peptides derived from the protein-transduction domains can be internalized in most cell types and are usually known as the cell penetrating peptides (CPP).[204, 206] These CPPs are either basic segments of RNA or DNA-binding proteins[207-209] such as pAntp(43-58) and TAT (48-60) or artificial peptides such as transportan,[210] model amphipathic peptide (MAP)[211] or other sequence based constructs[212, 213] such as oligoarginines. These peptides can act as cytosolic delivery vectors for both low and high molecular weight cargos like FITC,[208] proteins,[214-216] oligonucleotides,[217] peptide nucleic acids,[204] liposomes[218] and even particulates.[219]

Transactivator of Transcription (TAT peptide)

The transactivator of transcription (TAT) is an 86 residue protein derived from the human immunodeficiency virus (HIV). TAT trans-activates certain viral genes and is essential to viral replication. Independent studies using bacterially expressed[220] and chemically synthesized[221] TAT protein, respectively, showed that this protein can enter cells when added to the growth medium of cells in culture. The domain necessary for translocation across the membrane was determined to be the basic domain of the TAT protein.[208] The shortest sequence that is essential for internalisation is shown to be TAT (48-57) which has a sequence GRKKRRQRRR. The positively charged arginine residues are essential to the membrane penetration ability. This has been further confirmed by the fact that TAT-peptide mimetic composed of seven arginine residues[222] is able to gain entry into the cells. It has been concluded that the cationic guanidine moiety on arginine side chains confers the membrane translocating properties that are not observed in peptides containing similar amino acids such as lysine, ornithine or histidine.[223] The detailed mechanism of cellular internalisation of TAT peptide still remains to be determined.[224] Recent studies indicate an energy dependent endocytosis as the major mode of entry for TAT peptides.[225-228] However in addition to endocytosis, other mechanisms might exist as well.[229, 230] Although TAT allows efficient cellular uptake of molecules, the limiting factors are the inability of these conjugates to escape the endosomes and their subsequent lysosomal degradation.

Transport across the nuclear membrane

The eukaryotic nucleus is surrounded by the nuclear envelope that is composed of the inner and the outer membranes. The outer membrane is continuous with the endoplasmic reticulum (ER). Primarily, the nuclear membrane separates the DNA and the genetic machinery from the cytoplasm. The nuclear membrane is studded with large numbers of pores of huge size and elaborate construction.[231] Each nucleus has several thousand pores forming channels between the cytoplasm and the nucleoplasm for the trafficking of macromolecules in and out of the nucleus. These pores are usually referred as the nuclear pore complexs (NPC). Small molecules like ions diffuse freely through the central aqueous channel of the NPC in an energy independent way. Macromolecules are usually actively transported across the NPCs in a temperature sensitive and energy dependent manner.

Recent work has led to a better understanding of the mechanisms involved in the transport of proteins and RNA in and out of the nuclei.[232, 233] This transport involves nuclear localisation signals (NLSs) or export signals that bind to nuclear transport proteins (e.g Karyopherins α and β), which mediate their movement in or out of the nucleus through the nuclear pore complexes.

The nuclear transport across the NPC is a complex process and has been actively investigated[234] (see review articles[231, 235, 236]). There are a number of pathways available for nuclear import. Görlich recently reported on the kinetics of the translocation though the NPC.[237] A recent study by Read et al. showed that non-viral gene transfer based on NLS depends on the type of the NLS peptide, morphology of the DNA and the method of incorporation of the NLS peptide to the DNA.[238]

Nuclear Localisation Signal (NLS)

Selective nuclear import is mediated by nuclear localisation signals. The simian virus 40 (SV 40) large T antigen peptide was the first nuclear localisation signal that was identified[239] and was actively investigated by Feldherr.[240] Since then a large number of NLSs have been identified and they all include a stretch of basic amino acids. The SV 40 large T antigen NLS has one short cluster of basic amino acids and is therefore called the monopartite sequence. There are bipartite such as nucleoplasmin[241] and tripartite such as the PrnA NLSs[242] that contain two or three clusters of basic amino acids respectively.

The shortest functional sequence of the SV 40 large T antigen NLS is a heptapeptide with the sequence PKKKRKV and has a wide range of cargo import functions.[243] This NLS(126-132) binds to the Karyopherin α/β1 heterodimer, also known as importin α/β.[244] The karyopherin-α provides the NLS binding site[236] whereas the karyopherin-β, docks the heterotrimeric complex through the nuclear pore complex [245] and is subsequently translocated into the nucleus through the pore by an energy dependent mechanism that involves Ran.[246] (scheme 1.13).

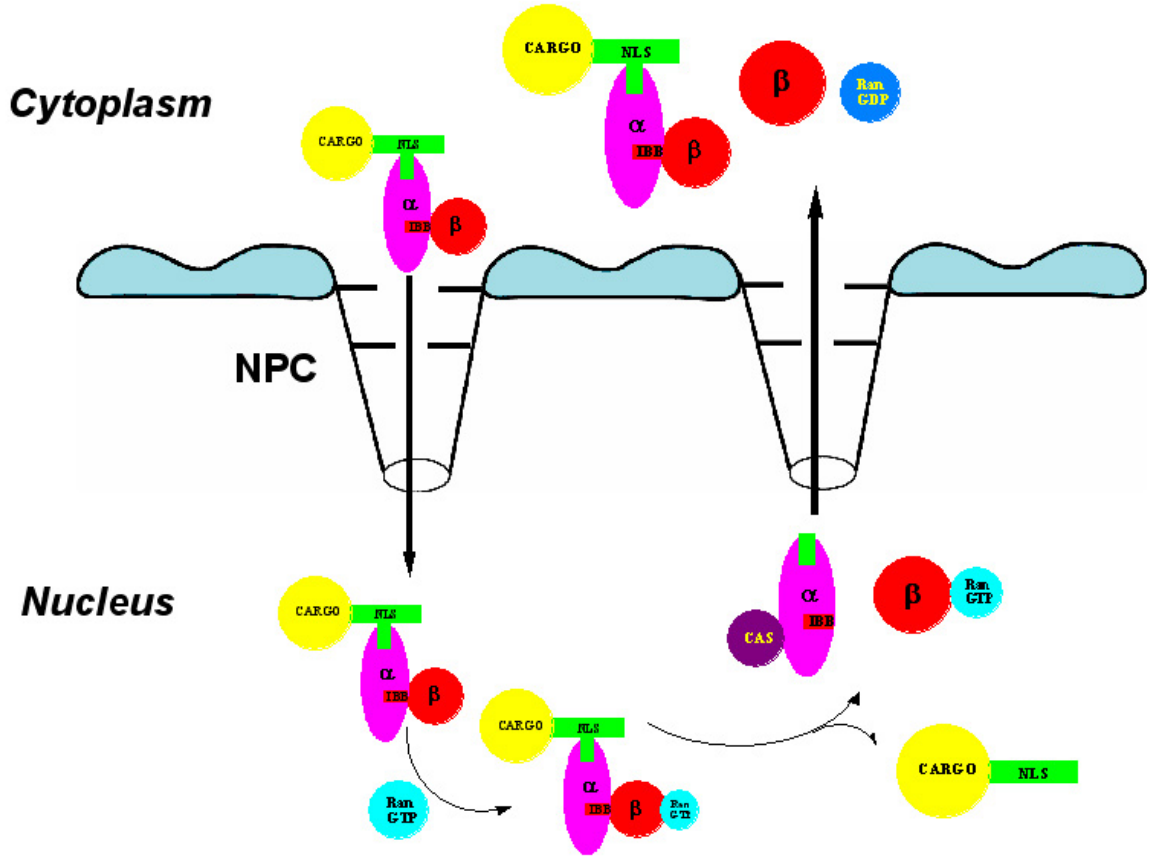

Scheme 1.13: Nuclear transport of NLS with a cargo through the nuclear pore complex.

The nuclear localisation signals have been used for gene delivery,[247] anti-gene PNA,[248] oligonucleotides,[249, 250] photosentisizers,[251] gold nanoparticles[252, 253] and radiolabelled intercalator.[254] To function properly, the NLS conjugate has to be located in the cytoplasm.[237] NLS conjugates, however, are not readily incorporated into the cells. Inefficient entry into the cells[255] or inability to escape endosomes[252] has been reported. More complicated conjugates have been devised to circumvent the problem of cellular uptake, for example NLS conjugates with lipophilic membrane anchoring peptide domains or Au clusters.[243, 251]

Small Regulatory Peptides

A number of human tumour tissues overexpress certain types of high affinity receptors on their surface. These receptors can be exploited for *in-vivo* imaging and therapy by the use of the so-called tumour affine peptides and their derivatives. These are small regulatory peptides and have been a continuous focus of attention since the last decade. These peptides can be used to localise tumours *in-vivo* and more recently to treat cancer with peptide

receptor radiation therapy (PRRT). The regulatory peptide receptors are overexpressed in various neuroendocrine tumours, breast, prostrate, gastrointestinal tract, pancrease and brain tumours. An excellent review appeared recently which highlights the tumours that overexpress the regulatory peptide receptors and the various regulatory/tumour affine peptides such as the gastrin releasing peptide, somatostatin, cholecystokinin-2, neurotensin, neuropeptide Y, bombesin, vasoactive intestinal peptide (VIP), substance P and the glucagon-like peptide.[256]

These regulatory peptides are usually small peptides (between 1 to 15 kDa). Due to their low molecular weight they can better penetrate into tumour tissues and can be rapidly cleared from the normal tissue and circulation. As such they lead to better tumour-to-background ratios than higher molecular weight compounds like monoclonal antibodies and their constructs. Therefore, radiolabelled neuropeptides can be used for imaging and therapy purposes.[257] The application of radiolabelled somatostatin and vasoactive intestinal peptide analogues for successful imaging of neuropeptide postive receptors has been reported.[258, 259] In addition, the development of further small regulatory peptides such as bombesin, cholecystokinin, neurotensin and substance P[260, 261] as potential imaging agents is actively pursued.

Of special interest are the gut peptides that function in an endocrine, paracrine and autocrine fashion. The gut peptides (gastrin, vasoactive intestinal peptide, neurotensin and bombesin) regulate, the growth, *in-vivo* and *in-vitro,* of some cancers in the gastrointestinal tract and pancreas.[263] Moreover, neurotensin plays important role in the central nervous system such as in nociception, pathophysiology of schizophrenia and in the mechanisms of action of antipsychotic drugs.

Neurotensin (NT)

Neurotensin is a brain and gastrointestinal peptide that carries out important central and peripheral functions in the organism. It is a 13 amino acid peptide (ELYGNKPRRPYIL) and was first isolated from bovine hypothalamus.[264] It has dual functions of a neurotransmitter/neuromodulator in the central nervous system and of a local hormone in the periphery. At central level, it is a neuromodulator of dopamine transmission[265] and anterior pituitary hormone secretion. It also has potent hypothermic and analgesic effects in the brain.[266, 267] In the periphery, neurotensin exerts paracrine and endocrine modulation of

the gastrointestinal tract and of the cardiovascular system.[268] Neurotensin has been shown to influence growth in a number of cancerous and non-cancerous cells by enhancing the proliferative effects of growth factors without itself inducing proliferation. Neurotensin for example, can potentiate the proliferative effects of insulin on human fibroblasts.[269]

In the brain, NT is exclusively found in nerve cells, fibers and terminals. Whereas in the periphery, it is mostly found in the endocrine N-cells of the intestinal mucosa.[264] Most of the actions of neurotensin are mediated through its interaction with the cell surface receptors. These receptors include the NTR1, NTR2 and the recently discovered NTR3 receptors.[270] The NTR1 and NTR2 receptors belong to the family of G-protein coupled receptors[271-273] with 7 transmembrane domains. The NTR3 receptor is different from these two receptors and has a single transmembrane domain.[274, 275] The NTR1 and NTR2 receptors have been studied in detail by radioligand-binding assays.[276] NTR1 receptor has a high binding affinity and a low capacity whereas the NTR2 receptors show low affinity and high capacity.[277, 278]

The structure activity studies have shown that the hexapeptide, NT(8-13) is equipotent or even more potent than the wild type NT in binding to the neurotensin receptors while maintaining its biological and pharmacological functions.[279] Point mutations have shown that the two guanidio groups of Arginines, the hydroxyphenyl group of tyrosine and the side chains of the isoleucine and leucine as well as the free carboxylic group at the *C*-terminal are necessary for the activity of NT.[280]

Scheme 1.14: A 3-D model of Neurotensin (8-13) and NTR1 complex.[281]

The activation of the NT receptors by binding of NT leads to the production of cGMP and cAMP or activation of the phosphatidylinositol pathway and calcium mobilisation.[282] The NT receptor is internalised by endocytosis after its interaction with the peptide and is destroyed.[270] In prostrate cancer cell lines, NT is metabolised by endogenous proteases.[283] The peptide bonds between Arg-Arg, Pro-Tyr and Tyr-Ile are the usual sites of cleavage by various endopeptidases.[284, 285] In human plasma the NT is rapidly degraded despite its high affinity.[286]

Over the years a large number of neurotensin analogues have been prepared and tested for various purposes in therapy as well as in tumour and receptor imaging. Neurotensin derivatives can serve as potent analgesics and antipsychotics especially in treatment of Parkinson's disease and Schizophrenia.[287, 288] A number of NT derivatives have been investigated for their use in the detection, localisation and treatment of malignant human tumours.[289-293] However the rapid degradation of NT derivatives and their inability to cross the blood brain barrier are major limiting factors.[264] Non-peptidic analogues have been reported.[294] In addition, various stabilised derivatives of the peptide have also been actively investigated.[295-298]

Objectives of present study

There is a huge potential of organometallic compounds in biology. Various bioactive peptides seem attractive targets. Incorporation of biologically functional organometallics in the exploitation of these targets will result in novel compounds with specific applications in detection, diagnosis and therapy or in lead compounds for further research.

The main objectives of the present research are:

- Solid phase peptide syntheses of various metal-peptide bioconjugates which include the metallocene (ferrocene and cobaltocenium carboxylic acids) bioconjugates of the SV 40 T antigen nuclear localisation signal peptide (NLS), Transactivator of transcription (TAT) and Neurotensin (NT) peptides. In addition, to carry out the solid phase syntheses of Platinum bioconjugates of NLS and NT.

- Optimization of syntheses procedures for metal as well as fluorescence labelling.

- Comprehensive characterization of the synthesized bioconjugates by means of NMR, HPLC, mass spectrometry and electrochemistry.

- Cellular uptake and nuclear localisation studies on the metallocene-NLS bioconjugates in human liver cancer cell line (Hep G2) and determination of their cytotoxic effects (if any).

- Cellular uptake and nuclear localisation studies on metallocene-TAT bioconjugates in Hep G2 cell line and study of their cytotoxicity.

- Determination of the cytotoxicity of Platinum-NLS bioconjugates in Hep G2 cell line.

- Receptor binding studies on various metal-neurotensin bioconjugates with NTR1 receptors in human adenocarcinoma (HT 29) cell line.

- Evaluation of the cytotoxic and genotoxic potential of various metal-peptide bioconjugates in a preliminary yeast assay.

Experimental Details

2.1 Syntheses and Characterisation

2.1.1 Materials and Apparatus

The compounds were synthesized using routine methods of solid phase peptide synthesis on Eppendorf automatic synthesizers. DMF for peptide synthesis was purchased from Roth Chemicals. All other solvents were reagent grade unless otherwise specified. All amino acids and resin were purchased from Novabiochem, Laufelfingen, Switzerland. Other reagents and chemicals were purchased from Aldrich-Sigma GmbH and used as received. FITC was purchased from Fluka Chemicals.

Mass spectra, MALDI-TOF were recorded on a Bruker Biflex Instrument and the ESI spectra (neg./pos.) on a Finnigan TSQ 700 at 4.5 kV, at the Institute of Organic Chemistry, University of Heidelberg. Only characteristic fragments are given with possible composition.

NMR spectra were measured at room temperature on a Bruker DRX 300 (^{1}H at 300.1316 MHz), Bruker AM (^{1}H at 366.1316 MHz), Bruker DRX (^{1}H at 500.1300 MHz) and Varian Unity Instruments (^{1}H at 399.896 MHz). The chemical shifts are reported in δ (ppm) referenced to TMS, using residual protio signals of deuterated solvents as internal standards. Coupling constants (*J*) are given in Hz. The peaks are identified as singlets (s), doublets (d), triplets (t) or multiplets (m). Depending upon the solubility of compounds, D_2O or CD_3OD were used as solvents.

Cyclic and square wave voltammograms were obtained with a three electrode cell on a Princeton Applied Research Basic Electrochemical System potentiostat. A Ag/AgCl (0.01 M AgCl in MeCN) reference electrode, a glassy carbon working electrode and a Pt wire auxiliary electrode in MeCN containing 0.1 M $TBAPF_6$ as supporting electrolyte were used. Ferrocene was used as an internal standard at a scan rate of 60 Hz.

Analytical HPLC was carried out on a Varian Prostar Instument using a Reverse Phase Varian Dynamax analytical column (C18 microsorb 60Å, diameter 4.5 mm, 250 mm length) with water and acetonitrile, both containing 0.1 % TFA, as eluents using a linear gradient, 5 to 95% acetonitrile, for 20 minutes. Purifications were done on a Varian Dynamax preparative column (C18 microsorb 60Å, diameter 21.4 mm, 250 mm length).

2.1.2 Methods and Analytical data

2.1.2.1 NLS(126-132) Bioconjugates

Solid Phase Peptide Synthesis

All NLS(126-132) bioconjugates were snythesized using standard SPPS methods using Fmoc strategy. Wang resin preloaded with Fmoc-Val-OH (0.63 mmol/g) was used. The resin was swelled in DMF for 1 h. Fmoc groups were cleaved using 20% piperidine in DMF for 10 minutes followed by 3x washing with DMF. 3 eq. of Fmoc-Lys(Boc)-OH, Fmoc-Arg(Pbf)-OH and Fmoc-Pro-OH along with equimolar quantities TBTU and HOBt as coupling reagents and DIPEA (8eq.) as base were used to synthesize the NLS part of the bioconjugates. The activation time was one minute and the coupling time for the amino acids was 35 minutes. The arginine and the lysine following the proline were coupled for one hour. The synthesized NLS has asequence of PKKKRKV. The terminal amino group of the peptide was used to carry the metallocene moiety, which was coupled using the standard method on solid phase (using 3 eq. cobaltocenium carboxylic acid or ferrocene carboxylic acid, 3 eq of TBTU and 3 eq. of HOBt with a longer activation time of 10 minutes).

For compounds **1** and **2**, the metallocene carboxylic acids were coupled on the resin to the *N*-terminal proline of the peptide. In case of compound **3,** Fmoc-Lys(mca)-OH which is commercially available was used in the second step of coupling. For Pt-bioconjugates **4** and **5**, the complexation was carried out with 6 eq. of K_2PtCl_4 in a 1:9 H_2O/DMF mixture. Aminoethyglycine (BB) and diaminopropionic acid (DAP) were used as ligands for platination. The complexation was carried out for 3 days. Upon successful complexation of the metal to the peptide, the resin changed colour from off white to brown. BB denotes the backbone (aminoethylglycine) and DAP the diaminopropionic acid ligands respectively.

For compounds **6-11**, after the NLS(126-132) sequence, another lysine, Fmoc-Lys(Mtt)-OH, was used as a linker and carrier of the fluorescent label. The metallocene carboxylic acid was then added to the *N*-terminal of the peptide and upon successful coupling of the metal complex to the peptide, the resin changed colour from off white to yellow or orange. For all compounds, the metallocene carboxylic acid was coupled to the free *N*-terminal of the peptide chain on the resin prior to labelling with the fluorescence marker. The side chain of the linker lysine was used for labelling with Fluorescein isothiocyanate (FITC). Compounds **12** and **13** are the truncated peptide-metallocene conjugates containing a lysine which is labelled with FITC.

The fluorescent label was added manually in the lab. The resin was washed with DMF to remove impurities. The resin carrying the bioconjugate had to be shrinked using MeOH for efficient removal of the methyltrityl (Mtt) protecting group. The side chain Mtt group was removed with 1% TFA in CH_2Cl_2 (using 5% TIS in the cleavage mixture). The resin was treated with 2 ml of the cleavage mixture for 2 min and this step is repeated 5 times. Afterwards the resin was washed with CH_2Cl_2 and again swelled for in DMF for 30 minutes. The resin was then shaken in the dark for 3 to 4 hours with a solution of FITC in DMF and 10 eq. of DIPEA.

At the end of the synthesis, the bioconjugates were washed repeatedly with DMF, CH_2Cl_2 and shrinked with MeOH. The resin was thoroughly dried over KOH under vaccum overnight prior to cleavage of the bioconjugate. Cleavage from the resin was achieved with 95 % TFA, 2.5 % TIS and 2.5 % H_2O for 3 h for all compounds except those containing ferrocene carboxylic acid as the metal moiety. For ferrocene containing compounds, the cleavage mixture consisted of 85% TFA, 10% phenol and 5% TIS. Whereas for Pt-bioconjugates, the cleavage mixture consisted of wet TFA containing 5 % H_2O.

The cleaved peptides were collected by filtration. The bioconjugates were precipitated from the filtrate upon addition of cold diethylether (-20 °C). The crude product was dried and lyophilized. Crude yield was quantitative in all cases. Purification was achieved by preparative HPLC.

HPLC conditions:

Analytical HPLC at 25°C

Method A	Linear gradient, 5 to 95% Acetonitrile in 20 minutes with water and acetonitrile both containing 0.1% TFA as eluents.
Method B	Linear gradient, 5 to 95% Methanol in 30 minutes with water containing 0.1% TFA and methanol as eluents.
Method C	Linear gradient, 5 to 95% Acetonitrile in 30 minutes with water and acetonitrile both containing 0.1% TFA as eluents.

Preparative HPLC at RT

Preparative HPLC was carried out using isocratic gradient with eluent concentrations ranging from 40 % to 55 % acetonitrile containing 0.1 % TFA. In case where methanol was used as an eluent, the purification was carried out at 70% methanol isocratic gradient.

Analytical data

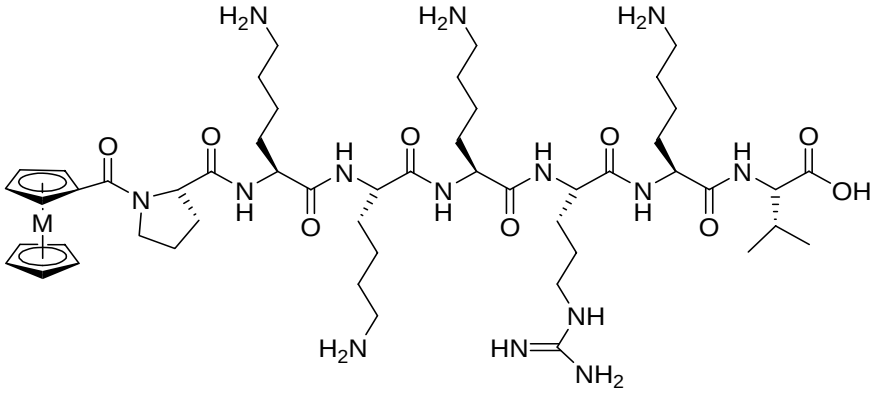

M = Co^+ **(1)**
Fe **(2)**

1: CcC(O)-NLS

Pale yellow solid, soluble in water and ethanol

$C_{51}H_{86}Co^+N_{14}O_9$ (1097.6 g/mol)

R_t = 6.9 minutes (Analytical HPLC; Method A)

ESI : *m/z* 366.9 $[M+3H]^{3+}$ 549.6 $[M+2H]^{2+}$

SWV: $E_{1/2}$ = -1.076 V vs. FcH / FcH^+

^{1}H-NMR (366 MHz, CD_3OD): δ_H 6.29 (s, 1H, substituted Cp) 6.24 (s, 1H, substituted Cp) 5.90 (pseudo t, 2H, substituted Cp) 5.87 (s, 5H, unsubstituted Cp) 4.50-4.60 (m, 1H, $H_{\alpha,Val}$) 4.23-4.42 (m, 7H, H_α) 3.72-3.79 (m, 2H, $H_{\delta,\ Pro}$) 3.20 (t, *J*=6.6 Hz, 2H, $H_{\delta,\ Arg}$) 2.91- 3.01 (m, 8H, $H_{\varepsilon,\ Lys}$) 2.38-2.32 (m, 1H, $H_{\beta,Val}$) 2.05-1.99 (m, 2H, $H_{\beta,\ Pro}$) 1.93-1.82 (m, 2H, $H_{\gamma,\ Pro}$) 1.79-1.64 (m, 20H, $H_{\beta,\ \delta,\ Lys}$, $H_{\beta,\ \gamma,\ Arg}$) 1.61-1.37 (m, 8H, $H_{\gamma,\ Lys}$) 0.98 (d, *J*=6 Hz, 6H, C*H*$_3$-Val)

2: FcC(O)-NLS

Orange solid, soluble in water and ethanol

$C_{51}H_{86}FeN_{14}O_9$ (1094.61 g/mol)

R_t = 9.91 minutes (Analytical HPLC; Method A)

MALDI-TOF: *m/z* 1094.8 $[M]^+$ 1134.8 $[M+K]^+$

SWV: $E_{1/2}$ = 247 vs. FcH / FcH^+

^{1}H-NMR (400 MHz, CD_3OD): δ_H 4.72 (broad s, 2H, H_α) 4.41 (broad s, 3H, substituted Cp, H_α) 4.34-4.22 (m, 4H, substituted Cp, H_α) 4.18 (s, 7H, unsubstituted Cp, H_α) 4.04-3.86 (m, 1H, $H_{\delta,\ Pro}$) 3.88-3.80 (m, 1H, $H_{\delta,\ Pro}$) 3.11 (pseudo t, 2H, $H_{\delta,\ Arg}$) 2.89-2.79 (m, 8H, $H_{\varepsilon,\ Lys}$) 2.27-2.19 (m, 1H, $H_{\beta,\ Val}$) 2.12-2.06 (m, 1H, $H_{\beta,\ Pro}$) 1.98-1.75 (m, 3H, $H_{\beta,\ \gamma,\ Pro}$) 1.70-1.56 (m, 20H, $H_{\beta,\ \delta,\ Lys}$, $H_{\beta,\ \gamma,\ Arg}$) 1.48-1.33 (m, 8H, $H_{\gamma,\ Lys}$) 0.89 (d, *J*=6.6 Hz, 6H, C*H*$_3$-Val)

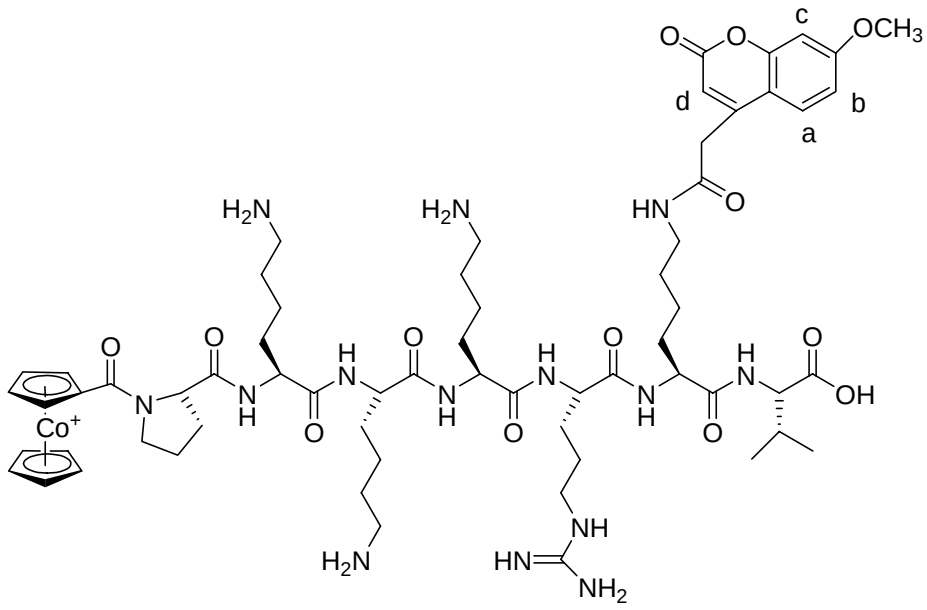

3: CcC(O)-NLS$_{mca}$

Light yellow solid, soluble in water and ethanol

$C_{63}H_{94}Co^{+}N_{14}O_{13}$ (1313.65 g/mol)

R_t = 11.14 minutes (Analytical HPLC; Method A)

ESI : *m/z* 438.9 $[M+3H]^{3+}$ 657.6 $[M+2H]^{2+}$

SWV: $E_{1/2}$ = -1.162V vs. FcH / FcH^{+}

^{1}H-NMR (300 MHz, D_2O): δ_H 7.50 (d, *J*=8.8 Hz, 1H, $H_{a,\ mca}$) 6.87 (d, *J*=8.7 Hz, 1H,$H_{c,\ mca}$) 6.80 (s, 1H, $H_{b,\ mca}$) 6.18-6.10 (m, 3H, $H_{d,\ mca}$, substituted Cp) 5.82 (pseudo t, 2H, substituted Cp) 5.75 (s, 5H, unsubstituted Cp) 4.48 (pseudo t, 1H, H_α) 4.14-4.28 (m, 6H, H_α) 3.85 (s, 3H, OC*H*$_3$-mca) 3.65 (broad s, 2H, $H_{\delta,\ Pro}$) 3.35 (pseudo t, 2H, $H_{\delta,\ Arg}$) 3.20-3.06 (m, 2H, $H_{\alpha,\ mca}$) 3.00-2.89 (broad s, 8H, $H_{\varepsilon,\ Lys}$) 2.45-2.30 (m, 1H, $H_{\beta,\ Val}$) 2.19-1.95 (m, 4H, $H_{\beta,\ \gamma,\ Pro}$) 1.81-1.59 (m, 20H, $H_{\beta,\ \delta,\ Lys}$, $H_{\beta,\ \gamma,\ Arg}$) 1.45-1.20 (m, 8H, $H_{\gamma,\ Lys}$) 0.86 (d, *J*=6.7 Hz, 6H, C*H*$_3$-Val)

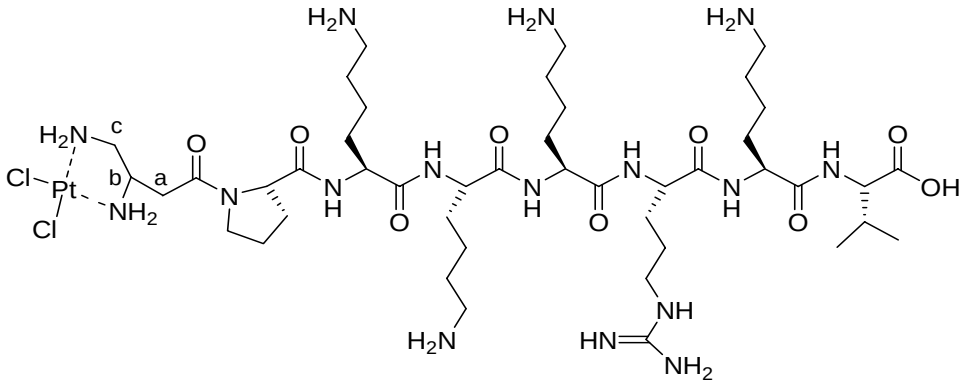

4: Pt(II)-BB-NLS

Silvery brown solid, soluble in water

$C_{44}H_{86}Cl_2N_{16}O_9Pt$ (1248.59 g/mol)

R_t = 9.4 minutes (Analytical HPLC; Method C)

MALDI-TOF: *m/z* 1248.7 $[M]^+$ 1288.7 $[M+H+K]^+$

^{1}H-NMR (400 MHz, D_2O): δ_H 4.35-4.28 (m, 1H, $H_{\alpha,\ Val}$) 4.28-4.17 (m, 6H, H_α) 3.56-3.40 (m, 2H, $H_{\delta,\ Pro}$) 3.07 (pseudo t, 2H, $H_{\delta,\ Arg}$) 2.95-2.82 (m, 11H, $H_{b,c,\ BB}$ $H_{\varepsilon,\ Lys}$) 2.64-2.49 (broad s, 2H, $H_{a,\ BB}$) 2.20-2.15 (m, 1H, $H_{\beta,\ Val}$) 2.10-2.03 (m, 1H, $H_{\beta,\ Pro}$) 1.92-1.83 (m, 3H, $H_{\beta,\ \gamma,\ Pro}$) 1.77-1.47 (m, 20H, $H_{\beta,\ \delta,\ Lys}$, $H_{\beta,\ \gamma,\ Arg}$) 1.36-1.22 (m, 8H, $H_{\gamma,\ Lys}$) 0.83 (d, *J*=7 Hz, 6H, C*H*$_3$-Val)

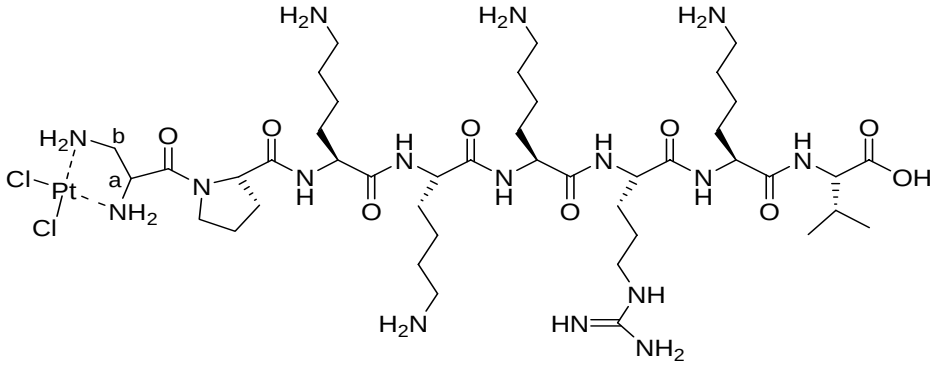

5: Pt(II)-DAP-NLS

Light brown solid, soluble in water

$C_{43}H_{84}Cl_2N_{16}O_9Pt$ (1233.56 g/mol)

R_t = 7.8 minutes (Analytical HPLC; Method C)

MALDI-TOF: *m/z* 1235.8 $[M+2H]^+$ 1275.8 $[M+2H+K]^+$

^{1}H-NMR (400 MHz, D_2O): δ_H 4.41-4.39 (m, 1H, $H_{\alpha,\ Val}$) 4.35-4.25 (m, 6H, H_α) 4.04-4.93 (m, 3H, $H_{a,\ DAP,}$ $H_{\delta,\ Pro}$) 3.78-3.72 (m, 1H, $H_{\delta,\ Pro}$) 3.60-3.55 (m, 2H, $H_{b,\ DAP}$) 3.19 (pseudo t, 2H, $H_{\delta,\ Arg}$) 3.05-2.96 (m, 8H, $H_{\varepsilon,\ Lys}$) 2.70-2.64 (m, 1H, $H_{\beta,\ Val}$) 2.35-2.25 (m, 1H, $H_{\beta,\ Pro}$) 2.12-1.99 (m, 3H, $H_{\beta,\ \gamma,\ Pro}$) 1.88-1.65 (m, 20H, $H_{\beta,\ \delta,\ Lys}$, $H_{\beta,\ \gamma,\ Arg}$) 1.54-1.38 (m, 8H, $H_{\gamma,\ Lys}$) 0.93-0.82 (m, 6H, C*H*$_3$-Val)

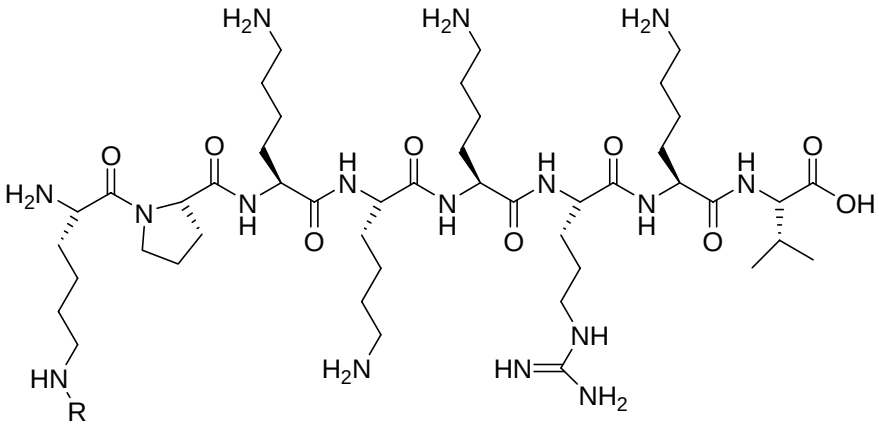

R = H **(6)**
= FITC **(7)**

6: H-Lys-NLS

White solid, soluble in water and ethanol

$C_{46}H_{90}N_{16}O_9$ (1010.71 g/mol)

R_t = 6.98 minutes (Analytical HPLC; Method A)

MALDI-TOF: *m/z* 1011 $[M+H]^+$ 1032.9 $[M+Na]^+$

^{1}H-NMR (300 MHz, D_2O): δ_H 4.52 (pseudo t, 1H, $H_{\alpha,\ Val}$) 4.40-4.25 (m, 6H, H_α) 4.16 (d, *J*=6 Hz, 1H, $H_{\alpha,\ Lys\ terminal}$) 3.83-3.74 (m, 1H, $H_{\delta,\ Pro}$) 3.67-3.58 (m, 1H, $H_{\delta,\ Pro}$) 3.22 (pseudo t, 2H, $H_{\delta,\ Arg}$) 3.09-2.99 (m, 10H, $H_{\varepsilon,\ Lys}$) 2.42-2.31 (m, 1H, $H_{\beta,\ Val}$) 2.19-1.99 (m, 1H, $H_{\gamma,\ Pro}$) 2.03-1.95 (m, 3H, H_{γ}, $H_{\beta,\ Pro}$) 1.90-1.67 (m, 24 H, $H_{\beta,\ \delta,\ Lys}$, $H_{\beta,\ \gamma,\ Arg}$) 1.58-1.39 (m, 10H, $H_{\gamma,\ Lys}$) 0.95 (2 overlapping d, *J*=6.8 Hz, 6H, CH_3-Val)

7: H-Lys(FITC)-NLS

Bright yellow solid, soluble in water and ethanol

$C_{67}H_{101}N_{17}O_{14}S^+$ (1399.74 g/mol)

R_t = 10.58 minutes (Analytical HPLC; Method A)

MALDI-TOF: *m/z* 1401.9 $[M+2H]^+$, 1442 $[M+2H+K]^+$

^{1}H-NMR (300 MHz, D_2O) δ_H 8.20 (s. 1H, FITC) 7.90 (s, 1H, FITC) 7.33-7.29 (m, Hz, 1H, FITC) 7.25-7.20 (m, 2H, FITC) 6.95 (s, 2H, FITC) 6.89 (d, *J*=8.2 Hz, 1H, FITC) 6.85-6.79 (m, 1H, FITC) 4.48-4.41 (m, 1H, H_α) 4.35-4.16 (m, 6H, H_α) 4.07-4.01 (m, 1H, H_α) 3.87-3.73 (m, 1H, $H_{\delta,\ Pro}$) 3.63-3.55 (m, 1H, $H_{\delta,\ Pro}$) 3.16-3.05 (m, 2H, $H_{\delta,\ Arg}$) 2.98-2.80 (m, 10H, $H_{\varepsilon,\ Lys}$) 2.30-2.22 (m, 1H, $H_{\beta,\ Val}$) 2.06-2.01 (m, 1H, $H_{\beta,\ Pro}$) 1.97-1.88 (m, 2H, $H_{\gamma,\ Pro}$) 1.79-1.55 (m, 24H, $H_{\beta,\ \delta,\ Lys}$, $H_{\beta,\ \gamma,\ Arg}$) 1.43-1.22 (m, 10H, $H_{\gamma,\ \delta,\ Lys}$) 0.88-0.80 (m, 6H, C$H_3$-Val)

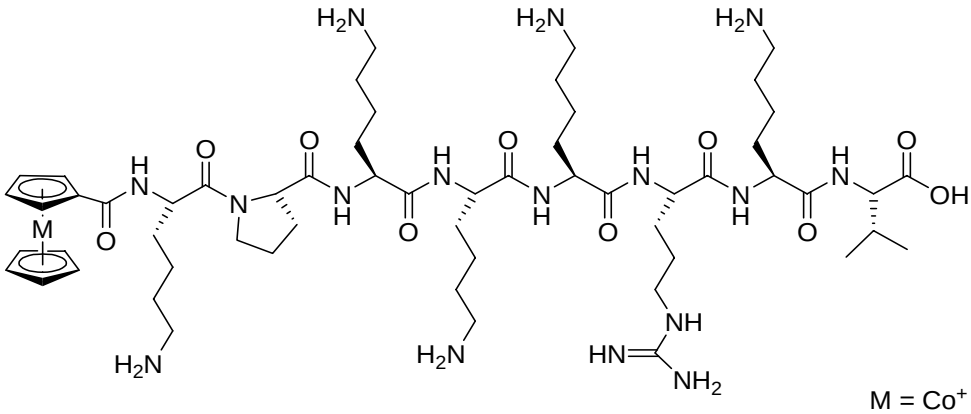

8: CcC(O)-Lys-NLS

Pale yellow solid, soluble in water and ethanol

$C_{57}H_{98}Co^{+}N_{16}O_{10}$ (1225.7 g/mol)

R_t = 8.14 minutes (Analytical HPLC; Method A)

MALDI-TOF: *m/z* 1226.5 $[M+H]^+$ 1266.5 $[M+K]^+$

SWV: $E_{1/2}$ = -1.38 V vs. FcH / FcH^+

^{1}H-NMR (400 MHz, D_2O) δ_H 6.25 (s, 1H, substituted Cp) 6.18 (s, 1H, substituted Cp) 5.82 (pseudo t, 2H, substituted Cp) 5.73 (s, 5H, unsubstituted Cp) 4.39 (pseudo t, 1H, H_α) 4.30-4.19 (m, 7H, H_α) 3.91-3.80 (m, 1H, $H_{\delta,\ Pro}$) 3.62-3.55 (m, 1H, $H_{\delta,\ Pro}$) 3.14 (pseudo t, 2H, $H_{\delta,\ Arg}$) 2.98-2.84 (m, 10H, $H_{\varepsilon,\ Lys}$) 2.31-2.20 (m, 1H, $H_{\beta,\ Val}$) 2.18-2.05 (m, 1H, $H_{\gamma,\ Pro}$) 2.01-1.90 (m, 2H, $H_{\beta,\ \gamma,\ Pro}$) 1.82-1.48 (m, 25 H, $H_{\gamma,\ Pro}$, $H_{\beta,\ \delta,\ Lys}$, $H_{\beta,\ \gamma,\ Arg}$) 1.39-1.25 (m, 10H, $H_{\gamma,\ Lys}$) 0.84 (d, *J*=7 Hz, 6H, C*H*$_3$-Val)

9: FcC(O)-Lys-NLS

Yellow solid, soluble in water and ethanol

$C_{57}H_{98}FeN_{16}O_{10}$ (1222.7 g/mol)

R_t = 9.7 minutes (Analytical HPLC; Method A)

MALDI-TOF: *m/z* 1223.5 $[M+H]^+$ 1246.6 $[M+Na]^+$

SWV: $E_{1/2}$ = 239 vs. FcH / FcH^+

^{1}H-NMR (400 MHz, D_2O): δ_H 4.50 (s, 2H, substituted Cp) 4.45-4.35 (m, 1H, $H_{\alpha,\ Val}$) 4.15 (broad s, 9H, unsubstituted Cp, H_α) 3.99-3.94 (m, 2H, H_α) 3.92-3.88 (m, 1H, $H_{\alpha,\ Lys\ terminal}$) 3.79-3.50 (m, 2H, $H_{\delta,\ Pro}$) 3.15 (pseudo t, 2H, $H_{\delta,\ Arg}$) 2.99-2.88 (broad s, 10H, $H_{\varepsilon,\ Lys}$) 2.30-2.24 (m, 1H, $H_{\beta,\ Val}$) 1.95-2.10 (m, 3H, $H_{\beta,\ \gamma,\ Pro}$) 1.90-1.60 (m, 25 H, $H_{\gamma,\ Pro}$, $H_{\beta,\ \delta,\ Lys}$, $H_{\beta,\ \gamma,\ Arg}$) 1.50-1.30 (m, 10H, $H_{\gamma,\ Lys}$) 0.85 (2 overlapping d, *J*=6 Hz, 6H, C*H*$_3$-Val)

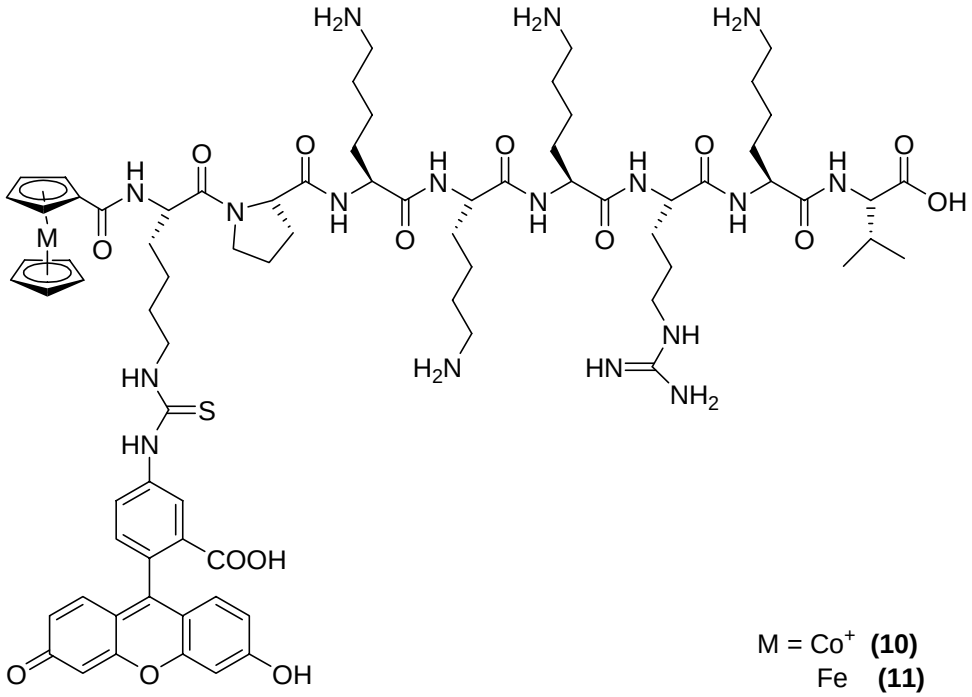

10: CcC(O)-Lys(FITC)-NLS

Bright orangish yellow solid, soluble in water and ethanol

$C_{78}H_{109}Co^{+}N_{17}O_{15}S$ (1614.73 g/mol)

R_t = 11.21 minutes (Analytical HPLC; Method A)

MALDI-TOF: *m/z* 1616.3 $[M+H]^+$

SWV: $E_{1/2}$ = -1.37 V vs. FcH / FcH^+

^{1}H-NMR (300 MHz, D_2O): δ_H 7.95 (s, 1H, FITC) 7.60 (d, *J*=6.8 Hz,1H, FITC) 7.30 (d, *J*=7.8 Hz,1H, FITC) 7.20 (d, *J*=8.6 Hz, 2H, FITC) 7.03 (s, 2H, FITC) 6.84 (d, *J*=6.8 Hz, 2H, FITC) 6.20 (pseudo t, 1H, substituted Cp) 6.17 (pseudo t, 1H, substituted Cp) 5.78 (s, 2H, substituted Cp) 5.73 (s, 5H, unsubstituted Cp) 4.40-4.32 (m, 1H, H_α) 4.25-4.10 (m, 6H, H_α) 4.05 (d, *J*=6 Hz, $H_{\alpha,\ Lys}$) 3.90-3.78 (m, 1H, $H_{\delta,\ Pro}$) 3.69-3.55 (m, 1H, $H_{\delta,\ Pro}$) 3.15-3.02 (m, 2H, $H_{\delta,\ Arg}$) 2.91-2.82 (m, 10H, $H_{\varepsilon,\ Lys}$) 2.05-1.79 (m, 5H, $H_{\beta,\ \gamma,\ Pro}$, $H_{\beta,\ Val}$) 1.71-1.42 (m, 24H, $H_{\beta,\ \delta,\ Lys}$, $H_{\beta,\ \gamma,\ Arg}$) 1.35-1.20 (m, 10H, $H_{\gamma,\ Lys}$) 0.86 (d, *J*=6 Hz, 6H, C*H*$_3$-Val)

11: FcC(O)-Lys(FITC)-NLS

Bright orange solid, soluble in water and ethanol

$C_{78}H_{109}FeN_{17}O_{15}S$ (1611.74 g/mol)

R_t = 12.23 minutes (Analytical HPLC; Method A)

MALDI-TOF: *m/z* 1614.2 $[M+2H]^+$ 1636.2 $[M+H+Na]^+$

SWV: $E_{1/2}$ = 166 mV vs. FcH / FcH^+

^{1}H-NMR (400MHz, CD_3OD): δ_H 8.29 (s, 1H, FITC) 7.75 (d, *J*=8.6 Hz, 1H, FITC) 7.39-7.31 (m, 1H, FITC) 7.22-7.17 (m, 1H, FITC) 6.76-6.68 (m, 3H, FITC) 6.58 (dd, *J*=6.2 Hz, 2H, FITC) 4.77-4.69 (pseudo t, 1H, $H_{\alpha,\ Val}$) 4.49-4.43 (m, 3H, H_α) 4.42 (s, 2H, substituted Cp) 4.38-4.31 (m, 4H, H_α) 4.29 (s, 2H, substituted Cp) 4.24 (s, 5H, unsubstituted Cp) 4.04-3.98 (m, 1H, $H_{\delta,\ Pro}$) 3.85-3.76 (m, 1H, $H_{\delta,\ Pro}$) 3.26-3.16 (m, 2H, $H_{\delta,\ Arg}$) 3.05-2.89 (m, 10H, $H_{\varepsilon,\ Lys}$) 2.34-2.26 (m, 1H, $H_{\beta,\ Val}$) 2.23-2.18 (m, 1H, $H_{\gamma,\ Pro}$) 2.06-1.98 (m, 2H, $H_{\beta,\ \gamma,\ Pro}$) 1.96-1.65 (m, 25 H, $H_{\beta,\ Pro}$, $H_{\beta,\ \delta,\ Lys}$, $H_{\beta,\ \gamma,\ Arg}$) 1.60-1.45 (m, 10H, $H_{\gamma,\ Lys}$) 1.00 (d, *J*=6.2 Hz, 6H, C*H*$_3$-Val)

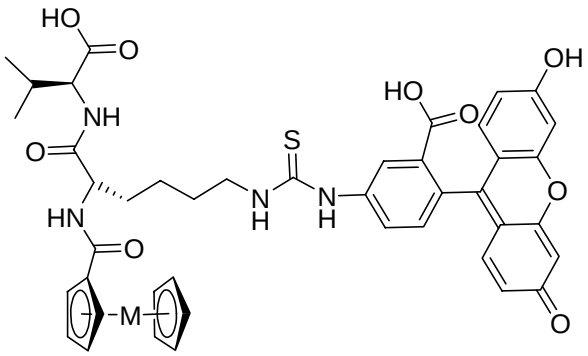

M = Co^+ **(12)**
Fe **(13)**

12: CcC(O)-Lys(FITC)-Val-OH

Bright orangish yellow solid, partially soluble in water and methanol, soluble in DMSO

$C_{43}H_{42}Co^+N_4O_9S$ (849.20 g/mol)

R_t = 13.75 minutes (Analytical HPLC; Method A)

MALDI-TOF: *m/z* 849.3 $[M]^+$

SWV: $E_{1/2}$ = -1.23 V vs. FcH / FcH^+

^{1}H-NMR (300 MHz, CD_3OD): δ_H 8.20 (s. 1H, FITC) 7.75 (d, *J=7* Hz, 1H, FITC) 7.09 (dd, *J=7.8* Hz, 1H, FITC) 6.65 (d, *J= 8.7* Hz, 2H, FITC) 6.52 (s, 2H, FITC) 6.50 (d, *J=7* Hz, 2H, FITC) 6.48 (pseudo t, 1H, substituted Cp) 6.28 (pseudo t, 1H, substituted Cp) 5.90 (pseudo t, 2H, substituted Cp) 5.85 (s, 5H, unsubstituted Cp) 4.38-4.34 (m, 2H, H_α) 3.70-3.61 (m, 2$H_{\varepsilon,\ Lys}$) 2.32-2.25 (m, 1H, $H_{\beta,\ Val}$) 2.08-1.95 (m, 2H, $H_{\beta,\ Lys}$) 1.87-1.75 (m, 2H, $H_{\delta,\ Lys}$) 1.68-1.57 (m, 2H, $H_{\gamma,\ Lys}$) 1.00 (d, *J=6* Hz, 6H, C*H*$_3$-Val)

13: FcC(O)-Lys(FITC)-Val-OH

Dark orange solid, soluble in DMSO and methanol, sparingly soluble in water

$C_{43}H_{42}FeN_4O_9S$ (846.2 g/mol)

R_t = 21.8 minutes (Analytical HPLC; Method B)

MALDI-TOF: *m/z* 847.5 $[M+H]^+$ 869.5 $[M+Na]^+$ 885.5 $[M+K]^+$

SWV: $E_{1/2}$ = 258 mV vs. FcH / FcH^+

^{1}H-NMR (400MHz, CD_3OD): δ_H 8.18 (s, 1H, FITC) 7.79 (d, *J*=8.2 Hz, 1H, FITC) 7.17 (d, *J*=8.2 Hz, 1H, FITC) 6.83-6.75 (m, 4H, FITC) 6.64 (d, *J*=8.2 Hz, 2H, FITC) 4.67 (pseudo t, 1H, $H_{\alpha,\ Val}$) 4.45-4.39 (m, 3H, substituted Cp, $H_{\alpha,\ Lys}$) 4.23 (s, 5H, unsubstituted Cp) 3.70 (broad s, 2H, $H_{\varepsilon,\ Lys}$) 2.29-2.19 (m, 1H, $H_{\beta,\ Val}$) 2.01-1.89 (m, 2H, $H_{\beta,\ Lys}$) 1.81-1.75 (m, 2H, $H_{\delta,\ Lys}$) 1.66-1.51 (m, 2H, $H_{\gamma,\ Lys}$) 1.03 (d, *J*=6.6 Hz, 6H, C*H*$_3$-Val)

2.1.2.2 NLS_{scr} (Scrambled sequence) Bioconjugates

Solid Phase Peptide Synthesis

The bioconjugates were synthesized using the routine methods of SPPS described in section 2.1.2.1. Wang resin preloaded with Fmoc-Arg-OH (0.58 mmol/g) was used. The NLS_{scr} has a sequence of KKVKPKR. Another Lysine was added at the *N*-terminal and its side chain was used as a carrier for the fluorescent label. Cobaltocenium and Ferrocene carboxylic acids were used as metal labels.

After the steps of synthesis, shrinking and cleavage from the resin, the crude products obtained in quantitative yields were dried and lyophilized. Purification was achieved by preparative HPLC.

Analytical data

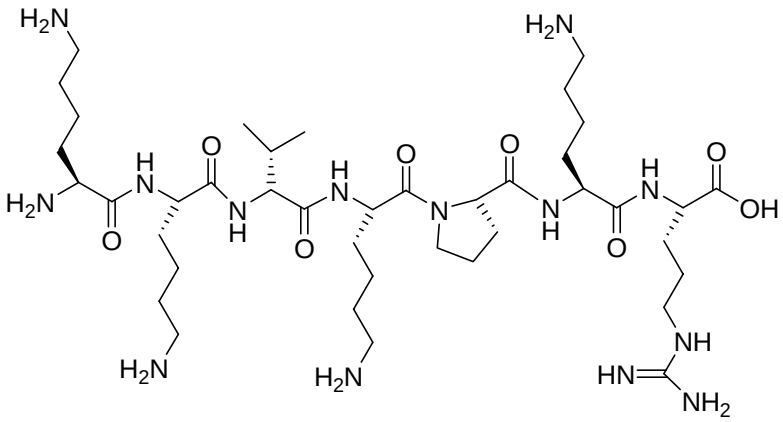

14: NLS_{scr}
White solid, soluble in water and ethanol

$C_{40}H_{78}N_{14}O_8$ (882.6 g/mol)

R_t = 7.4 minutes (Analytical HPLC; Method A)

MALDI-TOF: *m/z* 883.6 $[M+H]^+$

^{1}H-NMR (400 MHz, D_2O): δ_H 4.62-4.54 (m, 1H, $H_{\alpha,\ Val}$) 4.48-4.38 (m, 3H, $H_{\alpha,\ Lys}$) 4.30-4.20 (m, 1H, $H_{\alpha,\ Arg}$) 4.15-4.08 (m, 1H, $H_{\alpha,\ Pro}$) 4.05 (t, *J*=6.6 Hz, 1H, $H_{\alpha,\ terminal\ Lys}$) 3.92-3.82 (m, 1H, $H_{\delta,\ Pro}$) 3.70-3.60 (m, 1H, $H_{\delta,\ Pro}$) 3.21 (pseudo t, 2H, $H_{\delta,\ Arg}$) 3.05-2.95 (m, 8H, $H_{\varepsilon,\ Lys}$) 2.35-2.25 (m,1H, $H_{\beta,\ Val}$) 2.08-1.99 (m, 3H, $H_{\beta,\ \gamma,\ Pro}$) 1.92-1.56 (m, 21H, $H_{\gamma,\ Pro}$, $H_{\beta,\ \gamma,\ Lys}$, $H_{\beta,\ \gamma,\ Arg}$) 1.55-1.37 (m, 8H, $H_{\delta,\ Lys}$) 0.90 (t, *J*=7.0 Hz, 6H, CH_3-Val)

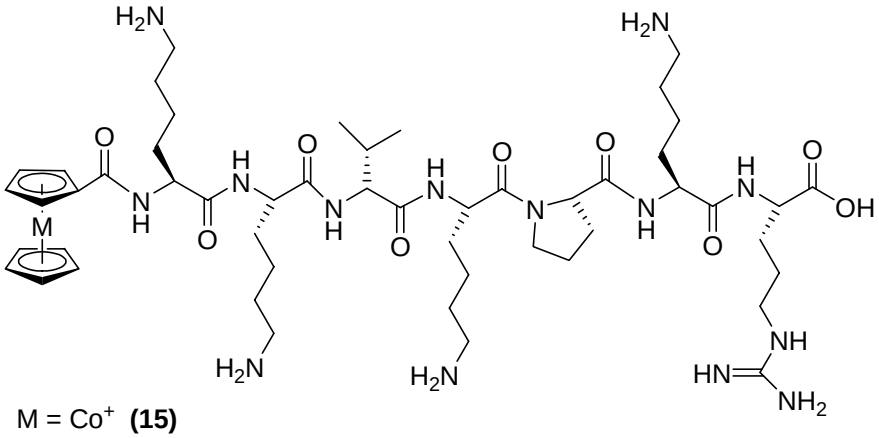

M = Co^+ **(15)**
Fe **(16)**

15: CcC(O)-NLS$_{scr}$

Pale yellow solid, soluble in water and ethanol

$C_{51}H_{86}Co^+N_{14}O_9$ (1097.6 g/mol)

R_t = 7.34 minutes (Analytical HPLC; Method A)

MALDI-TOF : *m/z* 1099 $[M+H]^+$ 1121 $[M+Na]^+$

SWV: $E_{1/2}$ = -1.09 V vs. FcH / FcH^+

^{1}H-NMR (400 MHz, D_2O): δ_H 6.29 (s, 1H, substituted Cp) 6.25 (s, 1H, substituted Cp) 5.89 (s, 2H, substituted Cp) 5.80 (s, 5H, unsubstituted Cp) 4.62-4.57 (m, 1H, $H_{\alpha,Val}$) 4.43-4.36 (m, 5H, H_α) 4.26 (pseudo t, 1H, H_α) 4.13-4.08 (m, 1H, H_α) 3.90-3.84 (m, 1H, $H_{\delta,\ Pro}$) 3.68-3.60 (m, 1H, $H_{\delta,\ Pro}$) 3.20 (pseudo t, 2H, $H_{\delta,\ Arg}$) 3.01-2.95 (m, 8H, $H_{\varepsilon,\ Lys}$) 2.34-2.23 (m, 1H, $H_{\beta,Val}$) 2.03-1.98 (m, 3H, $H_{\beta,\ \gamma\ Pro}$) 1.92-1.63 (m, 21H, $H_{\beta,\ Pro}$, $H_{\beta,\ \gamma,\ Lys}$, $H_{\beta,\ \gamma,\ Arg}$) 1.51-1.38 (m, 8H, $H_{\delta,\ Lys}$) 0.92-0.89 (m, 6H, C*H*$_3$-val)

16: FcC(O)-NLS$_{scr}$

Yellow solid, soluble in water and ethanol

$C_{51}H_{86}FeN_{14}O_9$ (1094.61 g/mol)

R_t = 9.5 minutes (Analytical HPLC; Method A)

MALDI-TOF: *m/z* 1096.5 $[M+2H]^+$ 1117.7 $[M+Na]^+$

SWV: $E_{1/2}$ = 252 mV vs. FcH / FcH^+

^{1}H-NMR (400MHz, CD_3OD): δ_H 4.65-4.60 (pseudo t, 1H, $H_{\alpha,Val}$) 4.55-4.44 (m, 6H, H_α, substituted Cp) 4.40-4.36 (m, 1H, H_α) 4.26 (s, 5H, unsubstituted Cp) 4.20 (d, *J*=7.03 Hz, 1H, H_α) 3.96-3.87 (m, 1H, $H_{\delta,\ Pro}$) 3.74-3.34 (m, 1H, $H_{\delta,\ Pro}$) 3.28-3.19 (m, 2H, $H_{\delta,\ Arg}$) 2.97 (d, *J*=7.0 Hz, 8H, $H_{\varepsilon,\ Lys}$) 2.32-2.23 (m, 1H, $H_{\beta,\ Val}$) 2.16-1.90 (m, 3H, $H_{\beta,\ \gamma,\ Pro}$) 1.80-1.64 (m, 21H, $H_{\beta,\ Pro}$, $H_{\beta,\ \gamma,\ Lys}$, $H_{\beta,\ \gamma,\ Arg}$) 1.63-1.47 (m, 8H, $H_{\delta,\ Lys}$) 0.97 (d, *J*=6.6 Hz, 6H, C*H*$_3$-Val)

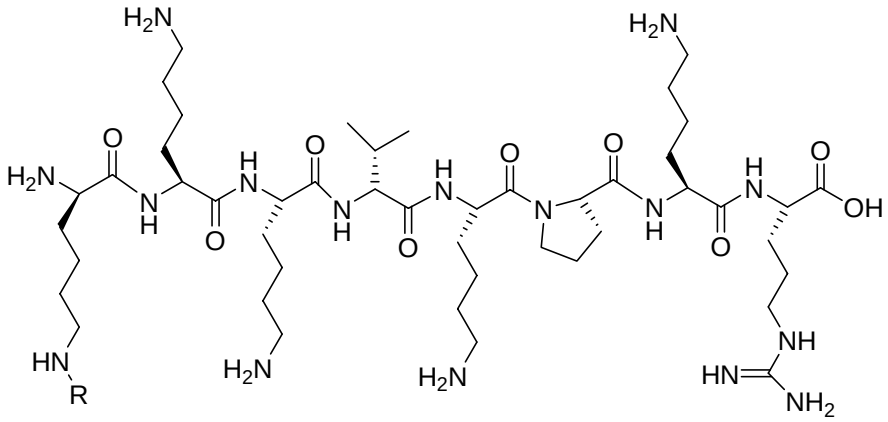

R = H **(17)**
= FITC **(18)**

17: H-Lys-NLS$_{scr}$

White solid, soluble in water and ethanol

$C_{46}H_{90}N_{16}O_9$ (1010.71 g/mol)

R_t = 6.7 minutes (Analytical HPLC, Method A)

MALDI-TOF: *m/z* 1011.8 $[M+H]^+$ 1033.8 $[M+Na]^+$

^{1}H-NMR (300MHz, D_2O): δ_H 4.63-4.56 (m, 1H, $H_{\alpha, Val}$) 4.47-4.41 (m, 1H, $H_{\alpha, Lys}$) 4.37-4.29 (m, 2H, $H_{\alpha, Lys}$) 4.28-4.22 (m, 2H, H_α) 4.14 (d, *J*=7.3 Hz, 1H, H_α) 4.06-3.92 (pseudo t, 1H, H_α) 3.92-3.83 (m, 1H, $H_{\delta, Pro}$) 3.71-3.62 (m, 1H, $H_{\delta, Pro}$) 3.21 (t, *J*=7 Hz, 2H, $H_{\delta, Arg}$) 3.05-2.93 (m, 10H, $H_{\varepsilon, Lys}$) 2.36-2.24 (m, 1H, $H_{\beta, Val}$) 2.08-1.98 (m, 2H, $H_{\beta, \gamma, Pro}$) 1.93-1.58 (m, 26H, $H_{\gamma, \beta, Pro}$, $H_{\beta, \delta, Lys}$, $H_{\beta, \gamma, Arg}$) 1.53-1.33 (m, 10H, $H_{\gamma, Lys}$) 0.92 (dd, *J*=6.2 Hz, 6H, C*H*$_3$-Val)

18: H-Lys(FITC)-NLS$_{scr}$

Bright yellow solid, soluble in water and ethanol

$C_{67}H_{101}N_{17}O_{14}S^+$ (1399.74 g/mol)

R_t = 10.14 minutes (Analytical HPLC; Method A)

MALDI-TOF: *m/z* 1402.2 $[M+2H]^+$, 1424.1 $[M+Na]^+$

^{1}H-NMR (400 MHz, D_2O) δ_H 8.06 (s. 1H, FITC) 7.69 (d, *J*=8.9 Hz, 1H, FITC) 7.42 (pseudo t, 1H, FITC) 7.37-7.27 (m, 1H, FITC) 7.20 (pseudo t, 1H, FITC) 7.01 (s, 2H, FITC) 6.86 (d, *J*=8.9 Hz, 2H, FITC) 4.40-4.25 (m, 7H, H_α) 4.15-4.05 (m, 1H, H_α) 3.90-3.82 (m, 1H, $H_{\delta, Pro}$) 3.70-3.65 (m, 1H, $H_{\delta, Pro}$) 3.58-3.51 (m, 2H, $H_{\delta, Arg}$) 3.05-2.90 (m, 10H, $H_{\varepsilon, Lys}$) 2.35-2.21 (m, 1H, $H_{\beta, Val}$) 1.95-1.86 (m, 3H, $H_{\beta, \gamma, Pro}$) 1.80-1.55 (m, 25H, $H_{\beta, Pro}$, $H_{\beta, \delta, Lys}$, $H_{\beta, \gamma, Arg}$) 1.49-1.31 (m, 10H, $H_{\gamma, Lys}$) 0.91 (d, *J*=6.6 Hz, 6H, C*H*$_3$-Val)

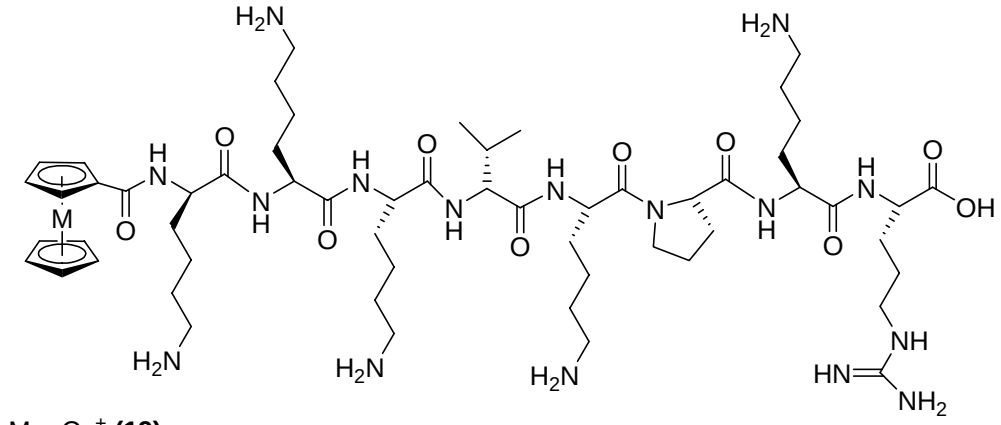

M = Co^+ **(19)**
Fe **(20)**

19: CcC(O)-Lys-NLS$_{scr}$

Pale yellow solid, soluble in water and ethanol

$C_{57}H_{98}Co^+N_{16}O_{10}$ (1225.7 g/mol)

R_t = 7.40 minutes (Analytical HPLC; Method A)

MALDI-TOF: *m/z* 1226.9 $[M+H]^+$ 1248.9 $[M+Na]^+$ 1282.9 $[M+K]^+$

SWV: $E_{1/2}$ = -1.38 V vs. FcH / FcH^+

^{1}H-NMR (400MHz, D_2O) δ_H 6.20 (s, 1H, substituted Cp) 6.18 (s, 1H, substituted Cp) 5.80 (s, 2H, substituted Cp) 5.70 (s, 5H, unsubstituted Cp) 4.51-4.44 (pseudo t, 1H, $H_{\alpha, Val}$) 4.35-4.28 (m, 2H, H_α) 4.26-4.19 (m, 3H, H_α) 4.18-4.13 (m, 1H, H_α) 3.99 (d, *J*=7.8 Hz, 1H, H_α) 3.80-3.78 (m, 1H, $H_{\delta, Pro}$) 3.61-3.58 (m, 1H, $H_{\delta, Pro}$) 3.09 (pseudo t, 2H, $H_{\delta, Arg}$) 2.93-2.83 (m, 10H, $H_{\varepsilon, Lys}$) 2.23-2.18 (m, 1H, $H_{\beta, Val}$) 1.98-1.90 (m, 3H, $H_{\beta, \gamma, Pro}$) 1.70-1.45 (m, 25 H, $H_{\beta, Pro}$ $H_{\beta, \gamma, Lys}$, $H_{\beta, \gamma, Arg}$) 1.38-1.18 (m, 10H, $H_{\gamma, Lys}$) 0.93 (d, *J*=7 Hz, 6H, C*H*$_3$-Val)

20: FcC(O)-Lys-NLS$_{scr}$

Yellow solid, soluble in water and ethanol

$C_{57}H_{98}FeN_{16}O_{10}$ (1222.7 g/mol)

R_t = 9.11 minutes (Analytical HPLC; Method A)

MALDI-TOF: *m/z* 1224.1 $[M+2H]^+$ 1246.6 $[M+Na]^+$

SWV: $E_{1/2}$ = 279 mV vs. FcH / FcH^+

^{1}H-NMR (300 MHz, D_2O): δ_H 4.53-4.60 (m, 2H, H_α) 4.34-4.38 (m, 2H, H_α) 4.17-4.30 (m, 7H, $H_{\alpha,}$ unsubstituted Cp) 4.05 (d, *J*=7.7 Hz, 2H, H_α) 3.87-3.76 (m, 1H, $H_{\delta, Pro}$) 3.64-3.55 (m, 1H, $H_{\delta, Pro}$) 3.15 (t, *J*=6.7 Hz, 2H, $H_{\delta, Arg}$) 3.00-2.80 (m, 10H, $H_{\varepsilon, Lys}$) 2.30-2.20 (m, 1H, $H_{\beta, Val}$) 2.08-1.92 (m, 4H, $H_{\beta, \gamma, Pro}$) 1.90-1.52 (m, 24 H, $H_{\beta, \delta, Lys}$, $H_{\beta, \gamma, Arg}$) 1.50-1.30 (m, 10H, $H_{\gamma, Lys}$) 0.91 (d, *J*=6.2 Hz, 6H, C*H*$_3$-Val)

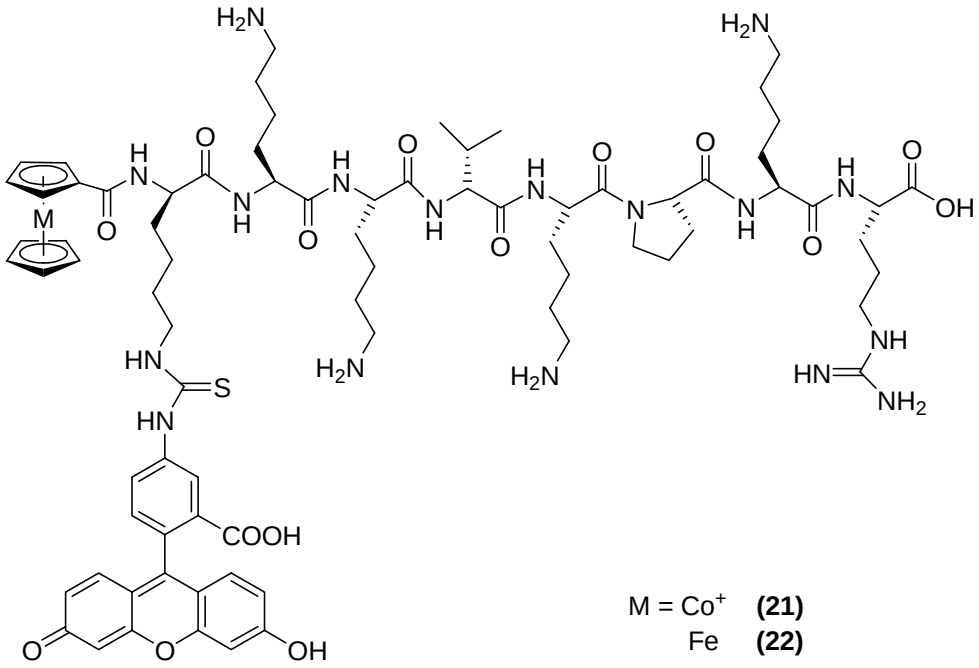

21: CcC(O)-Lys(FITC)-NLS$_{scr}$

Bright yellow solid, soluble in water and ethanol

$C_{78}H_{109}Co^{+}N_{17}O_{15}S$ (1614.73 g/mol)

R_t = 10.71 minutes (Analytical HPLC; Method A)

MALDI-TOF: *m/z* 1615.9 $[M+H]^+$ 1637.8 $[M+Na]^+$

SWV: $E_{1/2}$ = -1.35 mV vs. FcH / FcH^+

^{1}H-NMR (300MHz, D_2O): δ_H 7.93 (s, 1H, FITC) 7.60-7.53 (d, *J*=8.1, 1H, FITC) 7.32 (d, *J*=8 Hz,1H, FITC) 7.22-7.16 (m, 2H, FITC) 6.95 (s, 2H, FITC) 6.80 (dd, *J*=8.4 Hz, 2H, FITC) 6.20-6.15 (m, 2H, substituted Cp) 5.79 (pseudo t, 2H, substituted Cp) 5.72 (s, 5H, unsubstituted Cp) 4.50-4.00 (m, 7H, H_α) 3.80-3.37 (m, 2H, $H_{\delta,\ Pro}$) 3.15-3.04 (pseudo t, 2H, $H_{\delta,\ Arg}$) 3.00-2.89 (m, 10H, $H_{\varepsilon,\ Lys}$) 2.00-1.85 (m, 9H, $H_{\beta,\ \gamma,\ Pro}$, $H_{\beta,\ Val}$, $H_{\beta,\ \gamma,\ Arg}$) 1.84-1.56 (m, 20H, $H_{\beta,\ \delta\ ,\ Lys}$) 1.50-1.38 (m, 10H, $H_{\gamma,\ Lys}$) 0.85 (d, *J*=6.9 Hz, 6H, C*H*$_3$-Val)

22: FcC(O)-Lys(FITC)-NLS$_{scr}$

Bright orange solid, soluble in water and ethanol

$C_{78}H_{109}FeN_{17}O_{15}S$ (1611.74 g/mol)

R_t = 12.01 minutes (Analytical HPLC; Method A)

MALDI-TOF: *m/z* 1614.0 $[M+2H]^+$ 1637.2 $[M+H]^+$

SWV: $E_{1/2}$ = 279 mV vs. FcH / FcH^+

^{1}H-NMR (400 MHz, CD_3OD): δ_H 8.29 (s, 1H, FITC) 7.70 (d, *J*=8.2 Hz, 1H, FITC) 7.39-7.30 (m, 1H, FITC) 7.17 (d, *J*=8.2 Hz, 1H, FITC) 6.75-6.66 (m, 3H, FITC) 6.57 (dd, *J*=6.4 Hz, 2H, FITC) 4.62 (pseudo t, 1H, H_α,val) 4.50-4.34 (m, 10H, substituted Cp, H_α) 4.24 (s, 5H, unsubstituted Cp) 4.20 (d, *J*=7.4 Hz, 1H, H_α) 3.95-3.85 (m, 1H, $H_{\delta,\ Pro}$) 3.71-3.65 (m, 1H, $H_{\delta,\ Pro}$) 3.27-3.19 (m, 2H, $H_{\delta,\ Arg}$) 2.98 (broad s, 10H, $H_{\varepsilon,\ Lys}$) 2.32-2.21 (m, 1H, $H_{\beta,\ Val}$) 2.11-1.94 (m, 3H, $H_{\beta,\ \gamma,\ Pro}$) 1.85-1.65 (m, 25H, $H_{\beta,\ Pro}$, $H_{\beta,\ \delta,\ Lys}$, $H_{\beta,\ \gamma,\ Arg}$) 1.62-1.45 (m, 10H, $H_{\gamma,\ Lys}$) 0.98 (dd, *J*=6.2 Hz, 6H, C*H*$_3$-Val)

2.1.2.3 TAT (48-57) bioconjugates

Solid Phase Peptide Synthesis

All TAT bioconjugates were synthesized using the routine method of SPPS described in section 2.1.2.1. Wang resin preloaded with Fmoc-Arg(Pbf)-OH (0.35 mmol/g) was used. The synthesized TAT(48-57) peptide has a sequence of GRKKRRQRRR. Another Lysine was added at the *N*-terminal as a carrier of fluorescent label on its side chain. Cobaltocenium and ferrocene carboxylc acids were used as metal labels.

After the steps of synthesis, shrinking and cleavage from the resin, the crude products obtained in quantitative yields were dried and lyophilized. Purification was achieved by preparative HPLC.

Analytical data

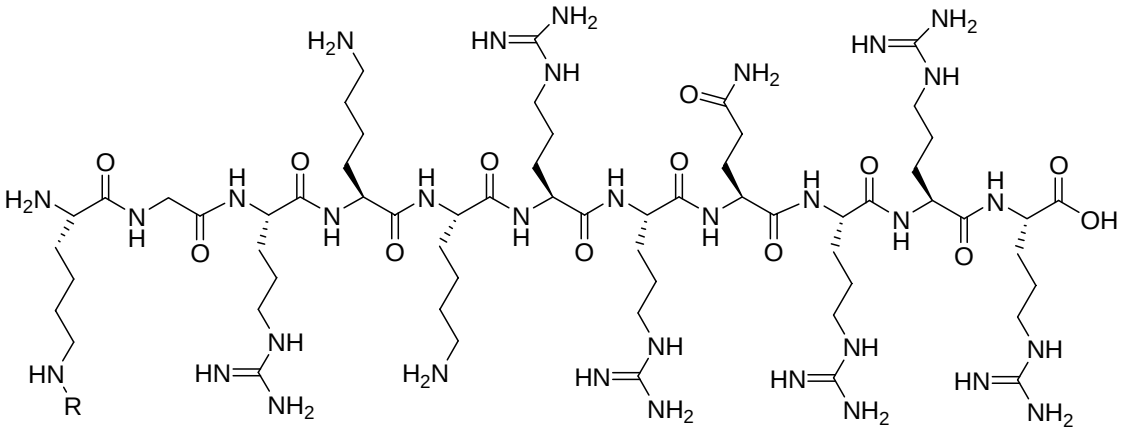

R = H (**23**)
= FITC (**24**)

23: H-K-TAT

White solid, soluble in water and ethanol

$C_{61}H_{121}N_{33}O_{13}$ (1523.98 g/mol)

R_t = 7.73 minutes (Analytical HPLC; Method A)

MALDI-TOF: *m/z* 1525.6 $[M+H]^+$

^{1}H-NMR (D_2O): δ_H 4.34-4.24 (m, 9H, H_α) 4.09 (pseudo t, 1H, $H_{\alpha,\ Arg}$) 4.02 (d, *J*=7.4 Hz, 2H, $H_{\alpha,\ Gly}$) 3.20-3.14 (m, 12H, $H_{\delta,\ Arg}$) 3.03-2.96 (m, 6H, $H_{\varepsilon,\ Lys}$) 2.35 (pseudo t, 2H, $H_{\gamma,\ Gln}$) 2.10-2.03 (m, 2H, $H_{\beta,\ Gln}$) 1.98-1.70 (m, 18H, $H_{\beta,\ Lys}$, $H_{\beta,\ Arg}$) 1.71-1.55 (m, 18 H, $H_{\delta,\ Lys}$, $H_{\gamma,\ Arg}$) 1.51-1.33 (m, 6H, $H_{\gamma,\ Lys}$)

24: H-K(FITC)-TAT

Bright dark yellow solid, soluble in water and ethanol

$C_{82}H_{132}N_{34}O_{18}S$ (1913.02 g/mol)

R_t =10.36 minutes (Analytical HPLC; Method A)

ESI (pos.): *m/z* 383.9 $[M+5H]^{5+}$ 704.6 $[M+TFA+2Na+K+H]^{3+}$

^{1}H-NMR (D_2O): δ_H 8.06 (s, 1H, FITC) 7.66 (broad d, *J*=8.2 Hz, 2H, FITC) 7.22 (d, *J*=7.8 Hz, 2H, FITC) 7.02 (s, 2H, FITC) 6.86 (d, *J*=8.2 Hz, 2H, FITC) 4.26-4.10 (m, 9H, $H_{\alpha)}$ 4.04-3.90 (m, 3H, $H_{\alpha,\ Arg}$, $H_{\alpha,\ Gly}$) 3.10-2.98 (m, 12H, $H_{\delta,\ Arg}$) 2.90- 2.82 (m, 6H, $H_{\varepsilon,\ Lys}$) 2.23 (pseudo t, 2H, $H_{\gamma,\ Gln}$) 1.90-1.80 (m, 2H, $H_{\beta,\ Gln}$) 1.75-1.60 (m, 18H, $H_{\beta,\ Lys}$, $H_{\beta,\ Arg}$) 1.55-1.40 (m, 18 H, $H_{\delta,\ Lys}$, $H_{\gamma,\ Arg}$) 1.33-1.23 (m, 6H, $H_{\gamma,\ Lys}$)

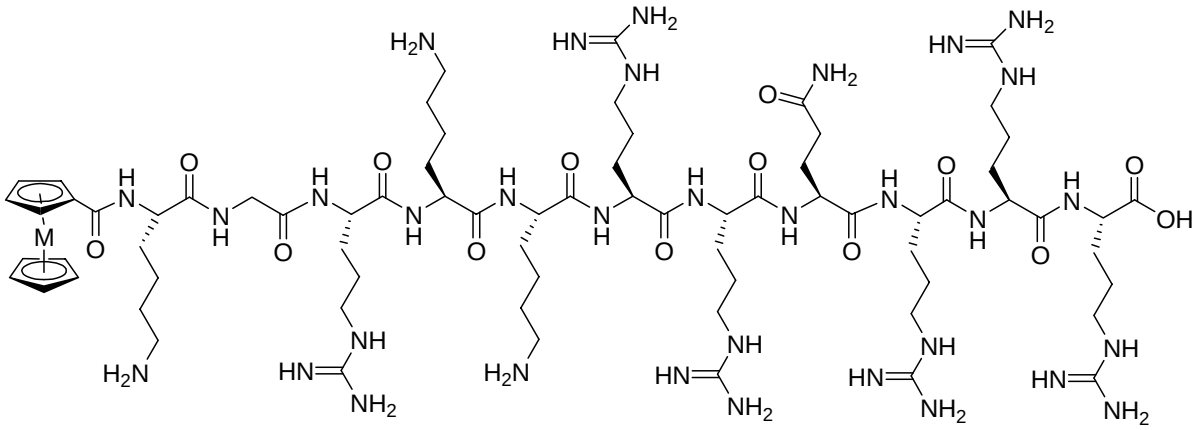

M = Co^+ (**25**)
Fe (**26**)

25: CcC(O)-K-TAT

Light yellow solid, soluble in water and ethanol

$C_{72}H_{129}Co^+N_{33}O_{14}$ (1738.97 g/mol)

R_t =7.26 minutes (Analytical HPLC; Method A)

MALDI-TOF: *m/z* 1740.2 $[M+H]^+$

SWV: $E_{1/2}$ = -1.32 V vs. FcH / FcH^+

^{1}H-NMR (D_2O): δ_H 6.30 (broad s, 2H, substituted Cp) 5.90 (pseudo t, 2H, substituted Cp) 5.81 (s, 5H, unsubstituted Cp) 4.49 (pseudo t, 1H, H_α) 4.34-4.25 (m, 9H, H_α) 4.02 (broad d, *J*=7.2 Hz, 2H, $H_{\alpha,\ Gly}$) 3.23-3.13 (m, 12H, $H_{\delta,\ Arg}$) 3.03-2.95 (m, 6H, $H_{\varepsilon,\ Lys}$) 2.35 (pseudo t, 2H, $H_{\gamma,\ Gln}$) 1.96-1.90 (m, 2H, $H_{\beta,\ Gln}$) 1.85-1.72 (m, 18H, $H_{\beta,\ Lys}$, $H_{\beta,\ Arg}$) 1.70-1.58 (m, 18 H, $H_{\delta,\ Lys}$, $H_{\gamma,\ Arg}$) 1.48- 1.38 (m, 6H, $H_{\gamma,\ Lys}$)

26: FcC(O)-K-TAT

Yellow solid, soluble in water and ethanol

$C_{72}H_{129}FeN_{33}O_{14}$ (1735.97 g/mol)

R_t = 9.24 minutes (Analytical HPLC; Method A)

MALDI-TOF: *m/z* 1736.8 $[M+H]^+$

SWV: $E_{1/2}$ = 199 mV vs. FcH / FcH^+

^{1}H-NMR (D_2O): δ_H 4.38 (pseudo t, 2H, substituted Cp) 4.26-4.21 (m, 9H, substituted Cp, H_α) 4.15 (s, 5H, unsubstituted Cp) 4.12-4.05 (m, 3H, $H_{\alpha,\ Gly}$, $H_{\alpha,\ Lys}$) 3.15-3.07 (m, 12H, $H_{\delta,\ Arg}$) 2.91-2.81 (m, 6H, $H_{\varepsilon,\ Lys}$) 2.36-2.25 (m, 2H, $H_{\gamma,\ Gln}$) 2.06-1.97 (m, 2H, $H_{\beta,\ Gln}$) 1.90-1.75 (m, 18H, $H_{\beta,\ Lys}$, $H_{\beta,\ Arg}$) 1.71-1.54 (m, 18 H, $H_{\delta,\ Lys}$, $H_{\gamma,\ Arg}$) 1.49-1.42 (m, 6H, $H_{\gamma,\ Lys}$)

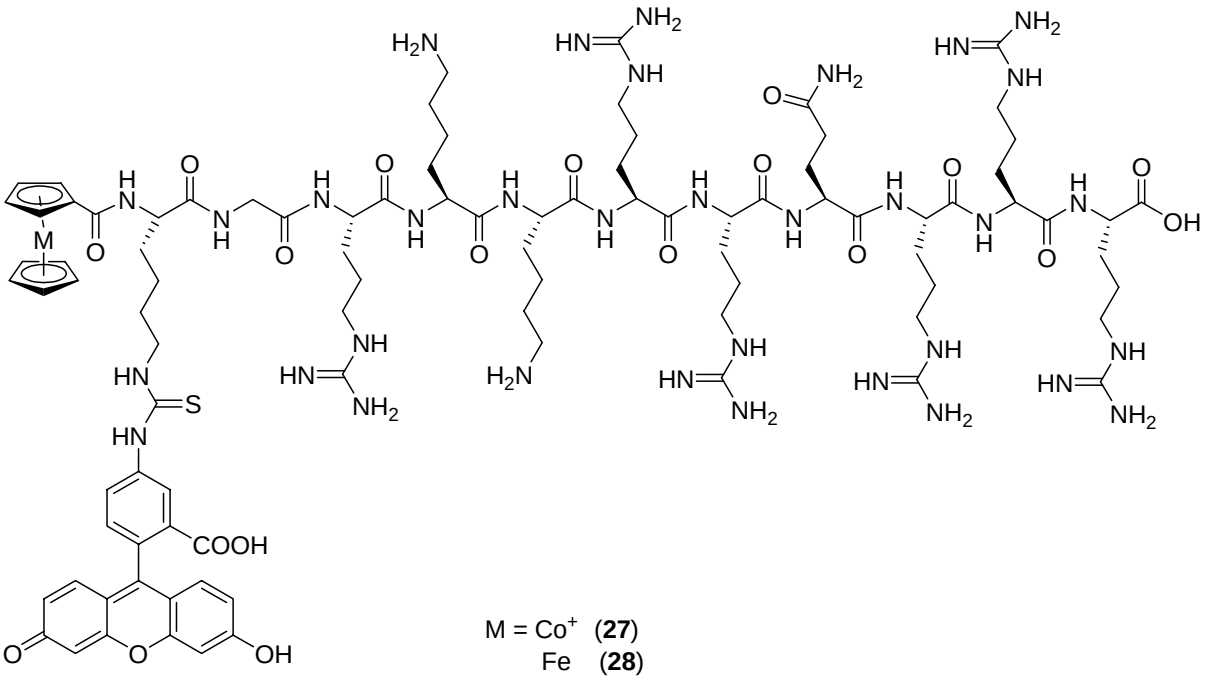

27: CcC(O)-K(FITC)-TAT

Bright orange yellow solid, soluble in water and ethanol

$C_{93}H_{140}Co^{+}N_{34}O_{19}S$ (2128.01 g/mol)

R_t = 10.74 minutes (Analytical HPLC; Method A)

MALDI-TOF: *m/z* 582.1 $[M+2Na+K+TFA]^{4+}$ 557.6 $[M+H+Na+2K]^{4+}$ 426.7 $[M+5H]^{5+}$ 355.8 $[M+6H]^{6+}$

SWV: $E_{1/2}$ = -1.38 V vs. FcH / FcH^{+}

^{1}H-NMR (D_2O): δ_H 8.12 (s, 1H, FITC) 7.90-7.88 (m, 2H, FITC) 7.24-7.21 (m, 1H, FITC) 7.19-7.12 (m, 1H, FITC) 6.93 (s, 2H, FITC) 6.77 (d, *J*=8.4 Hz, 2H, FITC) 6.17 (pseudo t, 2H, substituted Cp) 5.76 (pseudo t, 2H, substituted Cp) 5.69 (s, 5H, unsubstituted Cp) 4.23-4.10 (m, 10H, $H_{\alpha)}$ 3.90-3.85 (m, 2H, $H_{\alpha,\ Gly}$) 3.11-2.97 (m, 12H, $H_{\delta,\ Arg}$) 2.89-2.81 (m, 6H, $H_{\varepsilon,\ Lys}$) 2.21 (pseudo t, 2H, $H_{\gamma,\ Gln}$) 1.94-1.83 (m, 2H, $H_{\beta,\ Gln}$) 1.73-1.58 (m, 18H, $H_{\beta,\ Lys}$, $H_{\beta,\ Arg}$) 1.55-1.40 (m, 18 H, $H_{\delta,\ Lys}$, $H_{\gamma,\ Arg}$) 1.34-1.17 (m, 6H, $H_{\gamma,\ Lys}$)

28: FcC(O)-K(FITC)-TAT

Bright orange yellow solid, soluble in water and ethanol

$C_{93}H_{140}FeN_{34}O_{19}S$ (2125.01 g/mol)

R_t = 12.15 minutes (Analytical HPLC; Method A)

ESI (pos): *m/z* 532.6 $[M+4H]^{4+}$ 709.9 $[M+3H]^{3+}$

SWV: $E_{1/2}$ = 237 mV vs. FcH / FcH^+

^{1}H-NMR (D_2O): δ_H 8.16 (s, 1H, FITC) 7.66 (dd, *J*=8.2 Hz, 2H, FITC) 7.29-7.18 (m, 1H, FITC) 7.11-7.03 (m, 1H, FITC) 6.61 (s, 2H, FITC) 6.46 (d, *J*=7.03 Hz, 2H, FITC) 4.37-4.22 (m, 12H, substituted Cp, H_{α}) 4.13 (s, 5H, unsubstituted Cp) 4.10-4.07 (m, 2H, $H_{\alpha, Gly}$) 3.16-3.05 (m, 12H, $H_{\delta, Arg}$) 2.90-2.83 (m, 6H, $H_{\varepsilon, Lys}$) 2.40-2.22 (m, 2H, $H_{\gamma, Gln}$) 2.07-1.99 (m, 2H, $H_{\beta, Gln}$) 1.91-1.72 (m, 18H, $H_{\beta, Lys}$, $H_{\beta, Arg}$) 1.70-1.52 (m, 18 H, $H_{\delta, Lys}$, $H_{\gamma, Arg}$) 1.40-1.32 (m, 6H, $H_{\gamma, Lys}$)

2.1.2.4 NT(8-13) bioconjugates

Solid Phase Peptide Synthesis

All NT bioconjugates were snythesized using standard SPPS methods with Fmoc strategy. Wang resin preloaded with Fmoc-Ileu-OH (0.67 mmol/g) was used. The resin was swelled in DMF for 1 h. Fmoc groups were cleaved using 20% piperidine in DMF for 10 minutes. 3 eq. of Fmoc-protected amino acids along with 3 eq. TBTU and HOBt as coupling reagents and 8 eq. of DIPEA were used to synthesize the NT(8-13) with sequence (RRPWIL) or pseudo-NT (KKPWIL) part of the bioconjugates.

The terminal amino group was used to carry the metallocene moiety, coupled using the standard method on solid phase (using 3 eq. cobaltocenium or ferrocene carboxylic acid, 3 eq of TBTU and 3 eq. of HOBt and 8 eq. of DIPEA).

For Pt-bioconjugates, aminoethylglycine (BB) and diaminopropionic acid (DAP) were used as ligands for platination. The complexation was carried out with 6 eq. of K_2PtCl_4 in a 1:9 H_2O/DMF mixture for 3 days. Upon successful complexation of the metal complex to the peptide, the resin changed colour from off white to brown or biege.

At the end of the synthesis, the bioconjugates were washed repeatedly with DMF, CH_2Cl_2 and shrinked with MeOH. The resin was thoroughly dried over KOH under vaccum overnight prior to cleavage of the bioconjugate. Cleavage from the resin was achieved with 95 % TFA, 2.5 % TIS and 2.5 % H_2O for 3 h in case of cobaltocenium and non-metal bioconjugates. In case of ferrocene containing bioconjugates 10% phenol was added in a TFA/TIS mixture. Whereas, for Pt-bioconjugates, the cleavage mixture consisted of 95% TFA with 5% H_2O. After filtration, the bioconjugates were precipitated from the filtrate upon addition of cold diethylether (-20°C). The crude products in quantitative yields were dried and lyophilized. Purification was carried out by preparative HPLC.

Analytical data

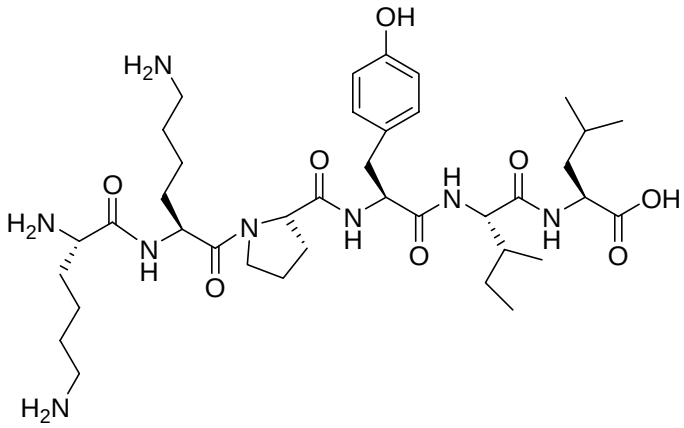

29: pNT(8-13, Lys^{8}-Lys^{9})

White solid, soluble in water and ethanol

$C_{38}H_{64}N_8O_8$ (760.48g/mol)

R_t = 10.68 minutes (Analytical HPLC; Method A)

MALDI-TOF: *m/z* 761.4 $[M+H]^+$ 799.3 $[M+K]^+$

^{1}H-NMR (300 MHz, D_2O) δ_H 7.05 (d, *J*=7.7 Hz, 2H, $H_{\textit{ortho}, Tyr}$) 6.75 (d, *J*=8.2 Hz, 2H, $H_{\textit{meta}, Tyr}$) 4.60-4.50 (m, 2H, $H_{\alpha, Ile}$, $H_{\alpha, Lys}$) 4.36-4.31 (m,1H, $H_{\alpha, Leu}$) 4.42-4.21 (m, 1H, $H_{\alpha, Pro}$) 4.07-4.04 (m, 1H, $H_{\alpha, Lys}$) 3.98-3.73 (m, 1H, $H_{\delta, Pro}$) 3.61-3.56 (m, 1H, $H_{\delta, Pro}$) 2.96-2.91 (m, 7H, $H_{\beta, Tyr}$, $H_{\varepsilon, Lys}$, $H_{\beta, Pro}$) 2.22-2.15 (m, 1H, $H_{\beta, Tyr}$) 1.99-1.92 (m, 2H, $H_{\beta, Ile}$, $H_{\gamma, Leu}$) 1.87-1.74 (m, 3H, $H_{\beta, Leu}$, $H_{\beta, Pro}$) 1.70-1.51 (m, 11H, $H_{\beta, \delta, Lys}$, $H_{\gamma, Pro}$, $H_{\gamma, Ile}$) 1.46-1.28 (m, 4H, $H_{\gamma, Lys}$) 1.12-0.98 (m, 1H, $H_{\gamma, Pro}$) 0.88-0.76 (m, 12H, CH_3-Leu, CH_3-Ile)

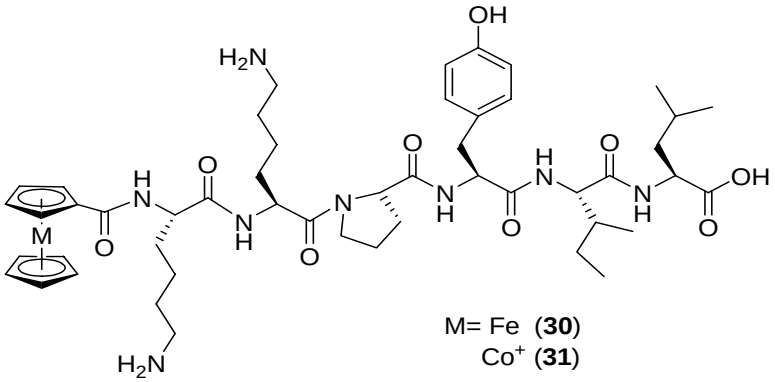

30: FcC(O)-pNT

Light yellow solid, soluble in water and ethanol

$C_{49}H_{72}FeN_8O_9$ (972.48 g/mol)

R_t = 12.8 minutes (Analytical HPLC; Method A)

MALDI-TOF: *m/z* 973.4 $[M+H]^+$ 995.4 $[M+Na]^+$ 1012.4 $[M+K]^+$

SWV: $E_{1/2}$ = 218 mV vs. FcH / FcH^+

^{1}H-NMR (300 MHz, D_2O): δ_H 7.05 (d, *J*=8.3 Hz, 2H, $H_{\textbf{\textit{ortho}},\ Tyr}$) 6.76 (d, *J*=8.2 Hz, 2H, $H_{\textbf{\textit{meta}},\ Tyr}$) 4.59-4.53 (m, 1H, $H_{\alpha,\ Tyr}$) 4.50 (s, 2H, substituted Cp) 4.41 (pseudo t,1H, $H_{\alpha,\ Leu}$) 4.33-4.28 (m, 1H, $H_{\alpha,\ Pro}$) 4.22 (s, 5H, unsubstituted Cp) 4.19-4.12 (m, 2H, $H_{\alpha,\ Ile}$, $H_{\alpha,\ Lys}$) 4.06 (d, *J*=8 Hz, 1H, $H_{\alpha,\ Lys}$) 3.80-3.74 (m, 1H, $H_{\delta,\ Pro}$) 3.62-3.52 (m, 1H, $H_{\delta,\ Pro}$) 2.99-2.88 (m, 7H, $H_{\beta,\ Tyr}$, $H_{\varepsilon,\ Lys}$, $H_{\beta,\ Pro}$) 2.22-2.10 (m, 1H, $H_{\beta,\ Tyr}$) 1.98-1.88 (m, 2H, $H_{\beta,\ Ile}$, $H_{\gamma,\ Leu}$) 1.81-1.50 (m, 13H, $H_{\beta,\ \delta,\ Lys}$, $H_{\gamma,\ Ile}$, $H_{\gamma,\ \beta,\ Pro}$, $H_{\beta,\ Leu}$) 1.48-1.27 (m, 4H, $H_{\gamma,\ Lys}$) 1.10-0.99 (m, 1H, $H_{\gamma,\ Pro}$) 0.89-0.71 (m, 12H, CH_3-Leu, CH_3-Ile)

31 :CcC(O)-pNT

Light yellow solid, soluble in water and ethanol

$C_{49}H_{72}Co^+N_8O_9$ (975.48 g/mol)

R_t = 11.33 minutes (Analytical HPLC; Method A)

MALDI-TOF: *m/z* 975.9 $[M]^+$ 998.9 $[M+Na]^+$

SWV: $E_{1/2}$ = -1.15 V vs. FcH / FcH^+

^{1}H-NMR (D_2O) δ_H 7.05 (d, *J*=8.2 Hz, 2H, $H_{\textbf{\textit{ortho}},\ Tyr}$) 6.76 (d, *J*=8.2 Hz, 2H, $H_{\textbf{\textit{meta}},\ Tyr}$) 6.23 (s, 1H, substituted Cp) 6.18 (s, 1H, substituted Cp) 5.84 (s, 2H, substituted Cp) 5.74 (s, 5H, unsubstituted Cp) 4.61-4.50 (m, 1H, $H_{\alpha,\ Ile}$) 4.4-4.31 (m,2H, $H_{\alpha,\ Lys}$, $H_{\alpha,\ Leu}$) 4.28-4.20 (m, 1H, $H_{\alpha,\ Pro}$) 4.10-4.02 (m, 1H, $H_{\alpha,\ Lys}$) 3.83-3.75 (m, 1H, $H_{\delta,\ Pro}$) 3.65-3.56 (m, 1H, $H_{\delta,\ Pro}$) 3.01-2.88 (m, 7H, $H_{\beta,\ Tyr}$, $H_{\varepsilon,\ Lys}$, $H_{\beta,\ Pro}$) 2.25-2.15 (m, 1H, $H_{\beta,\ Tyr}$) 2.01-1.90 (m, 2H, $H_{\beta,\ Ile}$, $H_{\gamma,\ Leu}$) 1.85-1.50 (m, 14H, $H_{\beta,\ Leu}$, $H_{\beta,\ Pro}$, $H_{\beta,\ \delta,\ Lys}$, $H_{\gamma,\ Pro}$, $H_{\gamma,\ Ile}$) 1.49-1.34 (m, 4H, $H_{\gamma,\ Lys}$) 1.10-1.01 (m, 1H, $H_{\gamma,\ Pro}$) 0.90-0.72 (m, 12H, CH_3-Leu, CH_3-Ile)

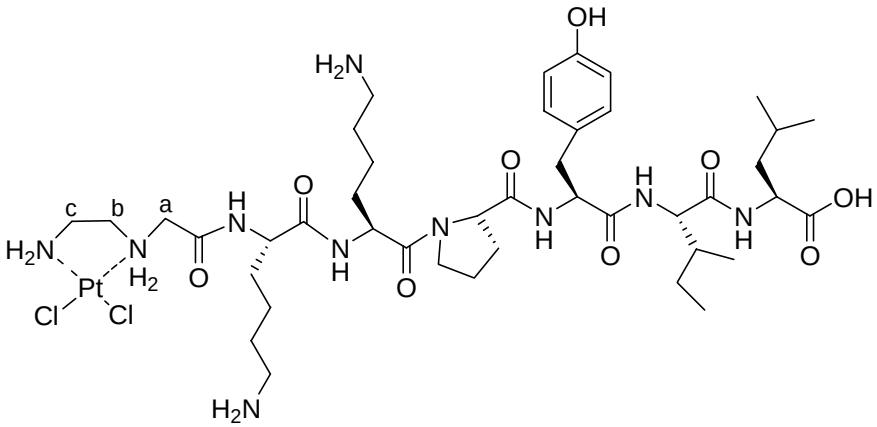

32: Pt(II)-BB-pNT

Dull yellow solid, soluble in water and ethanol

$C_{42}H_{72}Cl_2N_{10}O_9Pt$ (1125.45 g/mol)

R_t = 11.3 minutes (Analytical HPLC; Method A)

MALDI-TOF: *m/z* 1128.0 $[M+2H]^+$ 1150.0 $[M+H+Na]^+$ 1165.9 $[M+K]^+$

^{195}Pt-NMR (D_2O) : δ -1774 (Ref. H_2PtCl_6 in D_2O)

^{1}H-NMR (500 MHz, D_2O) δ_H 7.12 (d, *J*=8 Hz, 2H, $H_{\textit{ortho}, Tyr}$) 6.84 (d, *J*= 8 Hz, 2H, $H_{\textit{meta}, Tyr}$) 4.60-4.59 (m, 2H, $H_{\alpha, Ile}$, $H_{\alpha, Lys}$) 4.43-4.38 (m,1H, $H_{\alpha, Tyr}$) 4.34-4.28 (m, 2H, $H_{\alpha, Pro}$, $H_{\alpha, Leu}$) 4.16-4.11 (m, 1H, $H_{\alpha, Lys}$) 3.82-3.78 (m, 2H, $H_{\delta, Pro}$) 3.69-3.60 (m, 2H, $H_{a, BB}$) 3.04-2.97 (m, 6H, $H_{\beta, Tyr}$, $H_{\varepsilon, Lys}$, $H_{\beta, Ile}$) 2.90-2.85 (m, 1H, $H_{\beta, Tyr}$) 2.70-2.60 (m, 2H, $H_{b, BB}$) 2.03-2.24 (m, 1H, $H_{\beta, Tyr}$) 2.09-1.99 (m, 2H, $H_{c, BB}$) 1.90-1.75 (m, 4H, $H_{\beta, Lys}$) 1.77-1.65 (m, 10H, $H_{\delta, Lys}$, $H_{\beta, Pro}$, $H_{\beta, Ile}$, $H_{\beta, \gamma, Leu}$) 1.52-1.40 (m, 6H, $H_{\gamma, Lys}$, $H_{\gamma, Ile}$) 1.96-1.06 (m, 2H, $H_{\gamma, Pro}$) 0.96 (d, *J*=6 Hz, 3H, CH_3-Leu) 0.92-0.83 (m, 9H, CH_3-Leu, CH_3-Ile)

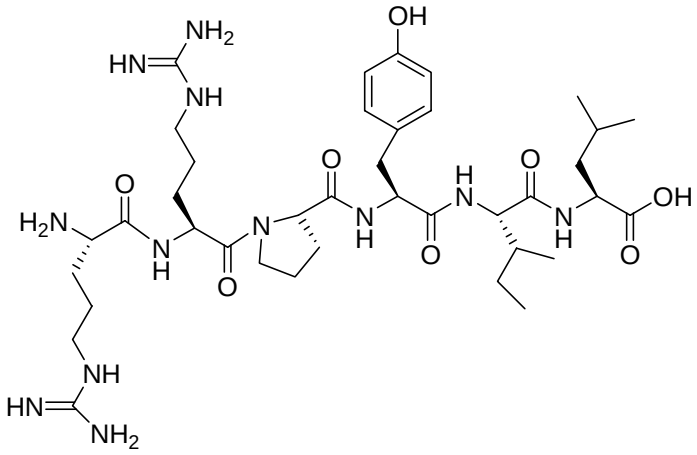

33: NT (8-13)

White solid, partially soluble in water and methanol, soluble in DMSO

$C_{38}H_{64}N_{12}O_8$ (816.99 g/mol)

R_t = 15.8 minutes (Analytical HPLC; Method B)

MALDI-TOF: *m/z* 817.4 $[M+H]^+$ 839.4 $[M+Na]^+$

^{1}H-NMR (300 MHz, CD_3OD): δ_H 7.03 (d, *J*=7.8 Hz, 2H, $H_{\textbf{\textit{ortho}},\ Tyr}$) 6.68 (d, *J*=7.6 Hz, 2H, $H_{\textbf{\textit{meta}},\ Tyr}$) 4.60-4.50 (m, 2H, $H_{\alpha,\ Ile}$, $H_{\alpha,\ Arg}$) 4.49-4.40 (m,2H, $H_{\alpha,\ Leu}$, $H_{\alpha,\ Pro}$) 4.30-4.26 (m, 1H, $H_{\alpha,\ Arg\ terminal}$) 3.83-3.79 (m, 1H, $H_{\delta,\ Pro}$) 3.71-3.62 (m, 1H, $H_{\delta,\ Pro}$) 3.28-3.14 (m, 4H, $H_{\delta,\ Arg}$) 3.10-3.00 (m, 1H, $H_{\beta,\ Tyr}$) 2.90-2.80 (m, 1H, $H_{\beta,\ Tyr}$) 2.21-2.10 (m, 1H, $H_{\beta,\ Pro}$) 1.52-1.42 (m, 2H, $H_{\gamma,\ Ile}$) 2.08-1.56 (m, 15H, $H_{\beta,\ \gamma,\ Arg}$, $H_{\beta,\ Pro}$, $H_{\beta,\ \gamma,\ Leu}$, $H_{\beta,\ Ile}$) 1.58-1.33 (m, 4H, $H_{\gamma,\ Arg}$) 0.88-0.76 (m, 12H, C*H*$_3$-Leu, C*H*$_3$-Ile)

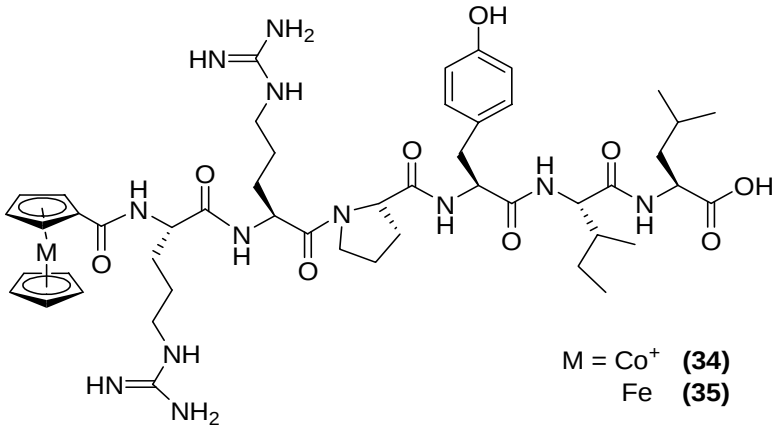

M = Co^+ **(34)**
Fe **(35)**

34: CcC(O)-NT

Yellow solid, soluble in water and ethanol

$C_{49}H_{72}Co^+N_{12}O_9$ (1031.49 g/mol)

R_t = 11.4 minutes (Analytical HPLC; Method A)

MALDI-TOF: *m/z* 1031.2 $[M]^+$ 1070.1 $[M+Na]^+$

SWV: $E_{1/2}$ = -1.31 V vs. FcH / FcH^+

^{1}H-NMR (300 MHz, D_2O): δ_H 7.05 (d, *J*=8.0 Hz, 2H, $H_{\textbf{\textit{ortho}}, Tyr}$) 6.75 (d, *J*=7.8 Hz, 2H, $H_{\textbf{\textit{meta}}, Tyr}$) 6.23 (s, 1H, substituted Cp) 6.18 (s, 1H, substituted Cp) 5.84 (s, 2H, substituted Cp) 5.73 (s, 5H, unsubstituted Cp) 4.54-4.49 (m, 1H, $H_{\alpha, Arg}$) 4.41-4.36 (m, 1H, $H_{\alpha, Ile}$) 4.33-4.28 (m,1H, $H_{\alpha, Leu}$) 4.20-4.18 (m, 1H, $H_{\alpha, Pro}$) 4.05 (d, *J*=8.5 Hz, 1H, $H_{\alpha, Arg}$) 3.80-3.74 (m, 1H, $H_{\delta, Pro}$) 3.65-3.58 (m, 1H, $H_{\delta, Pro}$) 3.22-3.12 (m, 5H, $H_{\delta, Arg}$, $H_{\beta, Ile}$) 3.00-2.88 (m, 2H, $H_{\beta, Tyr}$) 2.22-2.10 (m, 1H, $H_{\beta, Pro}$) 1.80-1.50 (m, 12H, $H_{\beta, \gamma, Arg}$, $H_{\gamma, \beta, Pro}$, $H_{\gamma, Leu}$) 1.58-1.48 (m, 2H, $H_{\beta, Leu}$) 1.29-1.24 (m, 2H, $H_{\gamma, Ile}$) 0.86-0.79 (m, 12H, CH_3-Leu, CH_3-Ile)

35: FcC(O)-NT

Yellow solid, soluble in water and ethanol

$C_{49}H_{72}FeN_{12}O_9$ (1028.02 g/mol)

R_t = 13.18 minutes (Analytical HPLC; Method A)

MALDI-TOF: *m/z* 1029.3 $[M+H]^+$ 1067.2 $[M+K]^+$

SWV: $E_{1/2}$ = 214 mV vs. FcH / FcH^+

^{1}H-NMR (400 MHz, CD_3OD): δ_H 7.08 (d, *J*=8.2 Hz, 2H, $H_{\textbf{\textit{ortho}}, Tyr}$) 6.72 (d, *J*=8.2 Hz, 2H, $H_{\textbf{\textit{meta}}, Tyr}$) 4.54-4.58 (m, 1H, $H_{\alpha, Tyr}$) 4.47 (s, 2H, substituted Cp) 4.45-4.42 (m,2H, $H_{\alpha, Leu}$, $H_{\alpha, Pro}$) 4.29-4.24 (m, 8H, unsubstituted Cp, $H_{\alpha, Ile}$, $H_{\alpha, Lys}$, $H_{\alpha, Lys}$) 3.86-3.78 (m, 1H, $H_{\delta, Pro}$) 3.70-3.60 (m, 1H, $H_{\delta, Pro}$) 3.30-3.20 (m, 5H, $H_{\beta, Tyr}$, $H_{\varepsilon, Lys}$) 3.10-3.00 (m, 1H, $H_{\beta, Pro}$) 2.95-2.85 (m, 1 H, $H_{\beta, Pro}$) 2.24-2.14 (m, 1H, $H_{\beta, Tyr}$) 2.10-1.51 (m, 19H, $H_{\beta, Ile}$, $H_{\gamma, Leu}$, $H_{\beta, \delta, Lys}$, $H_{\gamma, Ile}$, $H_{\gamma, \beta, Pro}$, $H_{\beta, Leu}$, $H_{\gamma, Lys}$) 1.24-1.10 (m, 1H, $H_{\gamma, Pro}$) 1.04-0.84 (m, 12H, CH_3-Leu, CH_3-Ile)

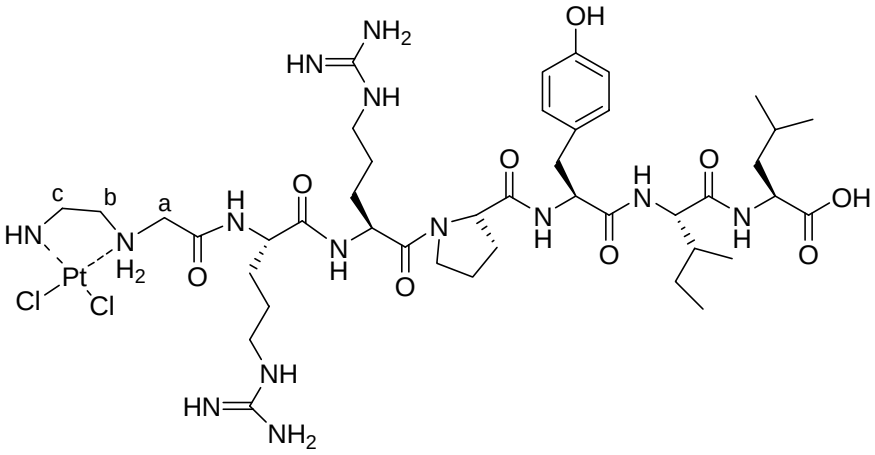

36: Pt(II)-BB-NT

Dull yellow solid, sparingly soluble in water and soluble in methanol

$C_{42}H_{72}Cl_2N_{14}O_9Pt$ (1181.46 g/mol)

R_t = 11.58 minutes (Analytical HPLC; Method A)

MALDI-TOF: *m/z* 1183.9 $[M+2H]^+$

^{195}Pt-NMR (D_2O) : δ -1865 (Ref. H_2PtCl_6 in D_2O)

^{1}H-NMR (500 MHz, CD_3OD): δ_H 7.77 (d, *J*=6.5 Hz, 2H, $H_{\textbf{\textit{ortho}}, Tyr}$) 7.41 (d, *J*=7.5 Hz, 2H, $H_{\textbf{\textit{meta}}, Tyr}$) 4.50-4.40 (m, 2H, $H_{\alpha, Arg}$) 4.31-4.29 (m,1H, $H_{\alpha, Tyr}$) 4.18-4.13 (m, 3H, $H_{\alpha, Leu}$, $H_{\alpha, Ile}$, $H_{\alpha, Pro}$) 3.93-3.88 (m, 4H, $H_{\delta, Arg}$) 3.70-3.60 (m, 2H, $H_{\delta, Pro}$) 3.50-3.40 (m, 2H, $H_{a, BB}$) 2.81-2.75 (m, 1H, $H_{\beta, Tyr}$) 2.70-2.60 (m, 3H, $H_{\beta, Ile}$, $H_{b, BB}$) 2.54-2.45 (m, 3H, $H_{\beta, Tyr}$, $H_{c, BB}$) 2.43-2.29 (m, 10H, $H_{\beta, Arg}$, $H_{\beta, Pro}$, $H_{\gamma, \beta, Leu}$, $H_{\gamma, Ile}$) 2.21-2.18 (m, 2H, $H_{\gamma, Pro}$) 1.89-1.85 (m, 5H, $H_{\gamma, Arg}$, $H_{\beta, Pro}$) 1.68 (d, *J*=6.5 Hz, 3H, C*H*$_3$-Ile) 1.67-1.56 (m, 9H, C*H*$_3$-Leu, C*H*$_3$-Ile)

2.1.2.5 Literature Syntheses

1. Cobaltocenium carboxylic acid

The cobaltocenium carboxylic acid was synthesized in two steps by a reported method.[299] The first step comprised of reaction of cyclopentadiene, methyl cyclopentadiene and cobalt (II) bromide in pyrrolidine. This yielded a mixture of mono and dimethyl cobaltocenium that was precipitated as hexafluorophosphate salt. The second step was the oxidation of the methyl group to acid using $KMnO_4$. The cobaltocenium monocarboxylic was separated from the disubstituted cobaltocenium or the starting material by soxhlet's extraction with acetone.

2. Fmoc-*t*-butyl-*N*-2-aminoethyl glycinate

The Fmoc-*t*-butyl-N-2-aminoethyl glycinate was synthesised by a reported method.[300] It was isolated as HCl salt. The other amino group was protected with Fmoc using the reported method.[190] The purification was carried out by flash chromatography and the yield was 71%.

3. Fmoc- *N*-2-aminoethyl glycine (BB)

Before reaction of the ligand to the peptide, the *t*-butyl group was removed by 90% TFA in CH_2Cl_2 at 0°C in 2 hours. The *t*-butyl alcohol and excess of TFA was removed by azeotropic distillation with toluene. The yield was 97%.

4. Fmoc protected *N,N*-diaminopropionic acid

Diaminopropionic acid is available commercially. The amino groups were protected according to a described method.[301] The purification was carried out by flash chromatography and yield was 30 %.

5. Platination

The platination was carried out as described by Roubillard.[190] Potassium tetrachloroplatinate was dissolved in a mixture of DMF/water (9:1 v/v) on an ultrasonic warm water bath (at 50°C) due to its poor solubility. The Fmoc groups of the BB and DAP ligands were removed by 20% piperidine. After washing, the resin was treated with the solution of K_2PtCl_2 for 40-72 hours in the dark with vigrous agitation.

2.2 Biological Studies

Uptake Studies and Cytotoxicity

Materials and Apparatus

Cell line

Human Hep G2 cell line (Human liver cancer)	DSMZ, Braunschweig, Germany

Chemicals

Gelatine	Merck, Darmstadt, Germany
Paraformaldehyde	Riedel-de-Haën AG, Seelze, Germany
DAKO® Fluorescent Mounting Medium	DAKO Diagnostics GmbH, Hamburg, Germany
Hoechst 33342 Dye	Molecular Probes, Göttingen, Germany
FM 4-64 Marker	Molecular Probes, Göttingen, Germany
Foetal Bovine Serum (FBS)	PAA Laboratories GmbH, Cölbe, Germany
RPMI 1640 with L-Glutamine	Gibco, Invitrogen GmbH, Karlsruhe, Germany
RPMI 1640 with L-Glutamine (Without phenol red)	Gibco, Invitrogen GmbH, Karlsruhe, Germany
Penicillin/Streptomycin/Glutamine (100x)	Invitrogen GmbH, Karlsruhe, Germany
Dulbecco's Phosphate buffered saline	Sigma-Aldrich, Taufkirchen, Germany
Trypsin-EDTA solution	Sigma-Aldrich, Taufkirchen, Germany
Trypanblue solution	Serva Feinbiochemika, Heidelberg, Germany
Triton x100	Serva Feinbiochemika, Heidelberg, Germany
WST-1 reagent (4-[3-(4-iodopheny)-2-(4-nitrophenyl)-2*H*-5-tetrazolio]-1,3-benzene disulfonate)	Roche Diagnostics, Mannheim, Germany
Crystal Violet	Merck, Darmstadt, Germany
Sodium-*n*-dodecyl sulphate	Boehringer, Mannheim, Germany

Cell culture media

Medium A RPMI 1640 with L-Glutamine, 10% FBS not heat inactivated, 100 Units/ml Penicillin G, 100 µg/ml Streptomycin, 0.292 mg/ml L-Glutamine

Medium B RPMI 1640 with L-Glutamine, 100 Units/ml Penicillin G, 100 µg/ml Streptomycin, 0.292 mg/ml L-Glutamine

Medium C Phenol red free RPMI 1640 with L-Glutamine, 100 Units/ml Penicillin G, 100 µg/ml Streptomycin, 0.292 mg/ml L-Glutamine

Apparatus

Cell culture flasks	Greiner bio-one, Frickenhausen, Germany.
Nunclon™surface 4-well plates	Nunc Roskilde, Denmark.
Microtest™96 plates	Becton Dickinson Labware, Franklin Lakes, NJ, USA.
Incubator	Direct Heat CO_2 Incubator Series 310, Forma Scientific.
Laminar Flow	Pretil® Laminarflow, Bemplingen, LaminAir® HB2448, Heraeus Instruments.
Centrifuge	Heraeus Multifuge 3_{S-R}, Osterode.
Microscope	Inverse microscope Nikon ECLIPSE TS 100/TS 100-F, Nikon Europe B.V., Badhoevedorp, Holland. Leica® BioMed microscope. Fluorescence microscope Zeiss Axioplan-2 with AxioCam, Jena, Germany.
Absorbance reader	Bio-Rad Microplate reader 550, Tokyo, Japan.

Methods

Cell Culture and Passaging

Hep G2 cells were cultured in 25 cm^2 or 75cm^2 culture flasks (as needed) in Medium A in a humified incubator maintained at 37°C in an atmosphere containing 5% CO_2. The cells were cultured at subconfluent numbers (65-70%) for three to four days.

The cell mono layer was once washed with PBS without Mg^{2+}/Ca,$^{2+}$ thereafter Trypsin-EDTA, 1ml per 25cm^2 of surface area, was added directly onto the cells. The culture flasks were then incubated at 37 °C for exactly 1 minute 45 seconds. Swiftly, the trypsin was neutralised with 0.5 ml FBS (5 ml of medium A) for 25 cm^2 culture flask. The cells were taken in a sterile plastic tube (blue cap). The culture flask rinsed 3 times with PBS and the volume was made up to 45 ml with sterile PBS. The blue cap tube was then centrifuged at 250xg for 5 minutes. The supernatant was discarded and the pellet of cells was resuspended in 5 ml of Medium A. The cell suspension was diluted to the required seeding density in a new labelled culture flask or plate containing pre-warmed medium for experiments. All the solutions for cell handling and passaging are kept at 37 °C during manipulations.

Cell Counting

Because a fixed number of cells were seeded for experiments, the counting of the cells is an important step before the actual experiments. For this, after normal passaging, the cell pellet was resuspended in 2 ml of medium A. 20 µl of this cell suspension was diluted with 30 µl of PBS in a 1.5 ml eppendorf tube and 50µl of Trypan blue solution was added. The tube was gently agitated and left for one minute. 10µl of this suspension was then taken in a Neubauer cell counting chamber and the cells counted under a microscope. Only the unstained (live) cells were counted.

For the calculation of the number of cells in one millilitre the following formula was used:

$$Y = n /4 \times 5 \times 10^4$$

Where, Y is the number of cells per millilitre of cell suspension under investigation, n is the total cell number in the 4 regions in the neubauer chamber in which the cells were counted, 5 is the dilution factor and 10^4 gives the number per millilitre.

2.2.1 Cellular Uptake Monitoring and Microscopy

The experiments were performed in 4-well plates. Each well was supplied with a glass cover slip which was coated with 0.2 % gelatine for 6 hours at 37°C. For experiments, 7.5 x 10^4 cells per well were seeded and grown for two days in Medium A. Before incubation with the compounds, cells were starved for 1 hour in Medium B. Hep G2 cells were incubated with

test compounds in a concentration range of 1mM to 10µM in medium B, for 24 h at 37 °C in a humified incubator (5 % CO_2).

Tested Concentrations

NLS-bioconjugates	1mM, 500µM and 100µM
TAT-bioconjugates	1mM, 500µM, 100µM and 50µM

Experiments with Live cells

After treatment, cells were washed twice with Medium A and once with phosphate buffered saline (PBS, 10mM). In case of the endosome marker, after the first washing with medium B, the cells were incubated in Medium B with 10 µM of FM 4-64 for 15 minutes. Afterwards, the cells were again washed twice with PBS. For nuclear staining, 100µl Hoechst 33342 dye (25µg/ml) was added for 1 minute to the cells and the cells were washed again with PBS three times for one minute each time.

The viability of the cells was checked by incubation with propidium iodide (8µg/ml; 15 minutes). The cover slips were mounted in a drop of PBS on a glass slide for microscopic observations. The cells were photographed within 5 minutes after mounting.

Experiments with Fixed Cells

The endosomal staining was carried out prior to the fixation of the cells. The cells were incubated in Medium B with 10 µM FM 4-64 for 15 minutes. After washing twice with PBS, the fixation was carried out by treating the cells with 2% paraformaldehyde for 20 minutes. Afterwards the cells were washed three times with 5 minute intervals. In this case the nuclear staining was carried out with 40µl of Hoechst 33342 dye (25µg/ml) after fixation of the cells. Afterwards the cells were washed again three times with PBS with 3 minute intervals. Finally, the cover slips were mounted upside down in DAKO's fluorescent mounting medium. All the fixed cells were preserved in dark at 5°C.

The cellular uptake and distribution was monitored by a fluorescence microscope (Axioplan-2, Zeiss, Jena, Germany) equipped with CY2 (green fluorescence), CY3 (red fluorescence) and UV (blue fluorescence) filters.

2.2.2 Proliferation Assay

The Tetrazolium salt WST-1 and Crystal violet assay

WST-1 cell proliferation assay

96-well plates were coated with 0.2% gelatine for 6 hours at 37° C. After one wash with PBS, 2.0 x 10^4 cells in medium A were seeded in each well. The plates were incubated for 12 hours. Since the doubling time for Hep G2 cells is reported to be 50-60 hours,[302, 303] the cells were incubated for 48 hours after treatment. A control plate with same number of cells was used to determine the background absorbance in case of WST-1 assay and the in case of the Cv assay to determine the cell number. The test compounds were introduced in concentrations of 1, 0.5 and 0.1 mM (4 wells for each concentration) and incubated in a humified atmosphere containing 5% CO_2. After treatment, the cells were washed twice with medium A, then once with medium C. Each well was then supplied with 100µl of the medium C, 10µl/well of WST-1 reagent was added and the plates were incubated at 37°C. The cleavage of WST-1 to formazan by metabolically active cells at 0, 60 and 90 minutes was quantified by scanning the plates at 415nm against a reference wavelength at 655nm in a microtiterplate reader.[304]

Crystal violet cell quantification assay

After the WST-1 assay, the cells were fixed with 4% paraformaldehyde for 5 minutes at room temperature and later washed three times with PBS and three times with 0.1% Triton x 100 buffer in PBS. 100µl of crystal violet [0.04% crystal violet in 4% (v/v) ethanol] was then added to each well and the plates were gently agitated for one hour at room temperature. After treatment with crystal violet the cells were washed 7 times with distilled water with two minute shaking intervals. Finally, 100µl of 1% SDS (sodium-*n*-dodecyl sulphate) was added to each well and the plates were incubated at room temperature with vigorous shaking, for 40 minutes. At the end, the absorbance was measured at 570 nm against a reference wavelength at 655nm.[305]

Statistical Analyses

All data are presented as mean values $\pm$standard errors of the mean (SEM). Depending on the mode of distribution, statistical procedures were performed by the Mann-Whitney Rank Sum test or by the Student's *t*-test using the Sigmastat 3.10 for windows. A *P* value of 0.05 or less was choosen for statistical significance.

2.2.3 Receptor Binding Studies

The binding studies were carried out by Dr. E. Garcia-Garayoa in collaboration with Prof. Dr. Bläuenstein of the Centre for Radiopharmaceutical Science, Paul Scherrer Institute, Switzerland.

Materials

Cell line

HT-29 cell line (human colon adenocarcinoma) was obtained from European Collection of Cell Culture (ECACC), Salisbury, England.

Chemicals

The following chemicals were from Gibco BRL Life Technologies AG, Basel, Switzerland;
McCoy's 5A +GLUTAMAX-I cell culture media
Fetal calf serum (FCS)
Antibiotic/antimycotic solution
Bovine serum albumin (BSA)
Trypsin-EDTA
Soybean Trypsin inhibitor

The following chemicals were from Sigma, Buchs, Switzerland;
HEPES (*N*-2-Hydroxyethypiperazine-*N´*-2-ethanesulfonic acid)
Chymostatin
Bacitracin
Neurotensin(8-13)

The following chemicals were from Merck, Dietikon, Switzerland;
HCl
NaCl
$MgCl_2$
NaOH
KCl

EGTA (Ethylene glycol-bis(β-aminoethylether)-*N, N, N´, N´*-tetraacetic acid) was from Fluka, Buchs, Switzerland.

[^{125} I]Tyr^{3}-NT was from Amersham, Zurich, Switzerland.

The radiotracer ^{99m} Tc-NT-II [retro-N^{α}-carboxymethylhistidine-NT(8-13)] was synthesised in the lab.

Apparatus

NaI gamma counter (Packard Canberra Cobra II Auto-Gamma) was used.

Method

The binding studies were carried out according to a reported method.[297]

Cell Culture

The HT-29 cells were maintained in McCoy's 5A-GLUTAMAX-I media at 37°C in a humified incubator under an atmosphere containing 7.5% CO_2 and passaged weekly. The culture media was supplemented with 10% FCS, 100 IU/ml penicillin, 100µg/ml streptomycin and 0.25 µg/ml amphotericin B.

Binding assays

Intact HT-29 cells at confluence were used for the binding assays. A day before the assay, 10^6 cells/0.4ml (equivalent to 0.3 mg protein) were seeded in 48 well plates. For experiments, a special binding buffer containing protease inhibitors (50 mM HEPES, 125 mM NaCl, 7.5 mM KCl, 5.5 mM $MgCl_2$, 1 mM EGTA, 5g/L bovine serum albumin, 2 mg/L chymostatin, 100 mg/L soyabean trypsin inhibitor, 50 mg/L bacitracin, pH 7.4) was used.

Cells were incubated for 1 hour at 37°C with 2 kBq/well of ^{99m}Tc-NT-II [retro-N^{α}-carboxymethylhistidine-NT(8-13)] and variable concentrations (0.01-30,000 nM) of the test compounds. The cells were then washed twice with cold binding buffer and afterwards solubilised with 1N NaOH at 37°C (0.4ml/well). The activity was determined in a γ-counter. Each experiment was performed in triplicate.

Results

3.1 Syntheses and Characterization

All bioconjugates were synthesized on solid phase using Fmoc strategy (scheme 3.1). The peptide sequences were synthesized either on automatic peptide synthesizers or manually. Wang resin preloaded with the first amino acid (with the *C*-terminal attached to the resin by a linker) was used.

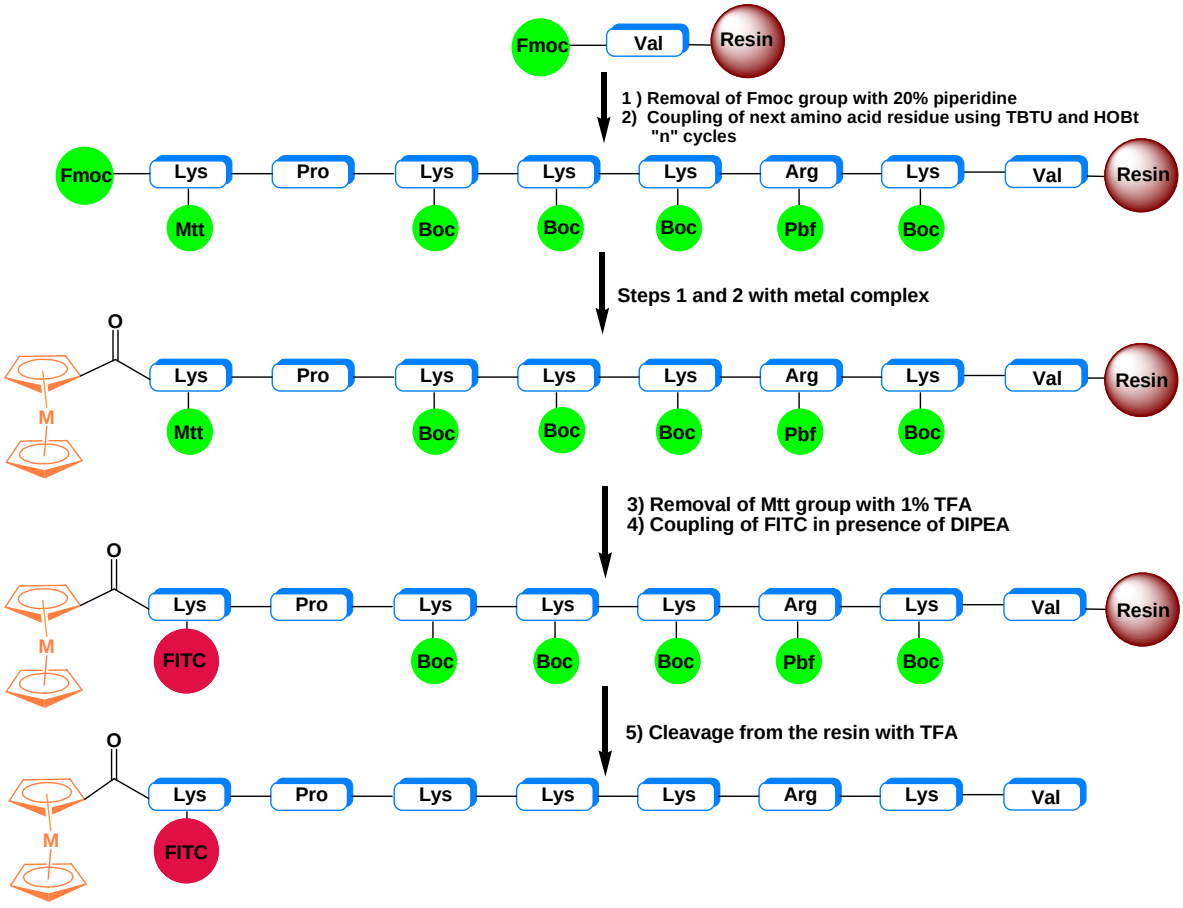

Scheme 3.1: SPPS of fluorescently labelled metallocene-NLS bioconjugates with Fmoc strategy.

In all cases, acid labile linker was used so as to obtain free acid group at the *C*-terminal upon acid cleavage (scheme 3.2).

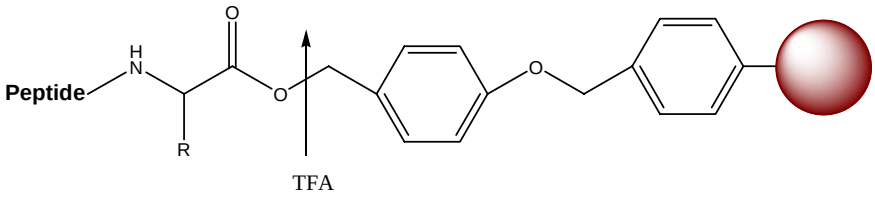

Scheme 3.2: Wang resin with an acid labile linker.

Ferrocene and cobaltocenium carboxylic acids were used as metal labels. Although both metal complexes resemble more or less in size and other properties, cobaltocenium carboxylic acid has cationic character as compared to the neutral ferrocene carboxylic acid (scheme 3.3). Both could be easily coupled to the peptides on the solid phase. However, cleavage conditions for ferrocene bioconjugates had to be modified to prevent the oxidative decomposition of the ferrocene moiety.

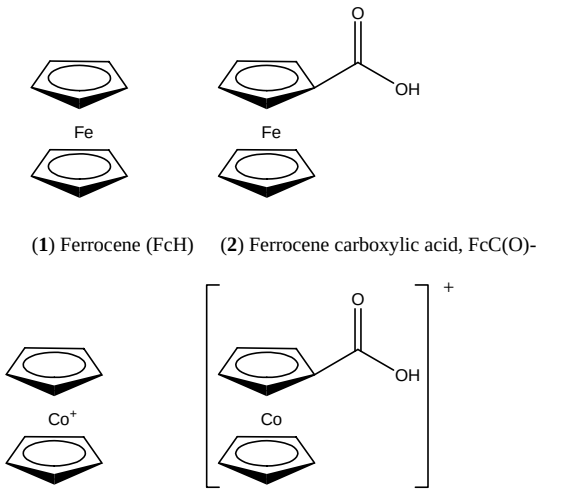

(**1**) Ferrocene (FcH) (**2**) Ferrocene carboxylic acid, FcC(O)-

(**3**) Cobaltocenium (CcH) (**4**) Cobaltocenium carboxylic acid, CcC(O)-

Scheme 3.3: Metallocene carboxylic acids.

Fluorescein isothiocyanate (FITC) was used as the fluorescent label and placed orthogonally on the side chain of the terminal Lysine. It was added manually in the last step of synthesis so as to minimise its exposure to harsh conditions of synthesis. The removal of Methytrityl (Mtt) group from Lysine side chain, with the help of dilute acid, is fully compatible with other acid labile protecting groups.

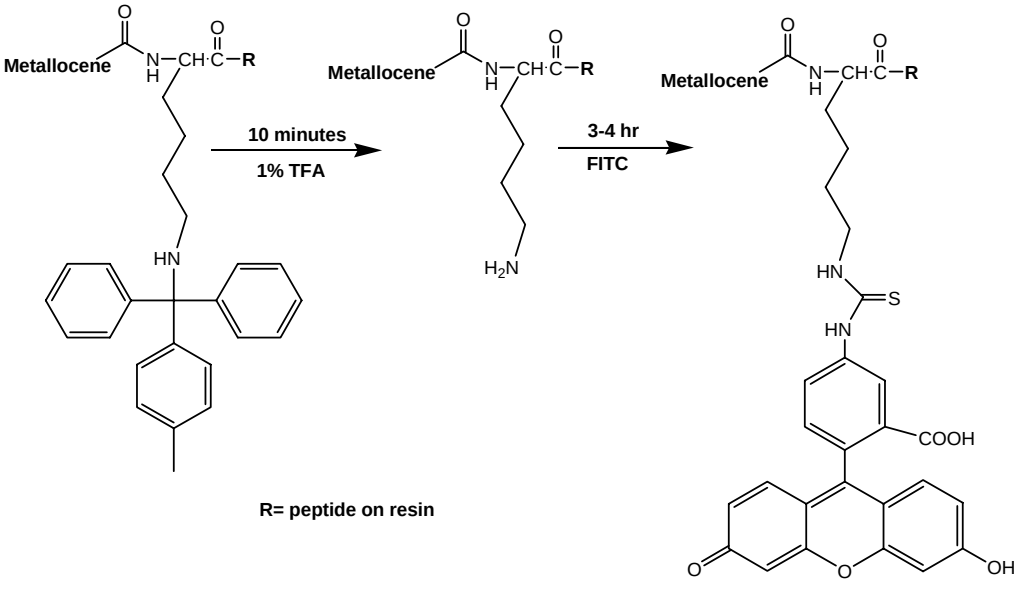

Scheme 3.4: Removal of Mtt group and labelling with FITC.

The coupling with FITC is also very efficient and simple washings are sufficient to remove most of the impurities. The HPLC chromatograms of some crude bioconjugates showed 98% purity. Therefore, labelling with FITC on solid phase is probably one of the cleanest and easy-to-handle methods.

In case of platinum containing compounds K_2PtCl_4 was used for platination. The poor solubility of K_2PtCl_4 in DMF was a problem but it could be dissolved in a mixture of 9:1 DMF/H_2O in few hours on an ultrasonic bath maintained at 50°C. K_2PtCl_4 was handled with care and all the steps of synthesis were carried out in the dark. The ligands were the aminoethylglycine (BB) and diaminopropionic acid (DAP) (scheme 3.5).

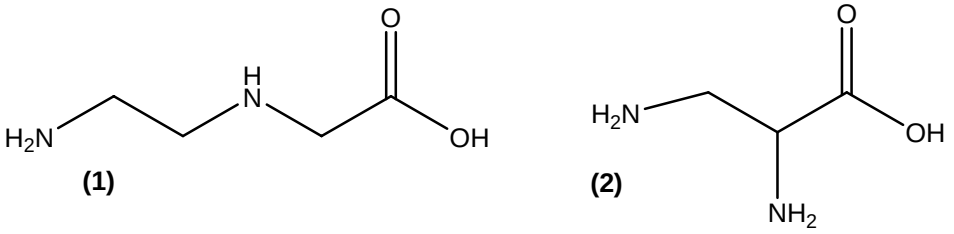

Scheme 3.5: Ligands used for platination: aminoethylglycine (BB) and diaminopropionic acid (DAP).

The ligands were coupled (with TBTU and HOBt) to the peptide and the amino groups were deprotected (with 20% piperidine) prior to platination. At least 40 hours were required for complexation. The change of colour of the resin indicated successful complexation. Afterwards the resin was washed with water in addition to CH_2Cl_2 and MeOH. The metal peptide bioconjugate was cleaved from the resin by a mixture of 95%TFA and 5% water in 2 to 3 hours.

All the bioconjugates were characterized by spectroscopic studies, HPLC and electrochemistry. The mass of each compound was determined by mass spectrometry MALDI-TOF or ESI. The ^{1}H-NMR spectra were also measured for all bioconjugates. One of the remarkable characterising feature is the signals arising from the cyclopentadienyl rings of the metallocenes, around 6 ppm (intensity 5:2:1:1) for the cobaltocenium group and around 4 ppm (intensity 5:2:2) for the ferrocene group. The FITC signals were identified in the aromatic region of the proton NMR spectra. The purity of the bioconjugates was analysed by RP-HPLC and subsequent purifications were carried out by preparative RP-HPLC using different isocratic conditions for different compounds. Since all the metal containing bioconjugates are electrochemically active, their redox potentials were determined.

The successfully synthesized bioconjugates are listed in the table 3.1. One letter codes are used to denote the amino acids. CcC(O)- and FcC(O)- are used to denote the cobaltocenium and ferrocene carboxylic acids. Pt indicates Platinum, BB stands for backbone (aminoethylglycine) and DAP for diaminopropionic acid. NLS stands for nuclear localisation signal, NLS_{mca} for methoxycoumarin substituted NLS, NLS_{scr} for the scrambled sequence of NLS, NT for neurotensin, pNT for pseudo neurotensin and TAT denotes the transctivaor of transcription peptide.

Table 3.1: List of synthesized bioconjugates

Comp. No.	Abbreviation	Sequence
1	CcC(O)-NLS	CcC(O)-PKKKRKV
2	FcC(O)-NLS	FcC(O)-KPKKKRKV
3	CcC(O)-NLS_{mca}	CcC(O)-PKKKRK$_{mca}$V
4	Pt-BB-NLS	Pt-BB-PKKKRKV
5	Pt-DAP-NLS	Pt-BB-PKKKRKV
6	K-NLS	KPKKKRKV
7	K(FITC)-NLS	K(FITC)-PKKKRKV
8	CcC(O)-K-NLS	CcC(O)-KPKKKRKV
9	FcC(O)-K-NLS	FcC(O)-KPKKKRKV
10	CcC(O)-K(FITC)-NLS	CcC(O)-K(FITC)-PKKKRKV
11	FcC(O)-K(FITC)-NLS	FcC(O)-K(FITC)-PKKKRKV
12	CcC(O)-K(FITC)-V	CcC(O)-K(FITC)-V
13	FcC(O)-K(FITC)-V	FcC(O)-K(FITC)-V
14	NLS_{src}	KKVKPKR
15	CcC(O)-NLS_{src}	CcC(O)-KKVKPKR
16	FcC(O)-NLS_{src}	FcC(O)-KKVKPKR
17	K-NLS_{src}	KKKVKPKR
18	K(FITC)-NLS_{src}	K(FITC)-KKVKPKR
19	CcC(O)-K-NLS_{src}	CcC(O)-KKKVKPKR
20	FcC(O)-K-NLS_{src}	FcC(O)-KKKVKPKR
21	CcC(O)-K (FITC)-NLS_{src}	CcC(O)-K(FITC)-KKVKPKR
22	FcC(O)-K(FITC)-NLS_{src}	FcC(O)-K(FITC)-KKVKPKR
23	K-TAT	KGRKKRRQRRR
24	K(FITC)-TAT	K(FITC)-GRKKRRQRRR
25	CcC(O)-K-TAT	CcC(O)-KGRKKRRQRRR
26	FcC(O)-K-TAT	FcC(O)-KGRKKRRQRRR
27	CcC(O)-K(FITC)-TAT	CcC(O)-K(FITC)-GRKKRRQRRR
28	FcC(O)-K(FITC)-TAT	FcC(O)-K(FITC)-GRKKRRQRRR
29	pNT	KKPYIL
30	FcC(O)-pNT	FcC(O)-KKPYIL
31	CcC(O)-pNT	CcC(O)-KKPYIL
32	Pt-BB-pNT	Pt-BB-KKPYIL
33	NT	RRPYIL
34	CcC(O)-NT	CcC(O)-RRPYIL
35	FcC(O)-NT	FcC(O)-RRPYIL
36	Pt-BB-NT	Pt-BB-RRPYIL

3.1.1 NLS Bioconjugates

Wang resin preloaded with Fmoc-Val-OH (0.63mmol/g) was used for the synthesis of all the NLS (126-132) bioconjugates. The synthesis was carried out in an eppendorf automatic peptide synthesizer. The metal labels were coupled manually in the lab. The synthesized bioconjugates were comprehensively characterized.

At the very beginning, it was investigated whether a metal carboxylic group could be coupled to the *N*-terminal of a peptide on the solid support. Therefore CcC(O)-NLS (**1)** was synthesized and characterized. It also led to optimisation of conditions. For cobaltocenium bioconjugates the purity of the metal label is very important. Besides longer activation time (5-10 minutes) for cobaltocenium carboxylic acid and longer coupling times (atleast 40 minutes) were necessary.

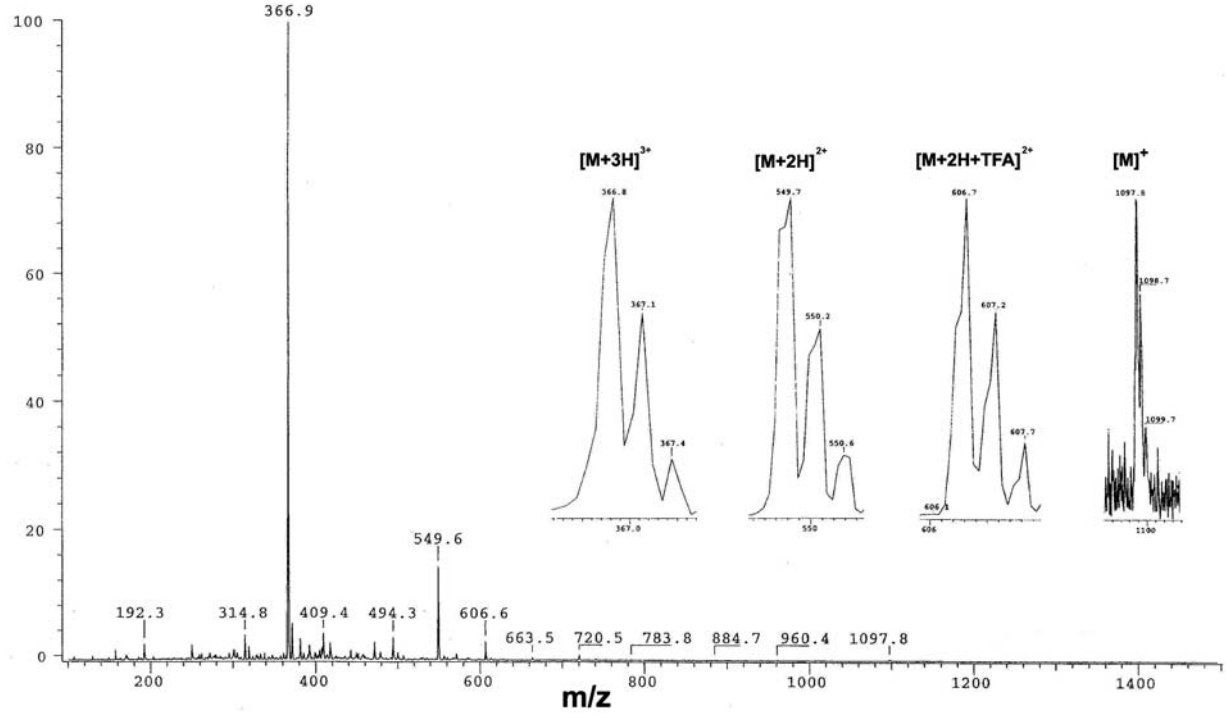

Fig. 3.1: ESI (pos.) spectrum of bioconjugate **1** showing characteristic peaks of mono, di and trications.

For the ferrocene containing bioconjugate **2**, problems were encountered when conventional cleavage mixture (95% TFA, 2.5% TIS and 2.5% H_2O) was used to cleave the bioconjugate from the resin. The coupling did not pose any greater challenge than as for the cobaltocenium carboxylic acid. However the cleavage conditions had to be modified using

10% phenol in the cleavage mixture to protect ferrocene from oxidation. The ^{1}H-NMR spectrum of compound **2** is given in Figure 3.2.

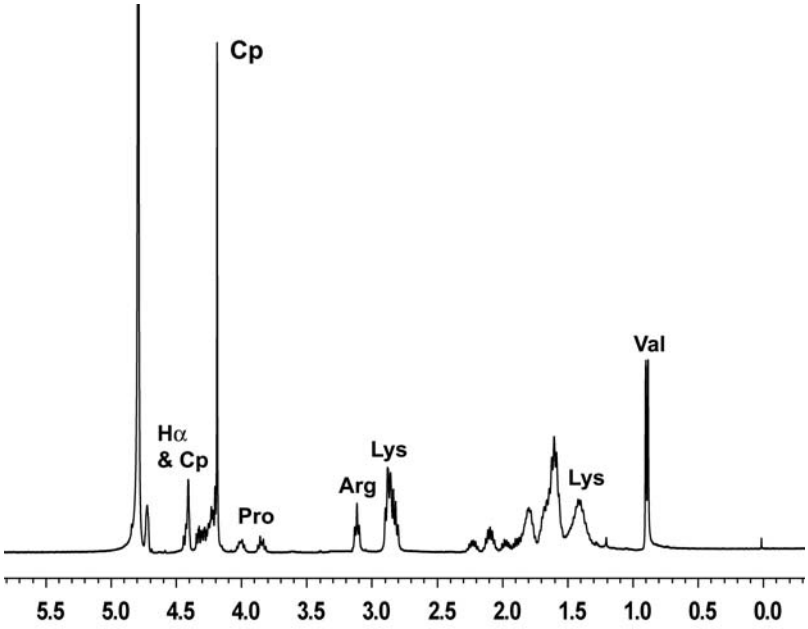

Fig. 3.2: ^{1}H-NMR spectrum of FcC(O)-NLS (**2**) in D_2O at room temperature. The characteristic peaks are indicated.

In case of compound **3**, a Lysine prelabelled with methoxycoumarin (mca) was used at position 131 of NLS(126-131) The objective was to synthesize a fluorogenically labelled metal-peptide conjugate to monitor the compound in cells. This is a fairly straightforward and very simple approach. However, due to incompatibility of this label with the microscopic facilities available, later another fluorescent label namely Fluorescein isothiocyanate (FITC) was used for labelling of all other compounds.

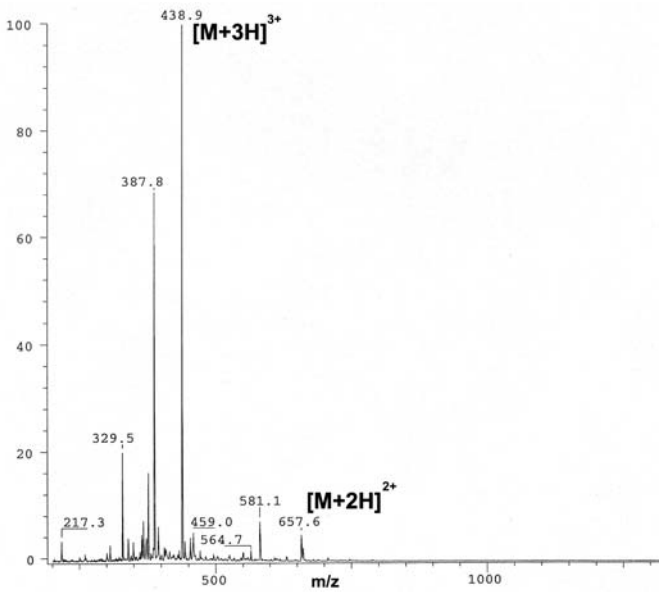

Fig. 3.3: ESI (pos.) spectrum of crude bioconjugate **3**.

First the metal-peptide bioconjugates with an additional lysine residue were synthesized and characterized. The metallocene carboxylic acids were coupled to the *N*-terminal of the peptide sequence. After cleavage of the bioconjugates from the resin the HPLC of most crude compounds showed 98-99% purity indicating the efficiency and cleanliness of the method. The HPLC chromatogram of CcC(O)-K-NLS (**8)** is depicted in Figure 3.4.

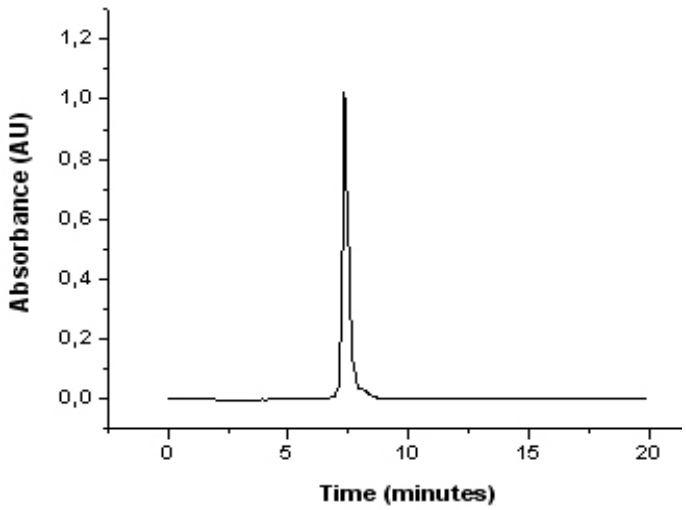

Fig. 3.4: HPLC chromatogram of compound **8;** RP-HPLC using method A, see experimental.

The electrochemical behaviour of the metal-peptide bioconjugates was also analyzed by measuring their square wave or cyclic voltammograms. The ferrocene bioconjugates showed a reversible wave with a redox potential in the range of 150 to 280 mV. Whereas the cobaltocenium bioconjugates showed a reversible wave at a high scan rate. Figure 3.5 depicts the cyclic voltammogram of ferrocene bioconjugate (**9**) exhibiting a reversible wave.

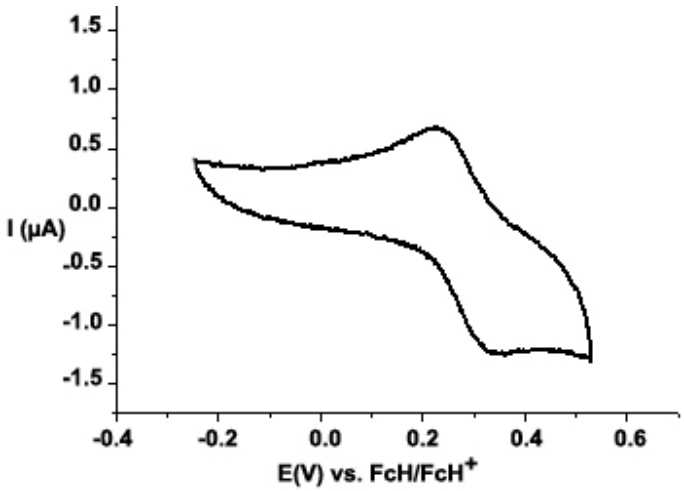

Fig. 3.5: Cyclic voltammogram of compound **9** measured in acetonitrile with $TBAPF_6$ as supporting electrolyte at room temperature.

Fluorescein isothiocyanate (FITC) was used in order to visualise the metallocene-NLS conjugates (**10**-**11**) inside the cells. The FITC labelling was carried out as the last step before the final cleavage of the peptide from the resin to ensure minimum of side reactions. After coupling of the metallocene moiety to the peptide as for CcC(O)-K-NLS, the lysine side chain was deprotected by removal of its "Mtt" group using dilute TFA. Reaction with FITC yielded the CcC(O)-K(FITC)-NLS conjugate (**10**) and FcC(O)-K(FITC)-NLS conjugate (**11**) on the solid support, which are bright dark orange in colour. All the compounds bearing FITC were stored and handled in dark. After cleavage and HPLC purification, the ^{1}H-NMR spectra clearly show the fluorescein signals in the aromatic region, in addition to the signals corresponding to the cyclopentadiene rings of the metallocenes and the peptide as well. Figure 3.6 depicts the comparison of the ^{1}H-NMR of the peptide with the metal labelled peptide as well as the two FITC labelled ferrocene and cobaltocenium bioconjugates of NLS(126-132).

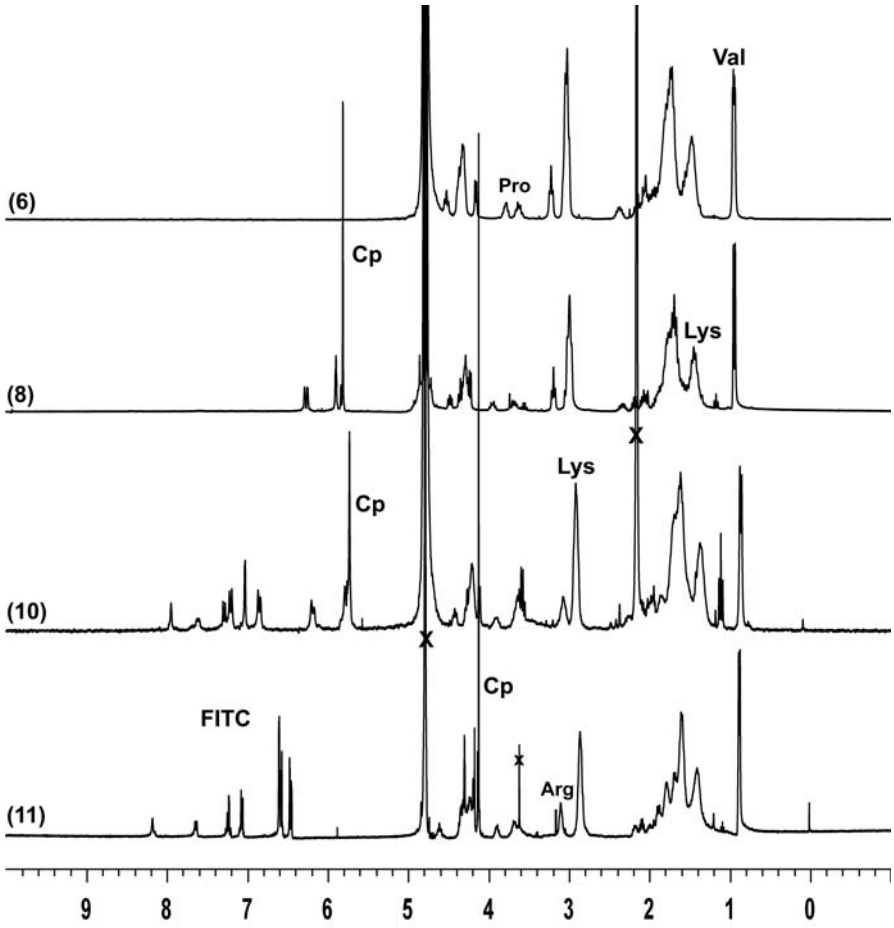

Fig. 3.6: ^{1}H-NMR spectra of FITC labelled compounds **10** and **11** in comparison with the unlabelled metal bioconjugate **8** and that of peptide **6** in D_2O at room temperature. The cyclopentadiene signals can be clearly observed around 6 ppm and 4 ppm for cobaltocenium and ferrocene bioconjugates respectively. The FITC signals can be seen in the aromatic region.

The MALDI-TOF spectrum of Ferrocene bioconjugate (**11**) with characteristic peaks is represented below;

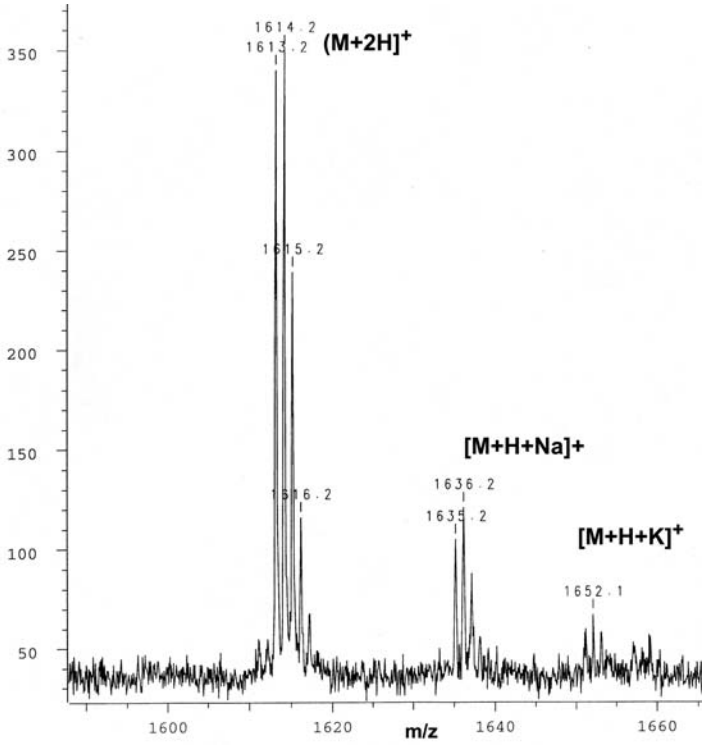

Fig. 3.7: MALDI-TOF mass spectrum of bioconjugate **11** showing characteristic peaks.

The HPLC chromatograms of the crude compounds **10** and **11** are depicted in Figure 3.8.

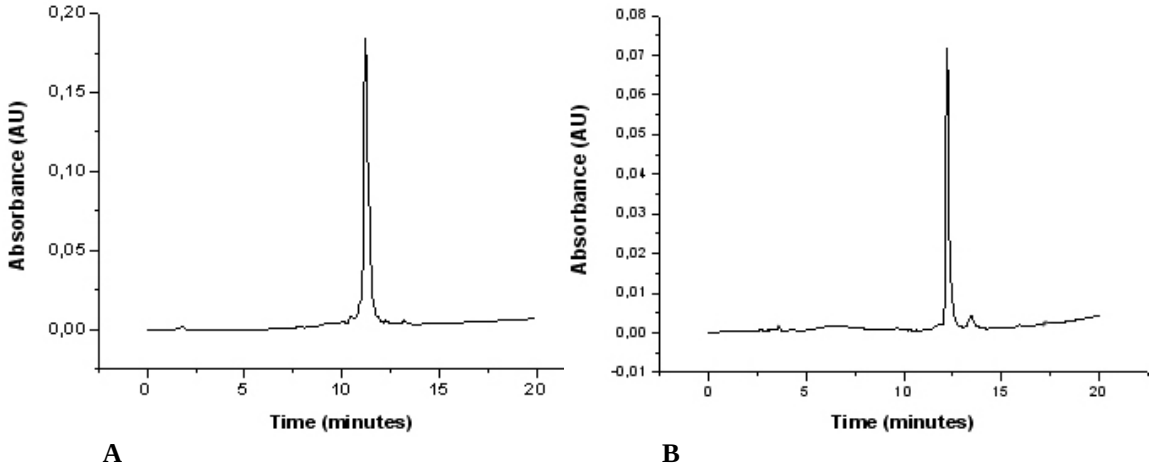

Fig. 3.8: HPLC chromatograms of bioconjugates **10** (A) and **11** (B) using method A, see experimental.

As controls, a fluorescent NLS conjugate without the metal group (K(FITC)-NLS) **7** as well as the truncated peptides, CcC(O)-K(FITC)-V (**12**) and FcC(O)-K(FITC)-V (**13**), were also prepared by solid phase synthesis. The purity of the synthesized compounds was

checked by RP-HPLC. Though lipophilic due to the cyclopentadienyl rings, the bioconjugate is soluble in water. The HPLC chromatogram of crude bioconjugate **12** analyzed using method A (see experimental for details) is depicted in Figure 3.9.

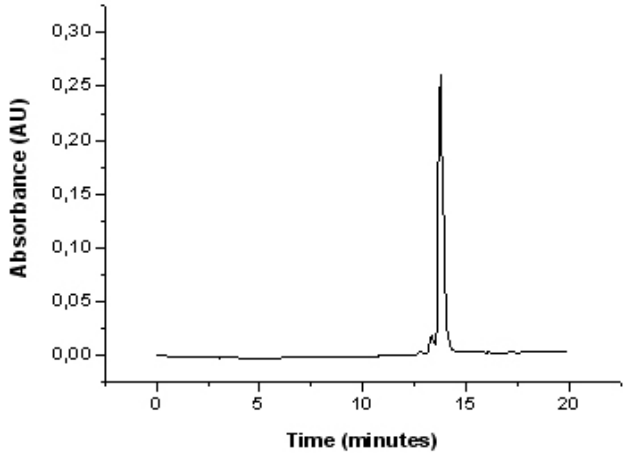

Fig. 3.9: HPLC chromatogram of bioconjugate **12**.

The mass of the bioconjugates was also determined by MALDI-TOF mass spectrometry. The mass spectrum of bioconjugate **13** is shown in Figure 3.10.

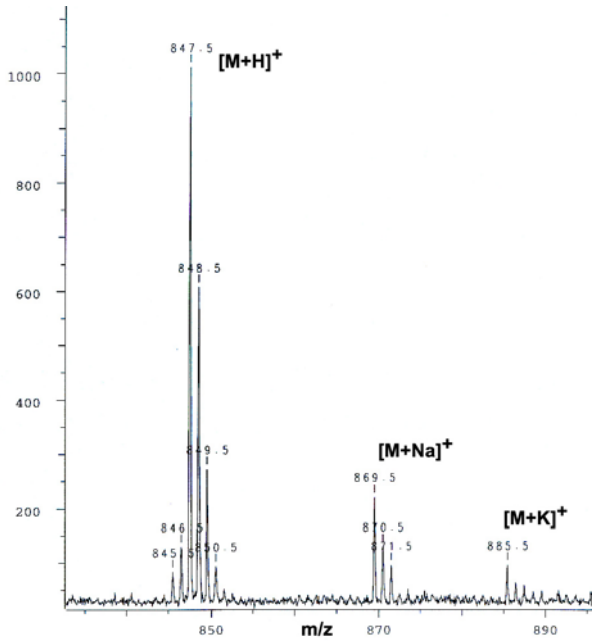

Fig. 3.10: MALDI-TOF spectrum of bioconjugate **13** showing characteristic peaks.

In addition to the metallocene bioconjugates, the platinum bioconjugates of the nuclear localisation signal, **4** and **5** with aminoethylglycine and diaminopropionic acid ligands respectively, were also successfully synthesized on the solid phase and comprehensively characterized.

3.1.2 NLS_{scr} Bioconjugates

The NLS_{scr} is the scrambled sequence of the nuclear localiszation signal (KKVKPKR). All the NLS_{scr} bioconjugates (**14-22**) were also synthesized on Wang resin. The square wave voltammogram of CcC(O)-K-NLS_{scr} (**19**) is depicted in Figure 3.11A and shows an E½ of -1.38 V vs. FcH/FcH^+ which is very similar to the bioconjugate **8** which contains the unscrambled sequence. Figure 3.11B shows the squarewave voltammogram of CcC(O)-K(FITC)-NLS_{scr}.

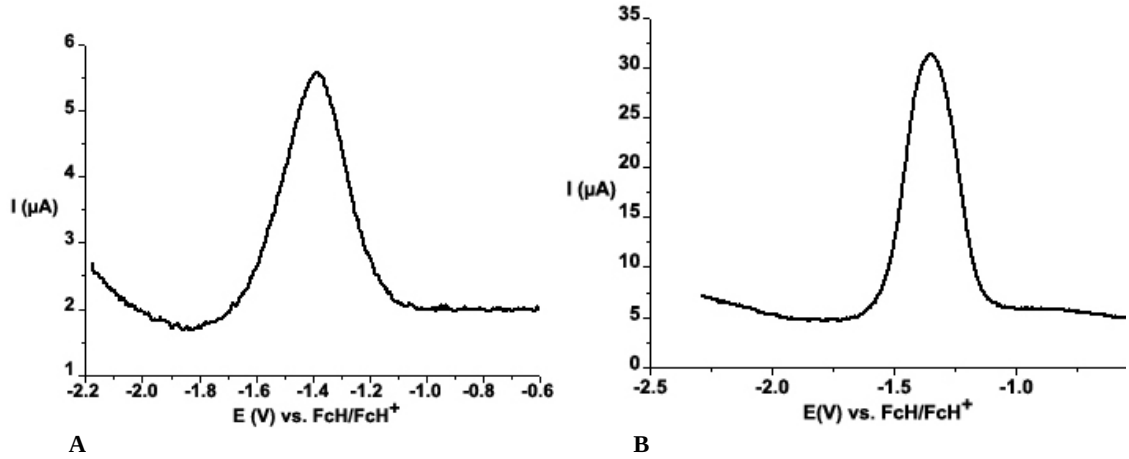

Fig. 3.11: Square wave voltammograms of bioconjugates **19** and **21**.

The metal-NLS_{scr} bioconjugates (**21** and **22**) were also labelled with FITC. As control the scrambled sequence of NLS labelled with FITC was synthesized. The ^{1}H-NMR spectra of all compounds were measured. Figure 3.12 depicts the ^{1}H-NMR of the unlabelled bioconjugate **17** and that of the double labelled (with ferrocene and FITC) bioconjugate **22**. Again characteristic peaks are visible corresponding to the FITC moiety as well as the cyclopentadienyl rings of the metallocene.

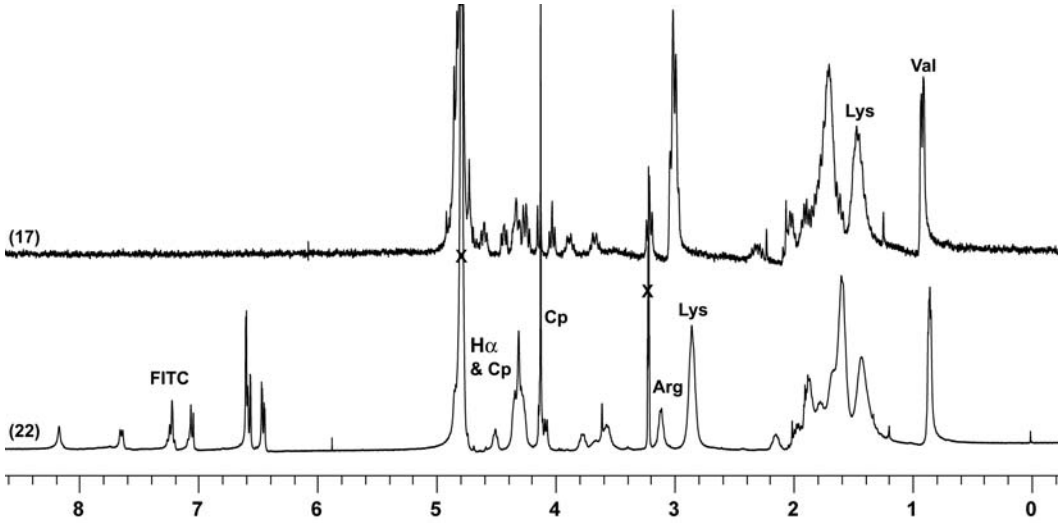

Fig. 3.12: ^{1}H-NMR spectra of the unlabelled peptide (**17**) and that of the FITC labelled metal peptide bioconjugate (**22**) measured in D_2O at room temperature.

The purity of all bioconjugates was also analyzed by RP-HPLC and the respective chromatograms of the crude FITC labelled bioconjugates, the metal-free (**18**) Cobaltocenium (**21**) and ferrocene(**22**) bioconjugates are represented in Figure 3.13.

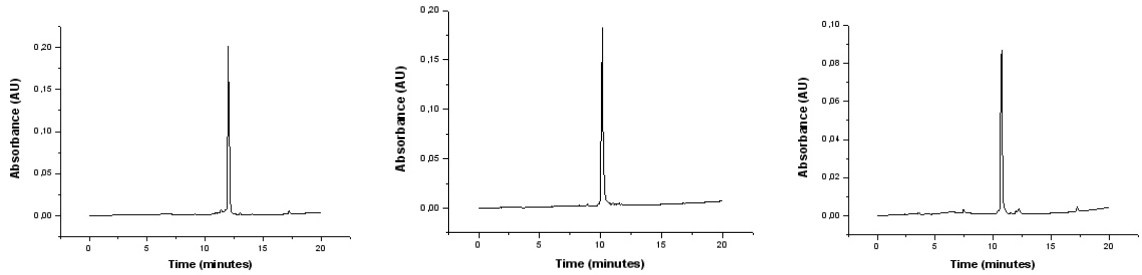

Fig. 3.13: HPLC chromatograms of bioconjugates **18** (A), **21** (B) and **22** (C) using method A, see experimental.

The following figure shows the MALDI-TOF spectrum of the bioconjugate **21**.

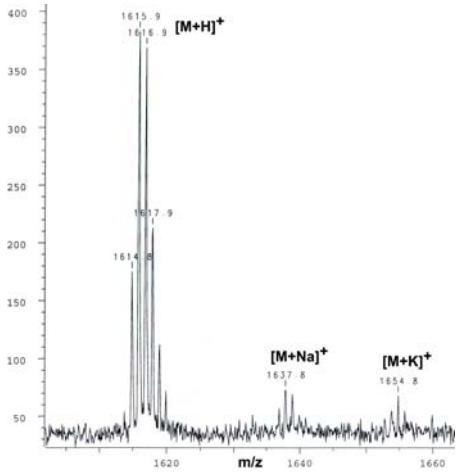

Fig. 3.14: The mass spectrum of bioconjugate **21** with characteristic peaks

3.1.3 TAT Bioconjugates

For the solid phase synthesis of the TAT sequence (KGKKRRQRRR) Wang resin preloaded with Fmoc-Arg(Pbf)-OH was used. All the metal labelled bioconjugates as well as the metal and FITC labelled bioconjugates were successfully synthesized and comprehensively characterized.

The HPLC chromatograms of the crude CcC(O)-K-TAT (**25**) and FcC(O)-K-TAT (**26**) showed high purity as show in Figure 3.15A and B.

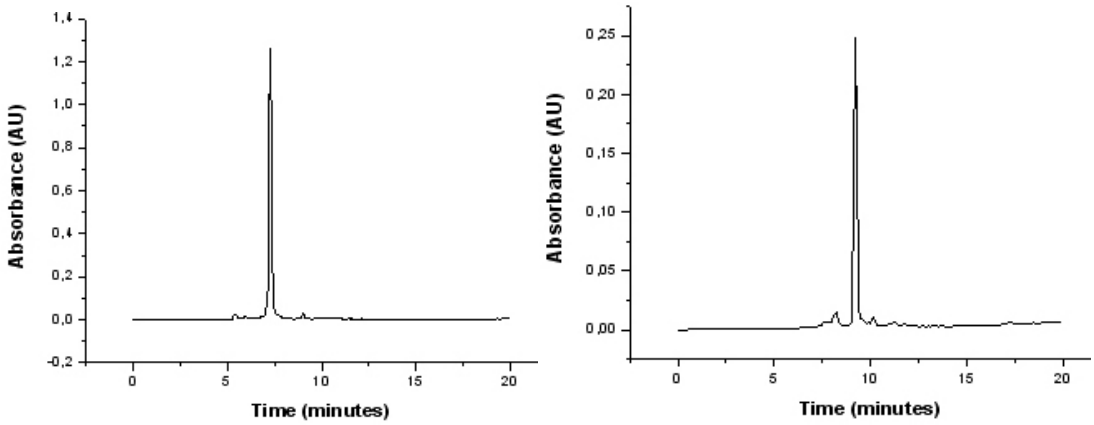

Fig. 3.15: HPLC chromatograms of crude bioconjugate **25** (A) and bioconjugate **26** (B) using method A, see experimental.

The ^{1}H-NMR spectra also shows all the characteristic signals arising from the FITC and the cyclopentadienyl rings as presented in Figure 3.16.

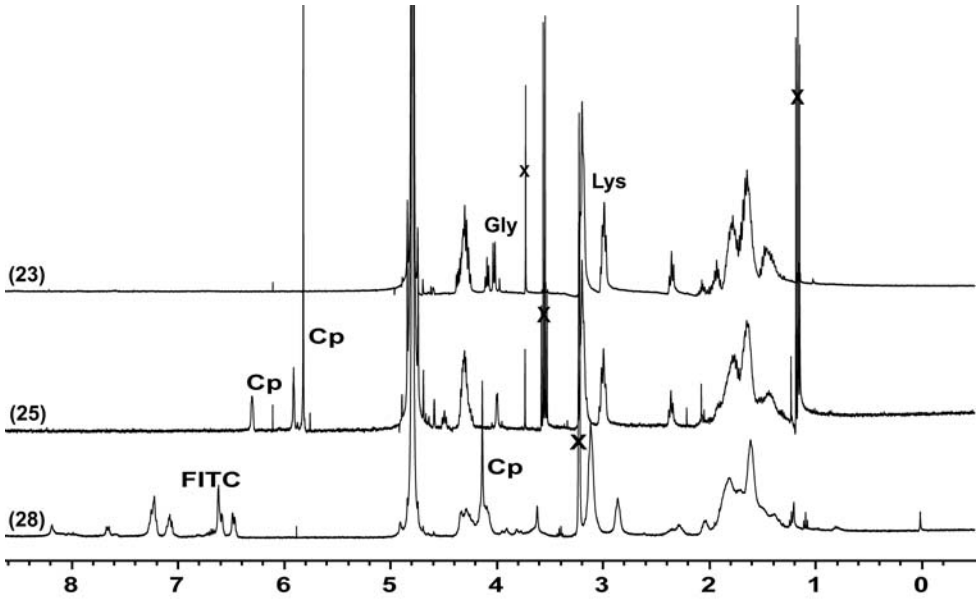

Fig. 3.16: ^{1}H-NMR spectra of the peptide **23**, the metal containing TAT peptide **25** and the FITC labelled Ferrocene-TAT bioconjugate **28** in D_2O at room temperature.

The electrochemical behaviour of the bioconjugates was also determined by measuring the cyclic or square wave voltammograms of the compounds. Figure 3.17A depicts the cyclic voltammogram of ferrocene bioconjugate **26** showing a reversible wave at 199 mV

vs. FcH/FcH^+. Whereas, the cobaltocenium bioconjugate (**27**) showed an E½ at -1.38 V vs. FcH/FcH^+ in square wave voltammetry, Figure 3.17B

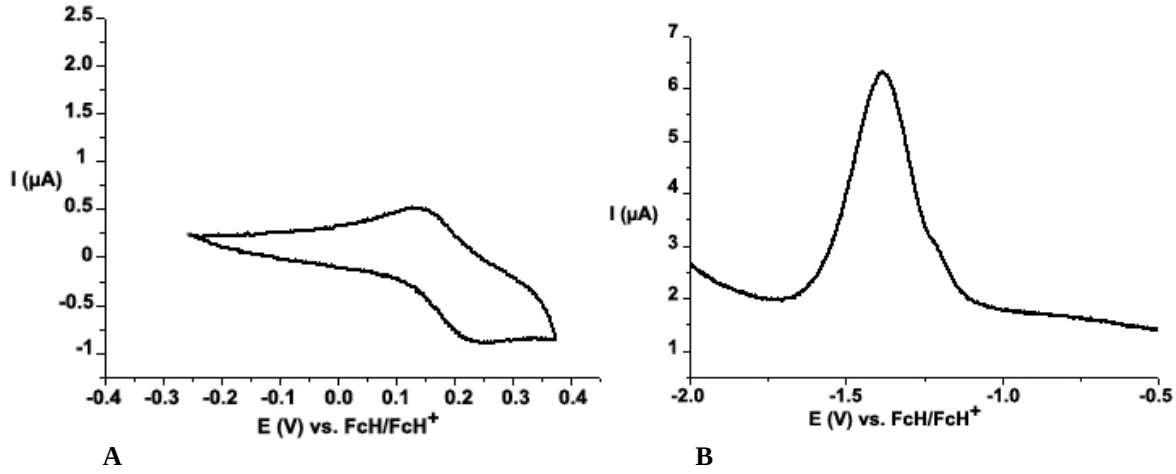

Fig. 3.17: Cyclic voltammogram of **26** (A) and the square wave voltammogram of **27** (B) in acetonitrile with $TBAPF_6$ as supporting electrolyte.

3.1.4 NT Bioconjugates

The metal-neurotensin bioconjugates were also synthesized by solid phase synthesis. In addition, the NT(8-13) sequence was slightly modified that is the Arg^8-Arg^9 motif was replaced with Lys-Lys and the sequence is designated as pseudo NT (pNT). All the bioconjugates were characterized and their purity was determined by RP-HPLC.

Bioconjugate **30** containing a ferrocene moiety exhibited a typical cyclic voltammogram as depicted in Figure 3.18 showing a reversible peak at 218 mV vs. FcH/FcH^+.

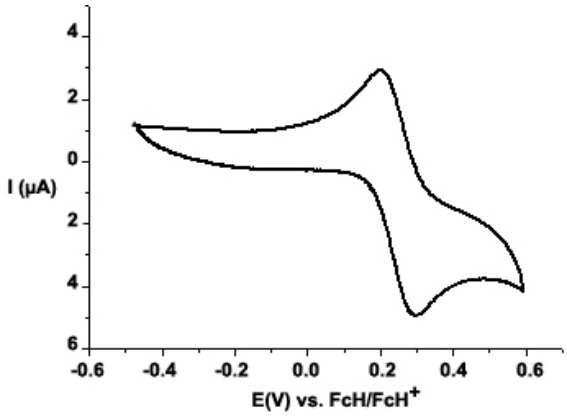

Fig. 3.18: Cyclic voltammogram of bioconjugate **30**.

In addition to the metallocene bioconjugates, the platinum conjugates of the neurotensin and pseudoneurotensin were also synthesized and characterized. The mass was determined using MALDI-TOF spectrometry as depicted below;

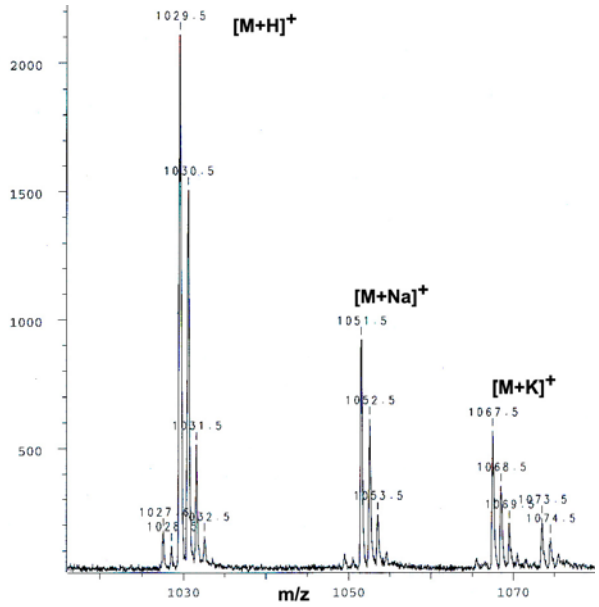

Fig. 3.19: Mass spectrum of bioconjugate **32** showing characteristic isotopic pattern of platinum.

The ^{1}H-NMR of the two metallocene-peptide bioconjugates are compared with the metal free neurotensin fragment as depicted in Figure 3.20 and show the characteristic signals of the cyclopentadienyl rings of the respective metallocenes.

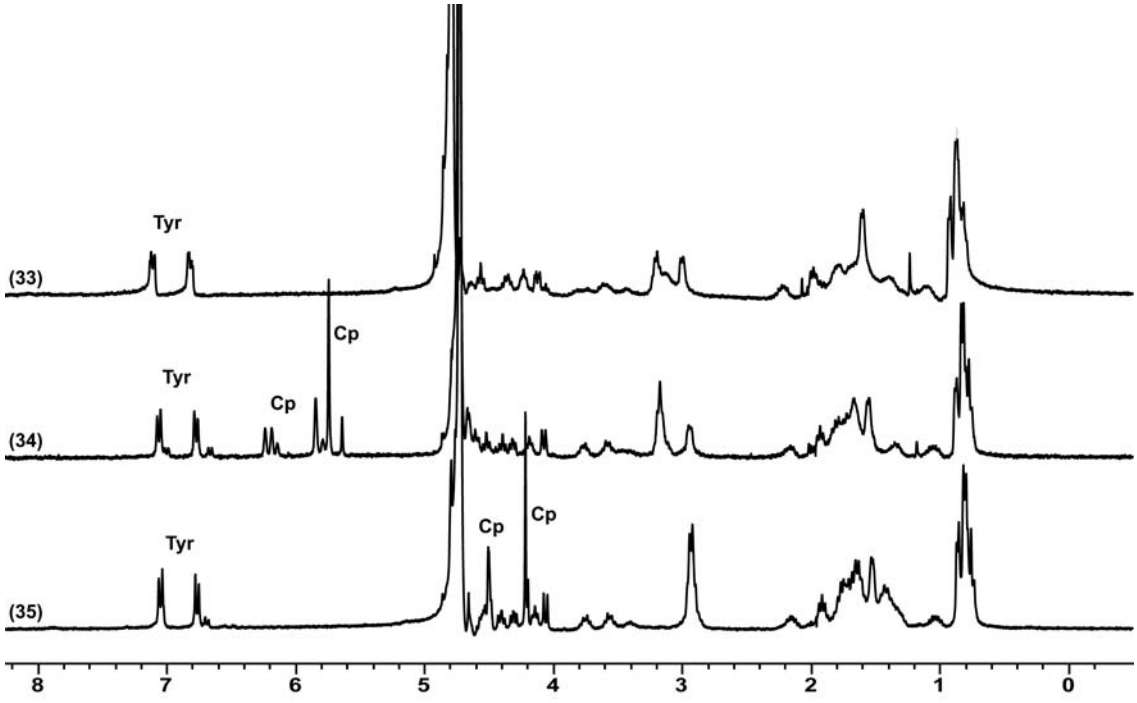

Fig. 3.20: ^{1}H-NMR spectra of the peptide **33** and the cobaltocenium-NT (**34**) and ferrocene-NT (**35**) in D_2O at room temperature.

RP-HPLC was used to check the purity of the compounds. The HPLC chromatograms of crude metallocene bioconjugates CcC(O)-NT (**34**) and FcC(O)-NT (**35**) are shown below in Figure 3.21 indicating a very high purity.

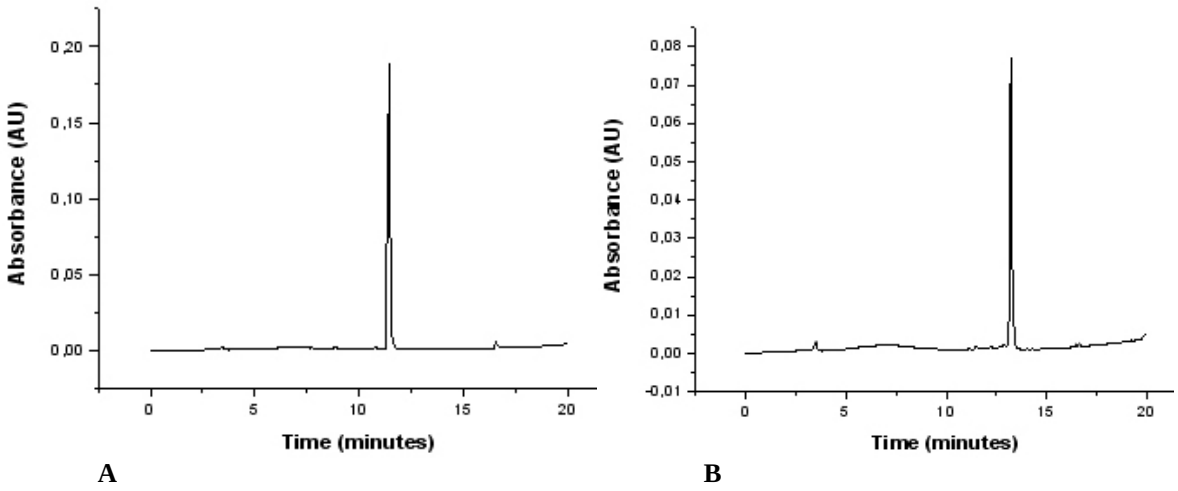

Fig. 3.21: HPLC chromatograms of crude bioconjugates **34** (A) and **35** (B) using method A, see experimental.

The cobaltocenium bioconjugate **34** was tested for its electrochemical behaviour and it exhibited an E½ at -1.31 V vs. FcH/FcH^+ as depicted in Figure 3.22.

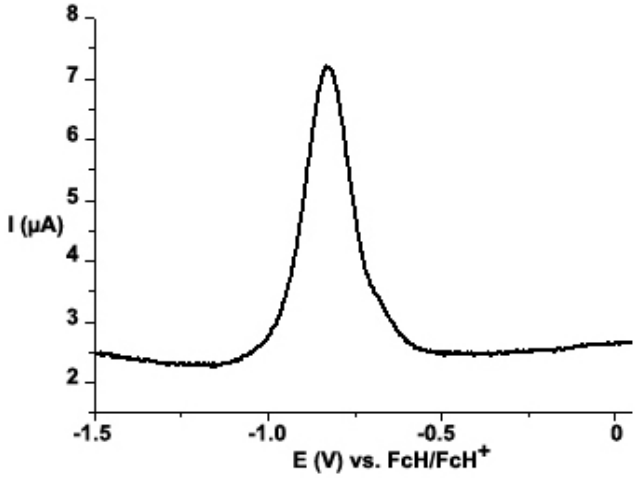

Fig. 3.22: Square wave voltammogram of **34** in acetonitrile with $TBAPF_6$ as supporting electrolyte.

3.2 Cellular Uptake and Nuclear Localisation

An immortalized human liver cancer cell line (Hep G2) was used for cellular uptake studies. Hep G2 cells were chosen, because they have relatively large nuclei. However, membrane translocation in this cell line is known to be rather difficult.[306] The cells were incubated with the test compounds in various concentrations for 24 h at 37°C in a humified incubator under an atmosphere containing 5% CO_2. The cells were washed twice with medium A in order to remove any adhereing metal-peptide bioconjugate. After the first washing step with PBS, the cells were treated according to the protocols. The experiments with live cells and fixed cells were carried out in parallel. Because recent reports indicate potential artificial redistribution of cell penetrating peptides into the nucleus upon fixation,[226, 307] it was essential to monitor the uptake and distribution of compounds in live cells. In addition, a complete duplicate of experiments was carried out with fixation of the cells with paraformaldehyde. This was done not only for the ease of handling, observation and photography, but also for the sake of comparison of the uptake and distribution in live and fixed cells in order to determine potential differences.

3.2.1 Experiments with Live Cells

3.2.1.1 NLS Bioconjugates

Cells incubated with Cobaltocenium bioconjugate (**10**) in a concentration of 1mM, showed three kinds of fluorescence; homogenous green fluorescence in the cytoplasm, and some dotted fluorescence in the cytoplasm and homogenous stronger fluorescence in the nuclei (Figure 3.2.1 A). Figures 3.2.1 C and D depict the co-localisation of the compound in the endosomes and the nucleus, respectively. The results indicate that the CcC(O)-K(FITC)-NLS (**10**) is readily taken up by the cells. The dot-like cytoplasmic distribution of compound **10** (Figure 3.2.1 C) overlapping with that of the endosome marker FM 4-64 indicate an active transport via endocytosis. The bioconjugate is probably internalised via endocytosis, released into the cytoplasm and then accumulated in the nucleus. The integrity of the cell membrane

was confirmed throughout the experimental procedure by verifying that the cells excluded propidium iodide (Figure 3.2.1 B).

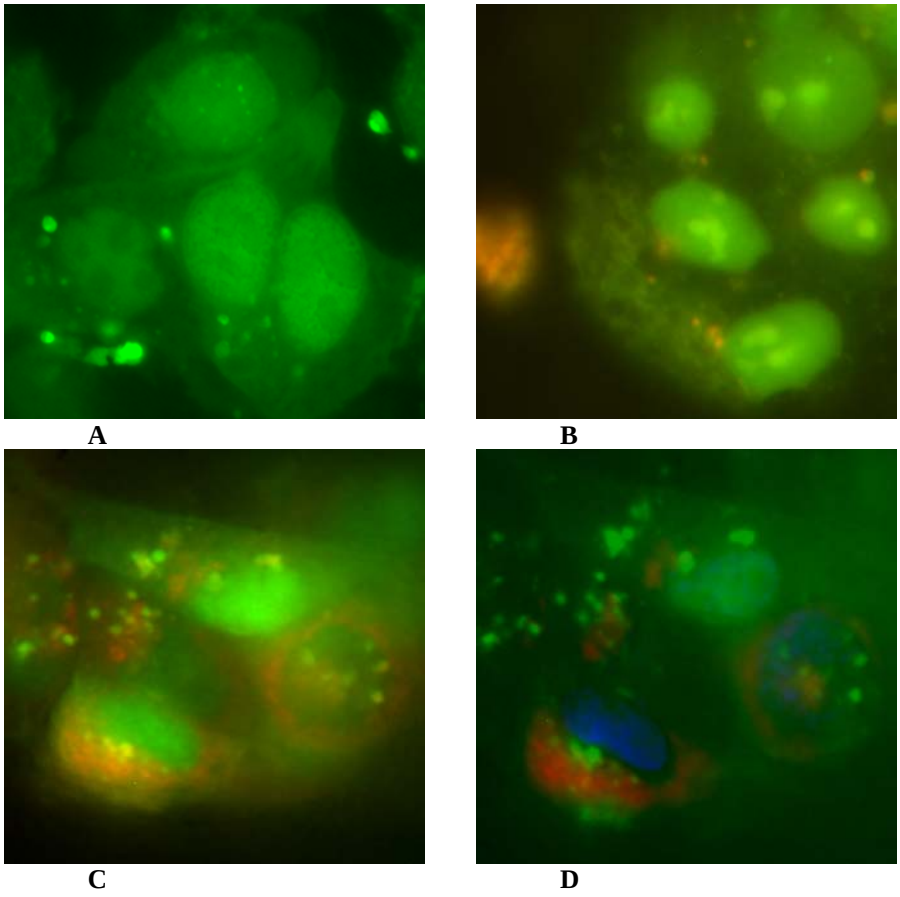

Fig. 3.2.1: Cellular uptake and nuclear localization of the cobaltocenium bioconjugate 10 (A); Integrity of cells after treatment with propidium iodide (B); Localisation in endosomes, cells after incubation with FM 4-64 (5µM) for 15 minutes (merged image, C); Merged image depicting endosomes and nucleus; CY3 and UV filters (D). Double Fluorescence microscopy, magnification 630x. Representative pictures of three independent experiments.

The ferrocene-NLS bioconjugate **11**, in a concentration of 500µM, was found to be localised in most nuclei (Figure 3.2.2 A). Fluorescence microscopy showed homogenous green fluorescence intracellularly being stronger in the nuclei. Some point-like fluorescence was also observed which seemed apparently extracellular although some small fluorescence might be located inside the cells. Figure 3.2.2 B depicts the endosomal and the nuclear staining in the same cells. Using double fluorescence microscopy, the endosomal marker FM 4-64 revealed that this bioconjugate was not co-localised in the endosomes (Figure 3.2.2 A). The same result was observed with the lower concentration (100µM) of this compound although less nuclear localisation was observed (see appendix for pictures) indicating a concentration-dependent uptake and nuclear translocation.

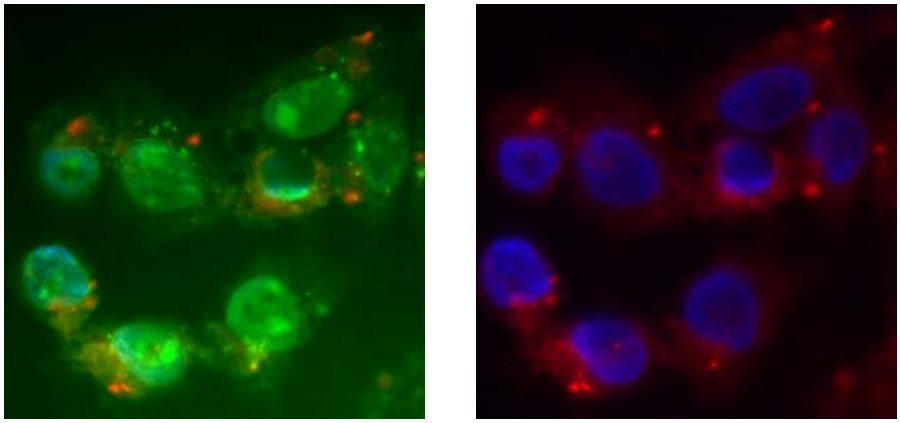

A B

Fig. 3.2.2: Localisation of bioconjugate 11 in the nuclei, merged image with CY2, CY3 and UV filters (A); Merged image depicting the endosomes and nuclei using CY3 and UV filters (B); Double Fluorescence microscopy, magnification 400x. Representative pictures of three independent experiments.

In contrast to metal-NLS bioconjugates, in case of the control compounds that is the metal-free K(FITC)-NLS (**7**)**,** the truncated peptides, CcC(O)-K(FITC)-V (**12**) and FcC(O)-K(FITC)-V (**13)**, an overall low and scattered fluorescence is observed with no or extremely weak fluorescence in the nuclei. For cells incubated with the non-metal containing conjugate **7** (Figures 3.2.3 A and B) very low fluorescence is seen in the cytoplasm and the nuclei.

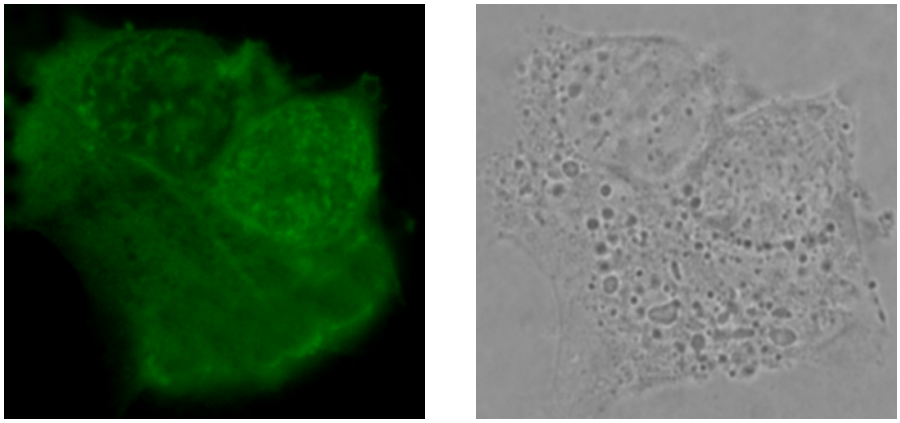

A B

Fig. 3.2.3: Distribution of metal-free bioconjugate 7, green fluorescence (CY2 filter) (A); Light microscopy (B); magnification 630x. Representative pictures of three independent experiments.

On the other hand, the truncated peptides **12** and **13** do not accumulate in the nuclei as observed by fluorescence microscopy. Most probably, these dipeptides entered the cells by diffusion but were not sufficiently accumulated to be visible intracellularly. In case of

CcC(O)-K(FITC)-V, the bioconjugate seems to adhere extracellulary on the membranes. Almost no fluorescence is seen intracellularly (Figures 3.2.4 A and B).

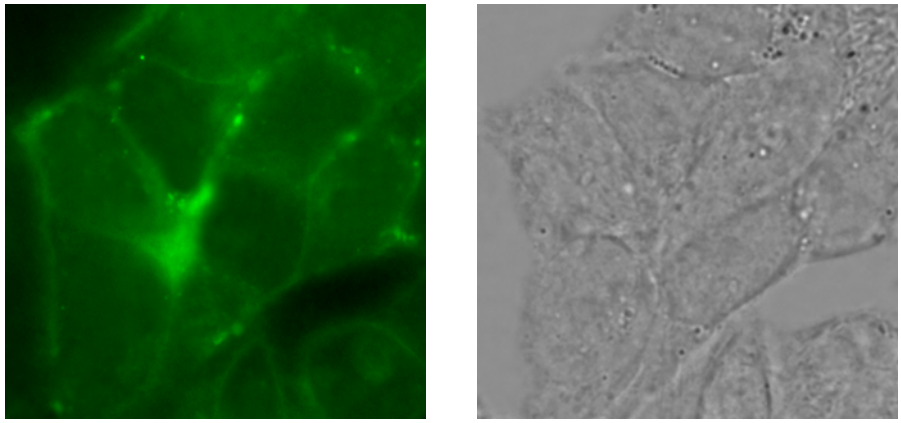

A B

Fig. 3.2.4: Distribution of truncated bioconjugate 12, green fluorescence (CY2) (A); Light microscopy (B); magnification 630x. Representative pictures of three independent experiments.

Similarly very low fluorescence was observed in the cytoplasm and none at all in the nuclei of the cells treated with FcC(O)-K(FITC)-V. In addition, bright dot like fluorescence was observed extracellularly (Fig. 3.2.5 A and B).

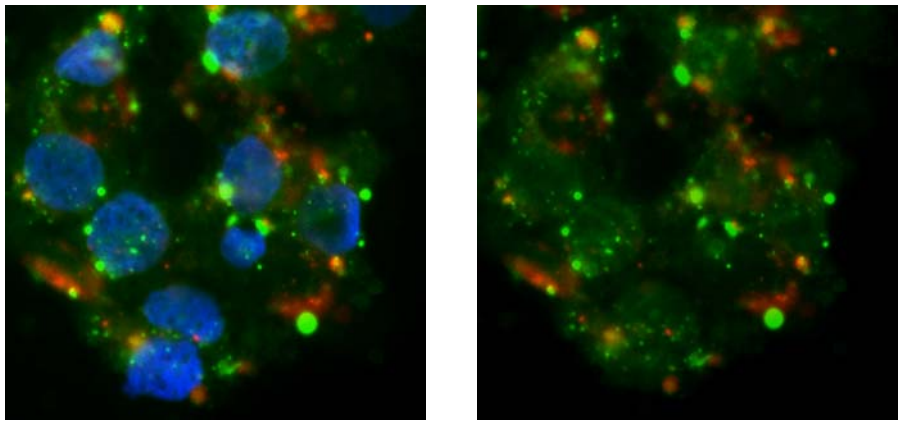

A B

Fig. 3.2.5: Localisation of bioconjugate 13, merged image, CY2, CY3 and UV filters (A); Merged image depicting the endosomes, CY2 and CY3 filters (B); Double Fluorescence microscopy, magnification 400x. Representative pictures of three independent experiments.

For all the metallocene-NLS and control compounds, some dot-like fluorescence is observed extracellularly and on the outer membrane, although to a varying degree (mostly for the control compounds, much less for the metallocene bioconjugates). It seems that these compounds adhere on the cell surface, a characteristic of basic cell penetrating peptides.

3.2.1.2 NLS_{scr} Bioconjugates

The role of the NLS upon cellular uptake and nuclear localisation could be determined by comparing the wild type NLS with the scrambled NLS. For this purpose, the scrambled sequence of the NLS (KKVKPKR) was used. Boffa et al have shown that this scrambled sequence is unable to target the nuclei of the cells. In this context it is necessary to note that the nuclear localisation function of the NLS is essentially dependent on the presence of Lys 128.[308]

Therefore, the ferrocene (**22**) and cobaltocenium conjugates (**21**) of the scrambled NLS sequence were synthesized. Both were similarly labelled with FITC for monitoring the uptake. FITC labelled metal-free scrambled peptide (**18**) was synthesized as a control. All the three compounds, **18**, **21** and **22**, showed similar behaviour: they were not localised in the endosomes, not distributed in the cytoplasm and no nuclear localization was observed in the concentrations tested (500µM and 100µM). Some bright green spots were seen extracellularly which is probably due to the tendency of these compounds to adhere to the cell membrane.

For the metal-free scrambled peptide **18**, the fluorescence was mostly extracellularly observed (Figures 3.2.6 A and B). This is probably due to adhering of the cationic peptide on the cell surface.

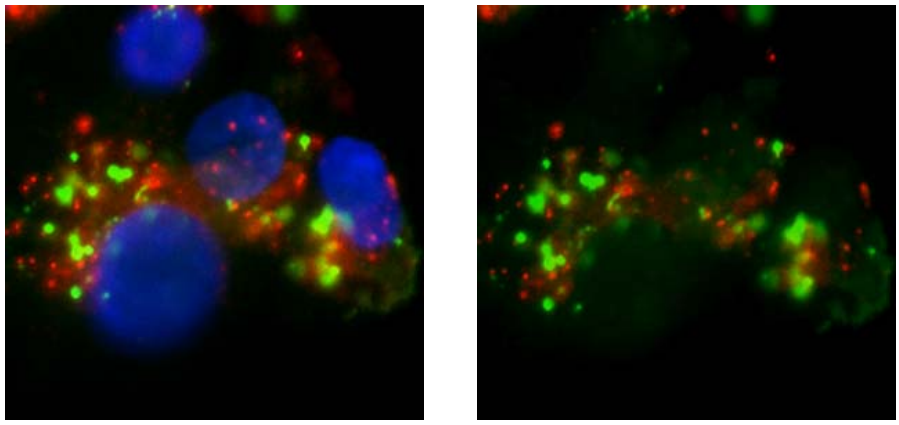

A **B**

Fig. 3.2.6: Distribution of bioconjugate 18, merged image green, red and blue fluorescence (A); Merged image depicting the endosomes, CY2and CY2 filters (B); Double Fluorescence microscopy, magnification 400x. Representative pictures of three independent experiments.

CcC(O)-K(FITC)-NLS_{scr} (**21**), was also unable toenter the cells. Figures 3.3.7 A and B, depict the endosomes and the nuclei. Some bright spots were visible extracellularly.

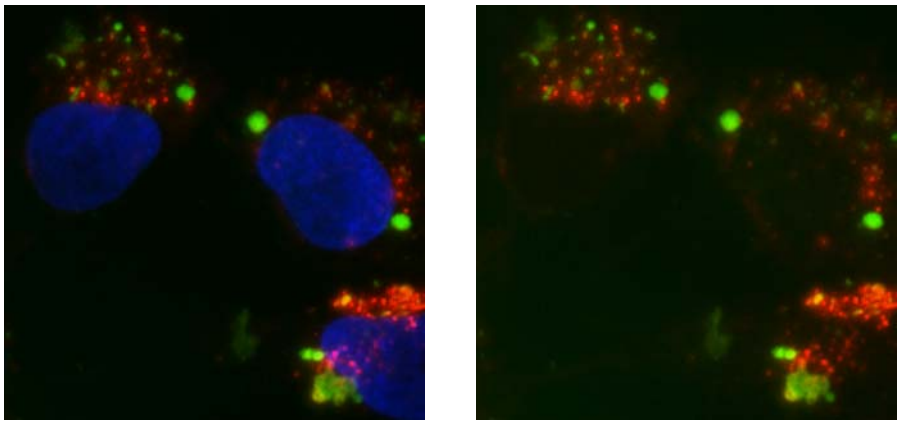

A **B**

Fig. 3.2.7: Distribution of bioconjugate 21, merged image green, red and blue fluorescence (A); Merged image depicting the endosomes, CY2 and CY3 filters (B); Double Fluorescence microscopy, magnification 400x. Representative pictures of three independent experiments.

Similarly in case of the Ferrocene bioconjugate of the scrambled NLS, **22**, no fluorescence was noted in either cytoplasm or in the nuclei while bright spots were visible extracellularly. (Figures 3.2.8 A and B).

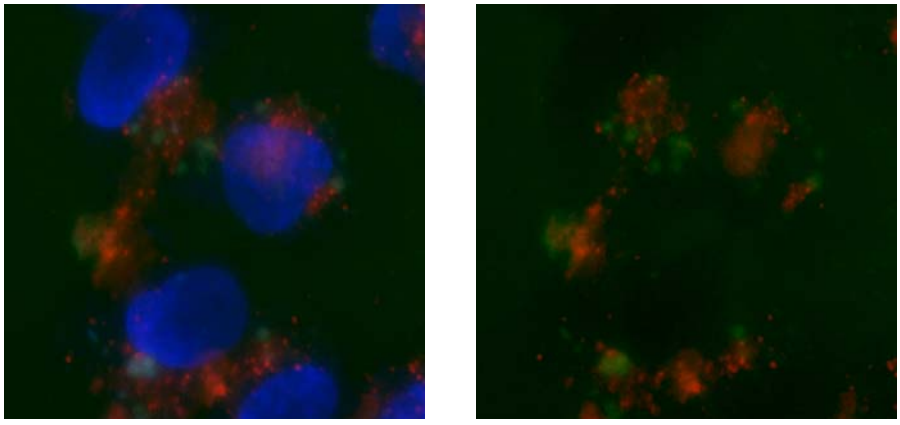

A **B**

Fig. 3.2.8: Distribution of bioconjugate 22, merged image green, red and blue fluorescence (A); Merged image depicting the endosomes, CY2 and CY3 filters (B); Double Fluorescence microscopy, magnification 400x. Representative pictures of three independent experiments.

3.2.1.3 TAT Bioconjugates

TAT is a sequence of 10 amino acids known as the viral transactivator of transcription. This Arginine rich cationic peptide (GRKKRRQRRR) functions as a carrier peptide and carries the cargos inside the cells across the cell membrane.

The TAT peptide was labelled with the cobaltocenium and ferrocene (bioconjugates **27** and **28** respectively) at the *N*-terminal. An additional Lysine was used for FITC labelling. As control, metal-free peptide **24** was also synthesized. All the three compounds were the tested using Hep G2 cells for cellular uptake and nuclear localisation.

The FITC labelled peptide (**24**) alone was not observed intracellularly in a concentration of 100µM. No fluorescence was noted in the cytoplasm or in the nuclei. Because some green fluorescence was observed extracellularly, the peptide seems to attach to the cell surface. (Figures 3.2.9 A and B).

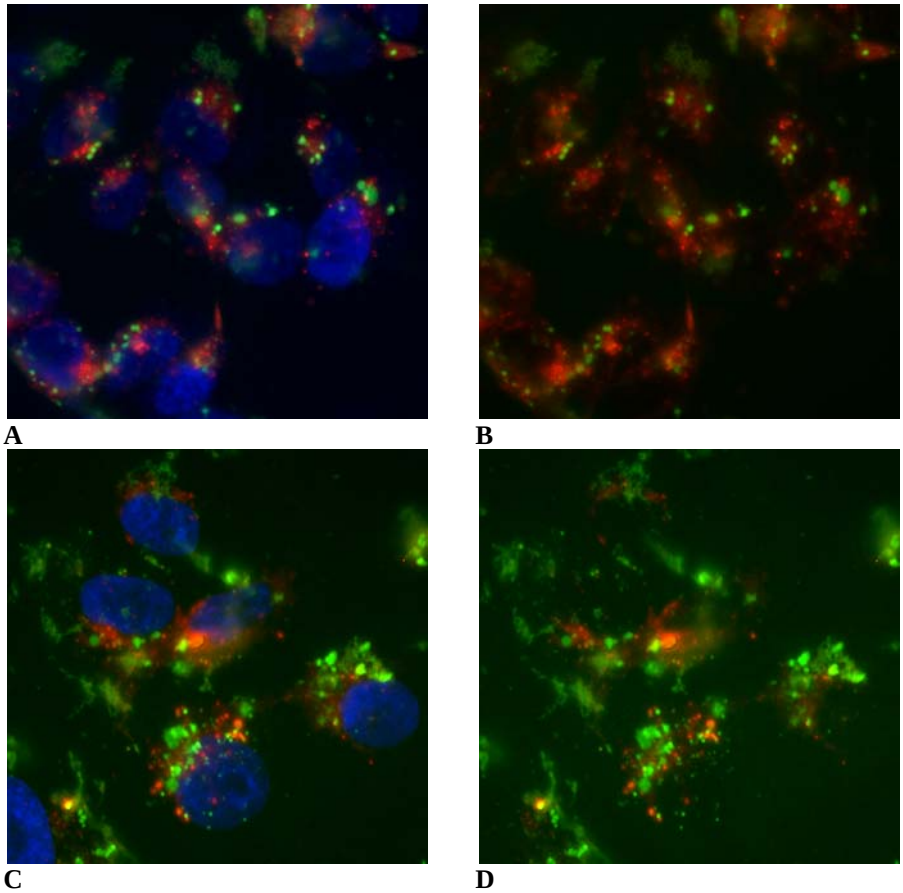

Fig. 3.2.9: Localisation of bioconjugate 24, merged image green, red and blue fluorescence (A); bioconjugate 24, merged image depicting the endosomes, CY2 and CY3 filters (B); Localisation of bioconjugate 27, merged image CY2, CY3 and UV filters (C); bioconjugate 27, merged image depicting the endosomes, CY2 and CY3 filters (D); Double Fluorescence microscopy, magnification 400x. Representative pictures of three independent experiments.

The CcC(O)-K(FITC)-TAT bioconjugate, **27** (100µM concentration), does not seem to gain access to either the intercellular compartments or the nuclei. Bright dot like fluorescence outside the cells indicates adhering of the compound on the cell surface (Figures 3.2.9 C and D).

In contrast, the ferrocene bioconjugate (**28**) at tested concentration of 10µM, seems to accumulate inside the cytoplasm of the cells as homogenous green fluorescence is observed intracellularly (Figure 3.2.10 A). However, the compound does not gain entry in the nuclei (Figure 3.2.10 B). The hydrophobic ferrocene moiety helps the internalisation of the peptide most likely by endocytosis and the escape from the endosomes seems to occur partially because a co-localisation of the compound in the endosomes is observed (Figure 3.2.10).

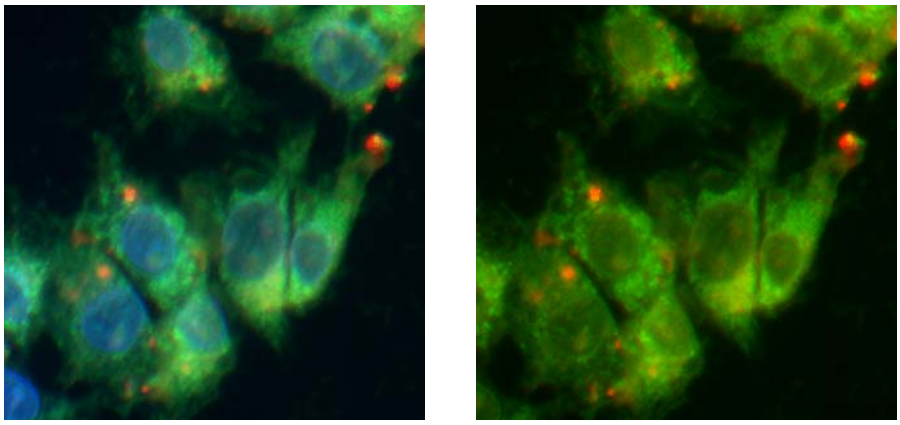

A **B**

Fig. 3.2.10: Distribution of bioconjugate 28, merged image CY2, CY3 and UV filters (A); bioconjugate 28, merged image depicting the endosomes, CY2 and CY3 filters; Double Fluorescence microscopy, magnification 400x. Representative pictures of three independent experiments.

3.2.2 Experiments with Fixed Cells

We also performed experiments using 2% paraformaldehyde for the fixation of the cells (20 minutes). After washing three times, the nuclei were stained with Hoechst dye for 5 minutes. For technical reasons the endosomal and nuclear staining was extremely difficult to carry out at the same time. Therefore, in one experiment cells were either stained with nuclear dye or with the endosomal marker. At the end, the coverslips were mounted in DAKO's Fluorescent mounting medium and stored at 4 °C in the dark.

3.2.2.1 NLS Bioconjugates

Identical results were obtained for cellular uptake and nuclear localisation for fixed or live cells. In case of the cobaltocenium bioconjugate (**10**) homogenous fluorescence is observed in the cytoplasm while stronger fluorescence is noted inside the nuclei (Figures 3.2.11 A and B). The endosomal staining indicates localisation of the bioconjugate in the endosomes but not extensively (Figures 3.1.11 C and D). Most probably the endosomes were permeable and opene after the time of treatment.

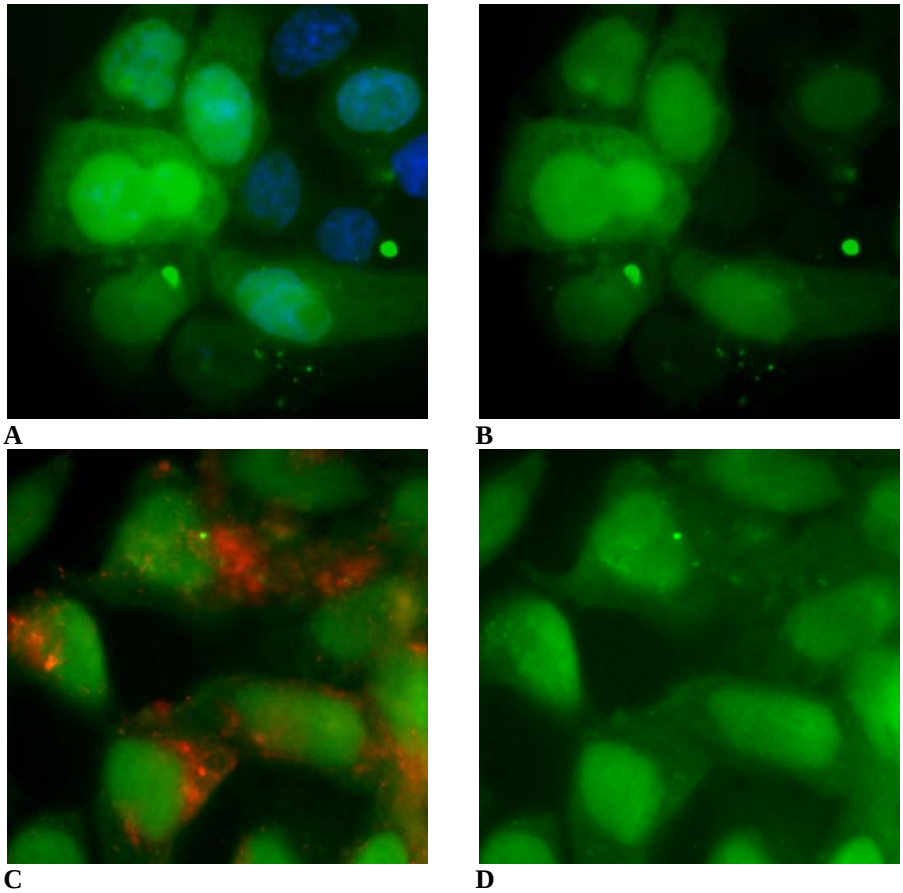

Fig. 3.2.11: Localisation of bioconjugate 10 after incubation with 5µM of the endosomal marker, FM 4-64 for 15 minutes or with Hoechest dye for nuclear staining for 5 minutes, merged image, CY2 and UV filters (A); bioconjugate 10, merged image depicting the endosomes, CY2 and CY3 filters; The cells were fixed with 2% paraformaldehyde and mounted in DAKO's fluorescent mounting medium. Double Fluorescence microscopy, magnification 630x. Representative pictures of three independent experiments.

Similarly, in case of the the ferrocene-labelled bioconjugate, **11** three kinds of fluorescence was observed. The bioconjugate was observed to be homogenously distributed in the cytoplasm and accumulated in the nuclei as shown by the strong green fluorescence in the

nuclei and weaker, but homogenous green fluorescence in the cytoplasm. Some bright dot like fluorescence was also observed extracellularly (Figures 3.2.12 A and B).

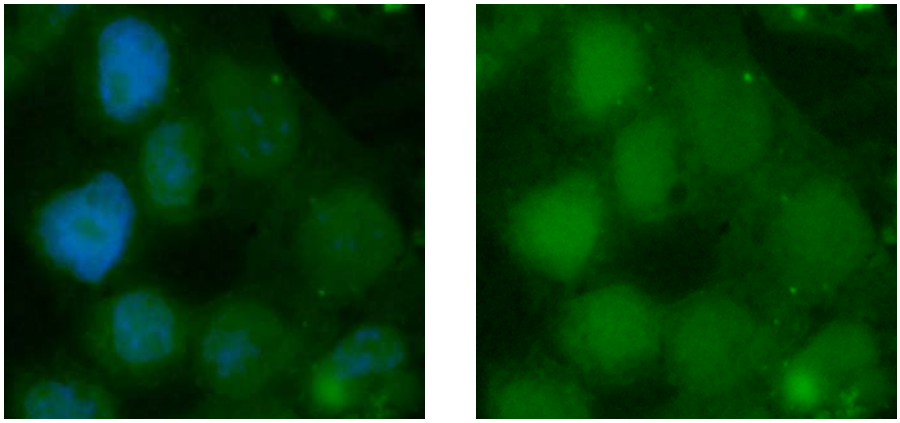

A **B**

Fig. 3.2.12: Localisation of bioconjugate 11, merged image, CY2 and UV filters (A); nuclear localization of bioconjugate 11 (B); The cells were fixed with 2 % paraformaldehyde and mounted in DAKO's fluorescent mounting medium. Double Fluorescence microscopy, magnification 630x. Representative pictures of three independent experiments.

The bioconjugate was co-localised with the endosomal marker (FM 4-64) (Fig. 3.2.13 A and B).

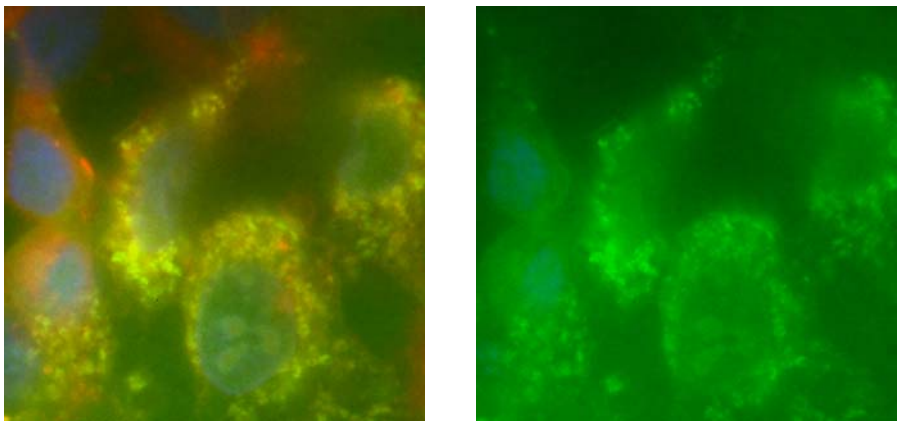

A **B**

Fig. 3.2.13: Localisation of bioconjugate 11 in the endosomes after incubation with 5µM of the endosomal marker FM 4-64 for 15 minutes, merged image, CY2, CY3 and UV filters (A); bioconjugate 11, CY2 filter; The cells were fixed with 2 % paraformaldehyde and mounted in DAKO's fluorescent mounting medium. Double Fluorescence microscopy, magnification 630x. Representative pictures of three independent experiments.

The control compound, the metal free peptide **7**, (Figures 3.2.14 A-D) very little internalisation is seen. Bright spots are visible extracellularly indicating adherance to the cell

surfaces or localisation among the cells. Due to its highly charged nature, the peptide seems to clump together therefore, dot-like fluorescence is observed extracellularly.

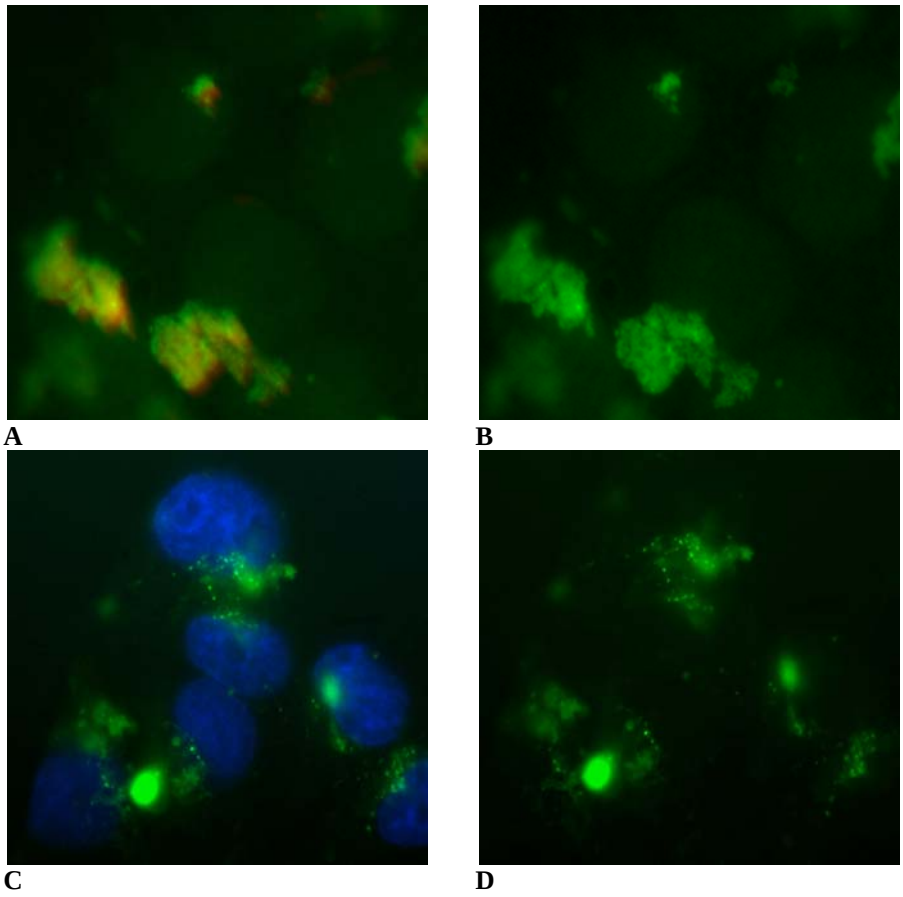

Fig. 3.2.14: Localisation of bioconjugate 7, after incubation with 5µM of the endosomal marker FM 4-64 for 15 minutes, CY2 and CY3 filters (A); Distribution of bioconjugate 7, CY2 filter (B) Localisation of bioconjugate 7, merged image, CY2 and UV filters (C); Distribution of bioconjugate 7 (D); The cells were fixed with 2% paraformaldehyde and mounted in DAKO's fluorescent mounting medium. Double Fluorescence microscopy, magnification 630x. Representative pictures of three independent experiments..

The truncated peptides CcC(O)-K(FITC)-V (**12**) and FcC(O)-K(FITC)-V (**13**), used as controls, do not gain access to the nuclei. They are not localised in the endosomes. Extracellular bright fluorescence is observed in both cases (Figures 3.2.15 A-D).

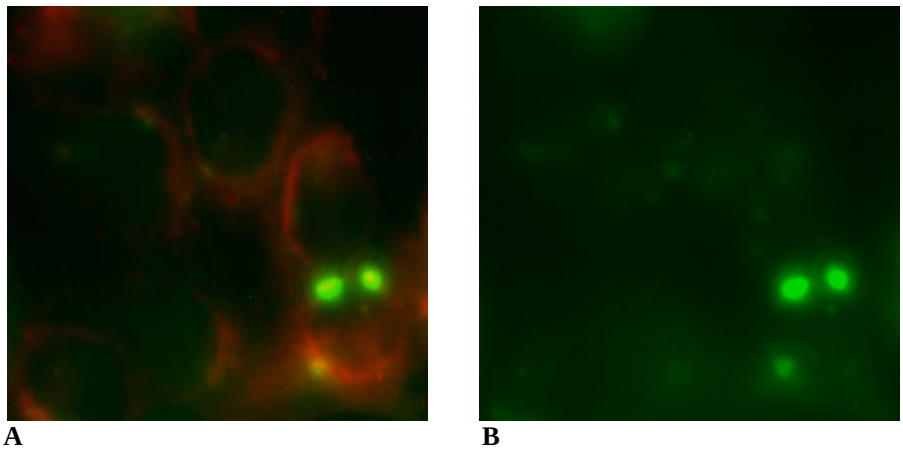

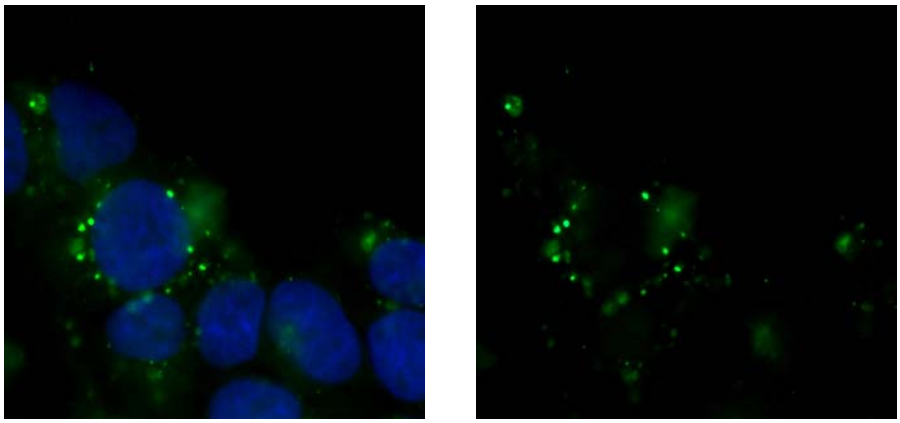

C D

Fig. 3.2.15: Cells after treatment with bioconjugate 12 and incubation with 5µM of the endosomal marker FM 4-64 for 15 minutes, CY2 and CY3 filters (A); Distribution of bioconjugate 12, CY2 filter (B) Localisation of bioconjugate 13, merged image, CY2 and UV filters (C); Distribution of bioconjugate 12 (D); Double Fluorescence microscopy, magnification 630x. Representative pictures of three independent experiments.

3.2.2.2 NLS_{scr} Bioconjugates

In case of the control, the metal-free peptide **18**, few bright spots are observed outside the cells. The compound is neither visible in the cytoplasm nor in the nuclei (Figure 3.2.16).

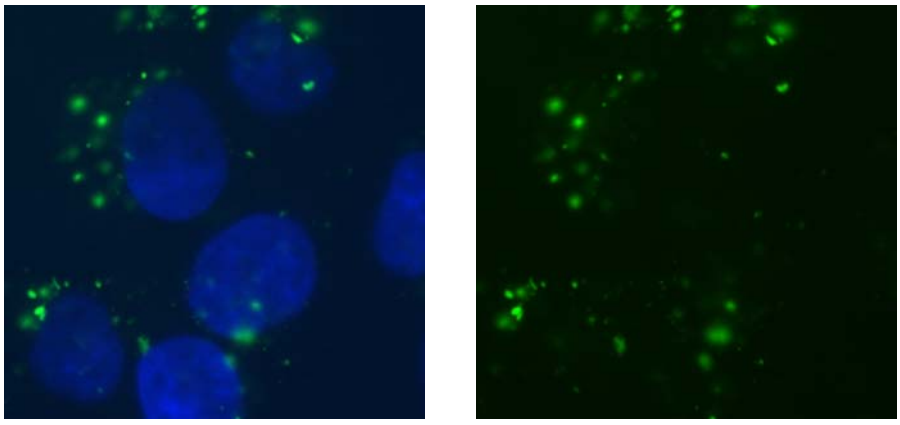

A B

Fig. 3.2.16: Localisation of bioconjugate 18, merged image, CY2 and UV filters (A); Distribution of bioconjugate 18, CY2 filter (B); The cells were fixed with 2 % paraformaldehyde and mounted in DAKO's fluorescent mounting medium. Double Fluorescence microscopy, magnification 630x. Representative pictures of three independent experiments.

The metal labelled peptides **21** and **22** (with cobaltocenium and ferrocene respectively), do not gain access to the nuclei and no fluorescence is observed in the cytoplasm as well (Figures 3.2.17 A-D). The peptide seems to clump together and adhere to the cell surface.

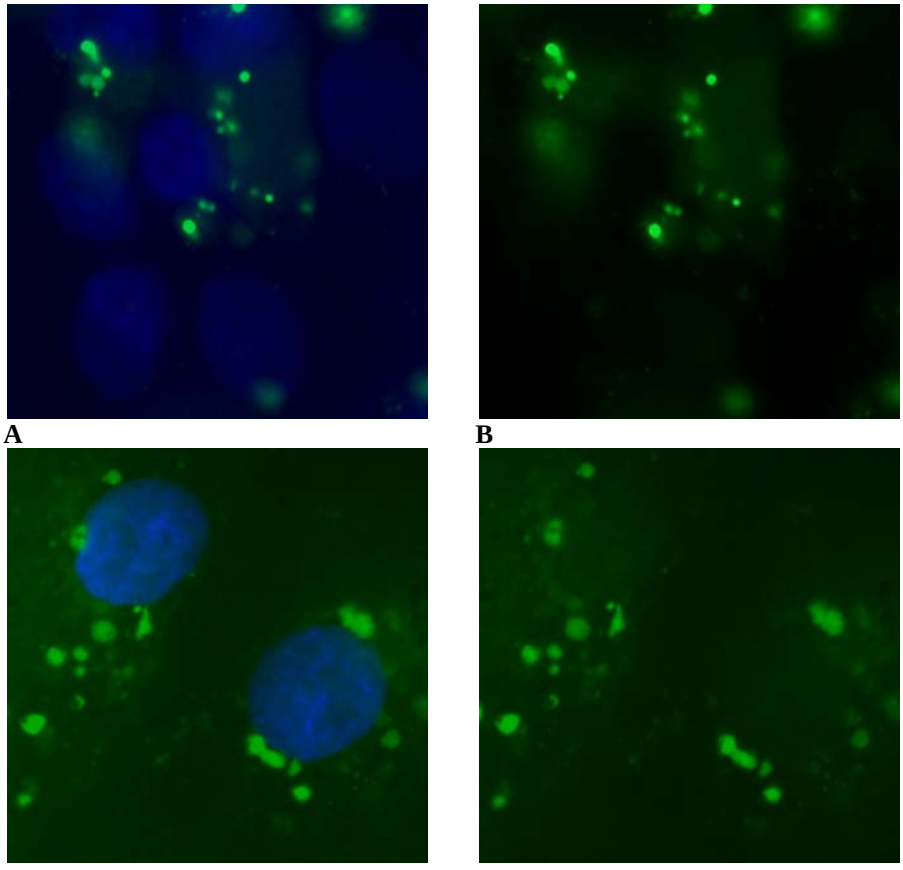

A **B**

C **D**

Fig.3.2.17: Localisation of bioconjugate 21, merged image, CY2 and UV filters (A); Distribution of bioconjugate 21, CY2 filter (B); Localisation of bioconjugate 22, merged image, CY2 and UV filters (C); Distribution of bioconjugate 22, CY2 filter (D); The cells were fixed with 2 % paraformaldehyde and mounted in DAKO's fluorescent mounting medium. Double Fluorescence microscopy, magnification 630x. Representative pictures of three independent experiments.

Some yellow spots are seen inside the cells indicating that some of the compounds might be trapped in the endosomes upon internalisation (Figures 3.2.18 A-D).

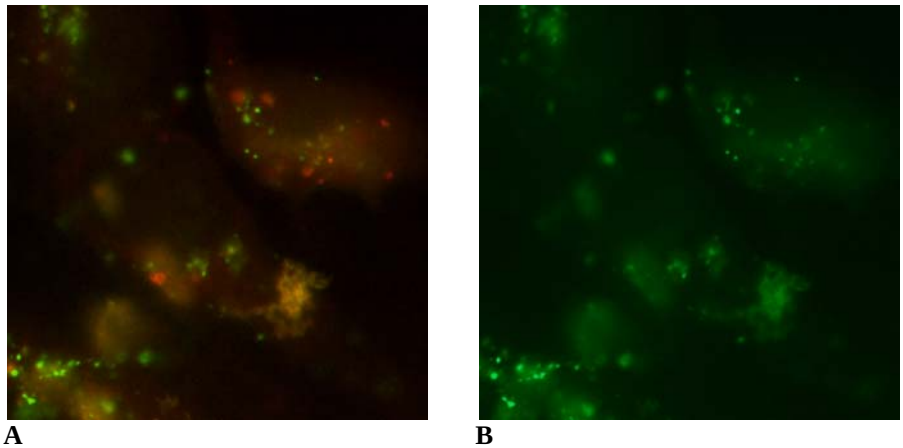

A **B**

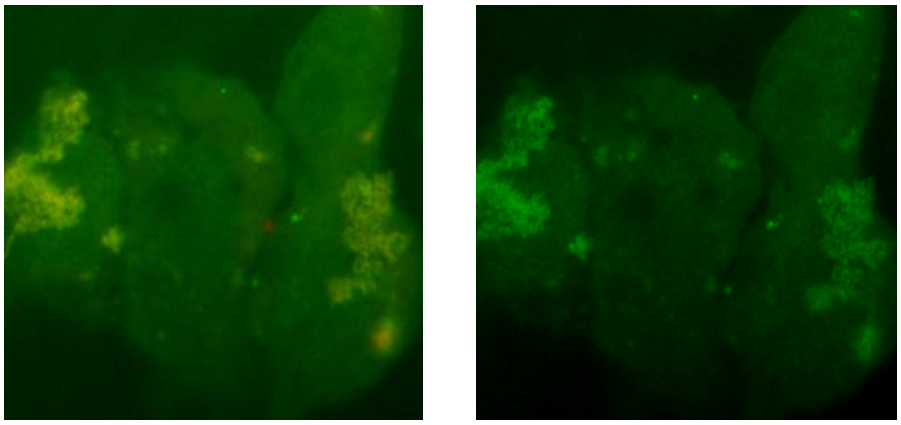

C D

Figure 3.2.18 : Localisation of bioconjugate 21 and endosomes after incubation with the endosomal marker FM 4-64 (5µM) for 15 minutes, merged image, CY2 and CY3 filters (A); Distribution of bioconjugate 21, CY2 filter (B); Localisation of bioconjugate 22, and endosomes after incubation with the endosomal marker FM 4-64 (5µM) for 15 minutes, merged image, CY2 and CY3 filters (C); Distribution of bioconjugate 22, CY2 filter (D); Double Fluorescence microscopy, magnification 630x. Representative pictures of three independent experiments.

3.2.2.3 TAT Bioconjugates

The TAT bioconjugates showed a different behaviour as compared to the NLS bioconjugates. The Ferrocene and cobaltocenium bioconjugates of TAT were synthesized and tested in a similar way as that of NLS under similar conditions.

The control, metal-free peptide **24**, was not found to be localised in the nuclei (Figure 3.2.19 A and B). However, in some cells scattered fluorescence is seen intracellularly (Figures 3.2.19 C and D).

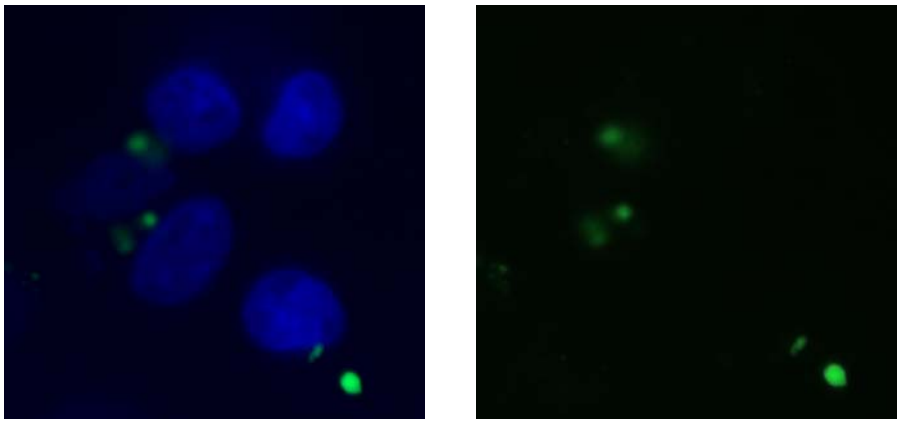

A B

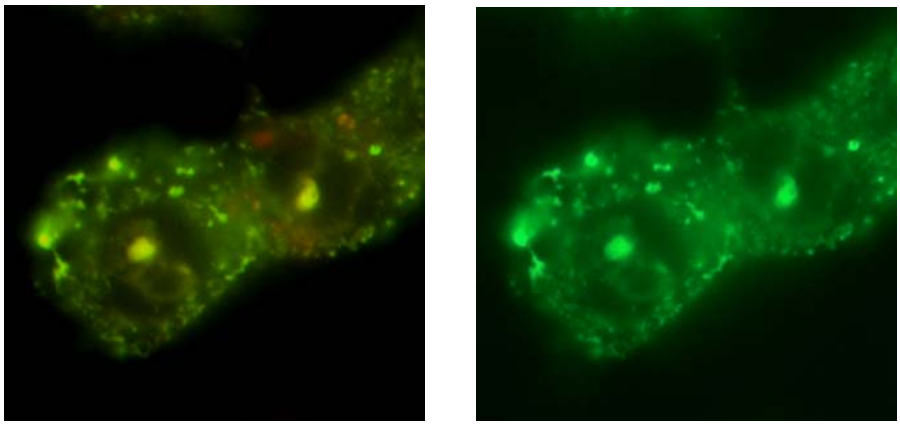

C D

Fig. 3.2.19: Localisation of bioconjugate 24 and nuclei after nuclear staining with Hoechst dye 33342 for 5 minutes, merged image, CY2 and UV filters (A); Distribution of bioconjugate 24, CY2 filter (B); Localisation of bioconjugate 24 and endosomes after incubation with the endosomal marker FM 4-64 (5µM) for 15 minutes, merged image, CY2 and CY3 filters (C); Distribution of bioconjugate 24, CY2 filter (D); The cells were fixed with 2 % paraformaldehyde and mounted in DAKO's fluorescent mounting medium. Double Fluorescence microscopy, magnification 630x. Representative pictures of three independent experiments.

After fixation of the cells, the cobaltocenium bioconjugate (**27**) is found to be localised intracellularly. Weak fluorescence is observed in the cytoplasm, but not in the nuclei (Figures 3.2.20 A and B). Some very bright spots are also observed outside the cells indicating adherence of the peptide on the cell surface.

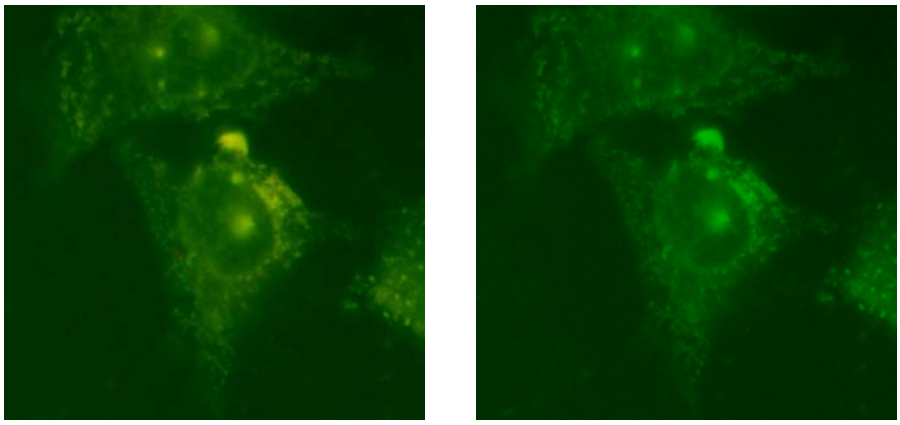

A B

Fig. 3.2.20: Localisation of bioconjugate 27 and endosomes after incubation with the endosomal marker FM 4-64 (5µM) for 15 minutes, merged image, CY2 and CY3 filters (A); Distribution of bioconjugate 27, CY2 filter (B); The cells were fixed with 2 % paraformaldehyde and mounted in DAKO's fluorescent mounting medium. Double Fluorescence microscopy, magnification 630x. Representative pictures of three independent experiments.

The ferrocene bioconjugate **28** seems to be internalised by the cells as indicated by the strong fluorescence in the cytoplasm. The bioconjugate, however, does not gain access to the nuclei (Figure 3.2.21). However, the bioconjugate is unable to enter the nuclei. It can not be proved whether this bioconjugate is localised with the endosomes.

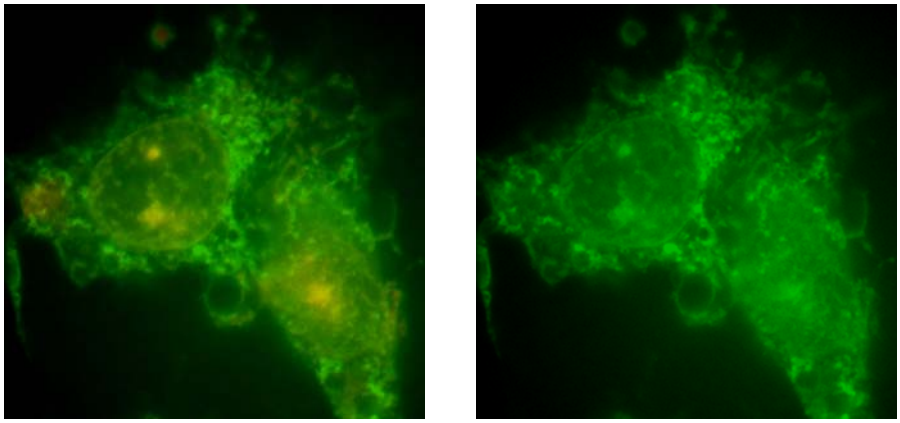

A **B**

Figure 3.2.21 : Localisation of bioconjugate 28 and endosomes after incubation with the endosomal marker FM 4-64 (5µM) for 15 minutes, merged image, CY2 and CY3 filters (A); Distribution of bioconjugate 28, CY2 filter (B); The cells were fixed with 2 % paraformaldehyde and mounted in DAKO's fluorescent mounting medium. Double Fluorescence microscopy, magnification 630x. Representative pictures of three independent experiments.

3.3 Proliferation Assay

WST/CV assay

For the screening of the compounds for their potential cytotoxic effects, the WST-1 assay, which is an easy, non-radioactive, spectrophotometric quantification of cell growth and viability was used. The WST-1 assay is a direct measurement of the cell viability. The tetrazolium salt WST-1 is cleaved to water soluble formazan dye by cellular enzymes (scheme 3.3.1). An expansion in the number of viable cells results in an increase in the overall activity of mitochondrial dehydrogenases in the sample which will in turn lead to an increase in the formation of the formazan dye. This increase in the formazan dye can be quantified by measurement of the absorbance on a microtiterplate reader and correlates directly to the number of metabolically active cells in the culture.

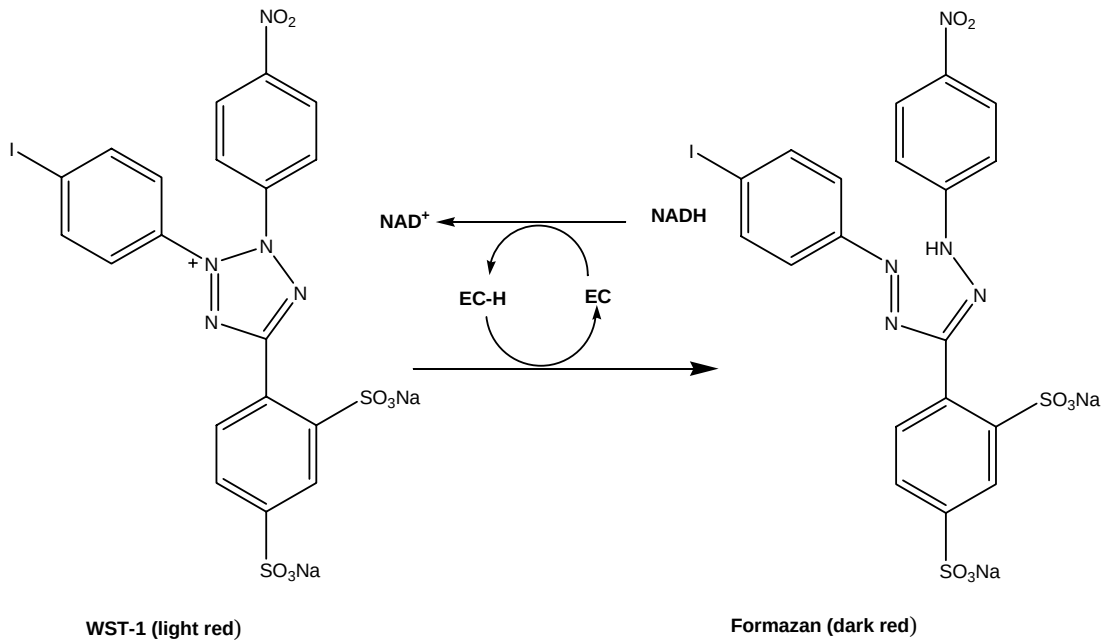

Scheme 3.3.1: Cleavage of the tetrazolium salt WST-1 to formazan (EC=electron coupling reagent)

The crystal violet cell quantification assay[305] was done after the WST-1 assay to determine the remnant number of adherent cells in order to correct the differences in cell numbers seeded in different wells. Crystal violet is a triphenylmethane dye that stains the membranes of viable cells. [305]

To begin with, the Hep G2 standard population curve was drawn using different cell populations and their treatment with crystal violet (Figure 3.3.1) in order to determine the optimal number of cells required for the assays.

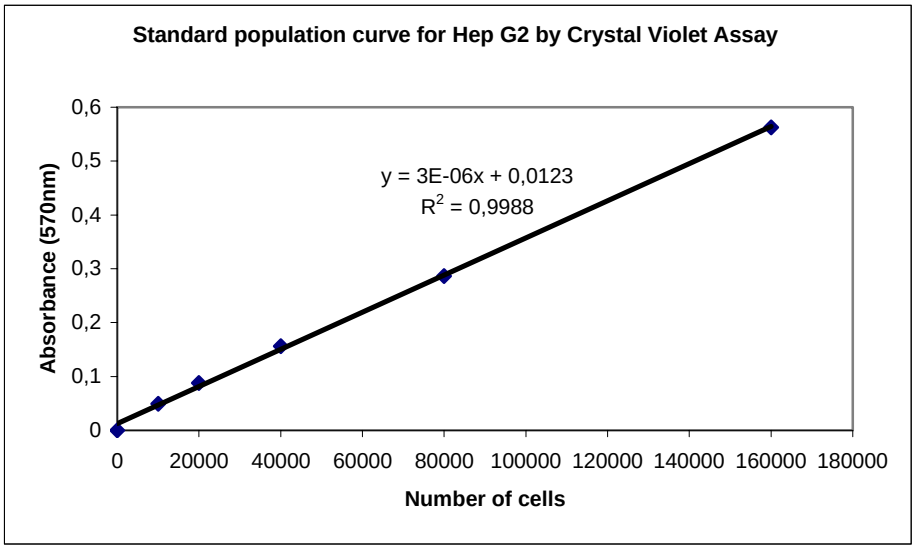

Fig. 3.3.1: Standard population curve for Hep G2 cells as determined by crystal violet cell quantification assay. After trypsinisation, the cells in suspension were first fixed with 4% paraformaldehyde for 5 minutes, diluted and centrifuged. After one washing the pellet was resuspended in 2 ml of Crystal violet solution and shaken for 1 hour. Following dilution, the cells were again centrifuged. The pellet was resuspended in distil water and centrifuged, this step of washing was repeated 5 times. Finally the pellet was resuspended in a fixed volume of water and the cells counted. Different dilutions containing different number of cells were made and taken in a 96-well plate (5 wells for each dilution). The cells were then treated with 1 %SDS solution for 30 minutes. The absorbance was measured on the ELISA reader at 570 nm against a reference wavelength at 655nm.

The standard population curve also shows that a linear relationship exists between the number of cells and the increase in the absorbance. The minimum number of cells for satisfactory measurement of absorbance was estimated to be around 20,000 cells per well. The doubling time of Hep G2 cells is 50-60 hours.[302, 303] Therefore, for all experiments 20,000 cells were seeded and treated with the test compounds after 12 hours and the assay was carried out after 48 hours.

Similarly, another experiment was carried out to determine the optimal time of incubation with WST-1 for Hep G2 cells. A fixed number of cells were seeded in 12 wells of a 96-well plate and incubated with WST-1 reagent at 37°C and measurements were recorded every 30 minutes for 4 hours. At the end the readings were further corrected by quantification of adherent cells by CV assay (Figure 3.3.2). It was observed that the maximum absorbance was achieved after one hour of incubation with WST-1 reagent after which a plateau was reached.

Therefore, one hour was taken as the optimal time for incubation of Hep G2 cells with WST-1 in all experiments.

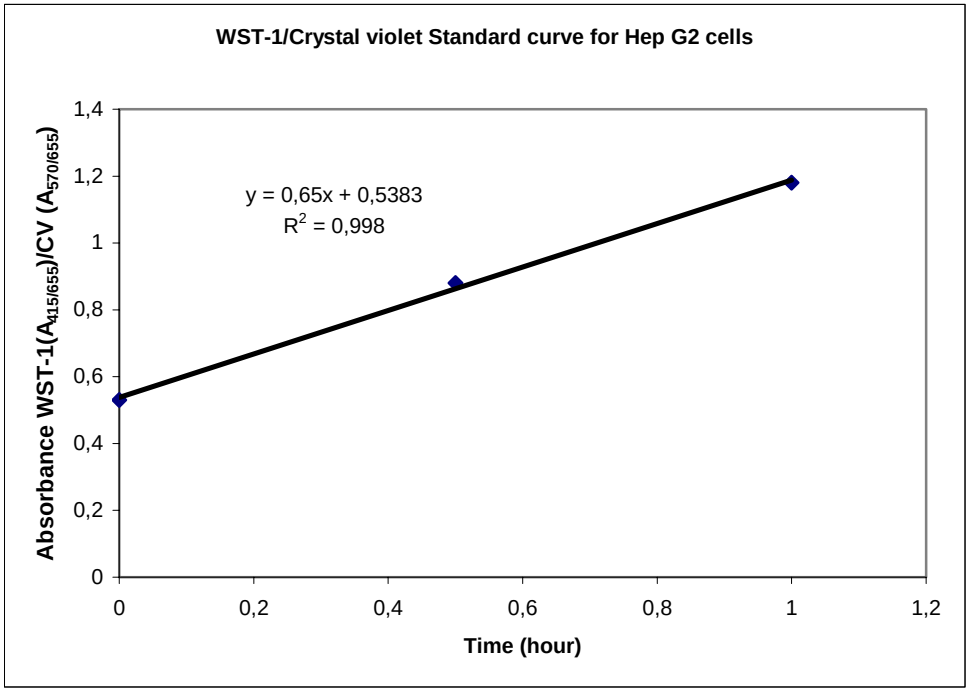

Fig. 3.3.2: Standard curve showing the optimal time of incubation of Hep G2 cells with WST-1 reagent. $5x10^4$ cells were seeded in 12 wells and incubated with 10 µl of WST-1 reagent at 37°C for 4 hours. Readings were taken every 30 minutes at 415 nm against a reference wavelength at 655 nm. The cells were then fixed with 4% PFA in PBS and after one washing, were treated with Crystal violet for 1 hour. After several washings the cells were treated with 1 % SDS for 40 minutes and the absorbance was measured at 570 nm against a reference at 655 nm.

Determination of the optimum number of Hep G2 cells and the optimal time of incubation with WST-1 reagent, permitted to proceed further with the actual cytotoxic screening of the synthesized compounds. The metal-peptide bioconjugates, not labelled with FITC, were screened for cytotoxic effects in the same concentrations as were used for the uptake studies. It should be noted that Vinblastine sulphate was used as the positive control in same concentrations as for the test compounds and was found to be cytotoxic in all the tested concentrations. Untreated cells represent the negative control and will be simply denoted as control in later descriptions.

Metallocene-NLS (wild type & scrambled) Bioconjugates

The proliferation rates are presented in Figure 3.3.3 as percentage of the control with ± SEM. The compounds K-NLS, CcC(O)-K-NLS and FcC(O)-K-NLS, in all tested concentrations (0.1, 0.5 and 1mM) revealed no statistically significant difference in the proliferation of the Hep G2 cells when compared to the control. Similarly, in case of K-NLS_{scr} and FcC(O)-K-NLS_{scr} no statistically significant difference in cell proliferation was found with respect to the control. In contrast, CcC(O)-K-NLS_{scr} exhibited a slightly significant difference compared with control in concentrations of 1mM and 0.5mM, indicating a stimulatory effect of this compound on the proliferation of the Hep G2 cells.

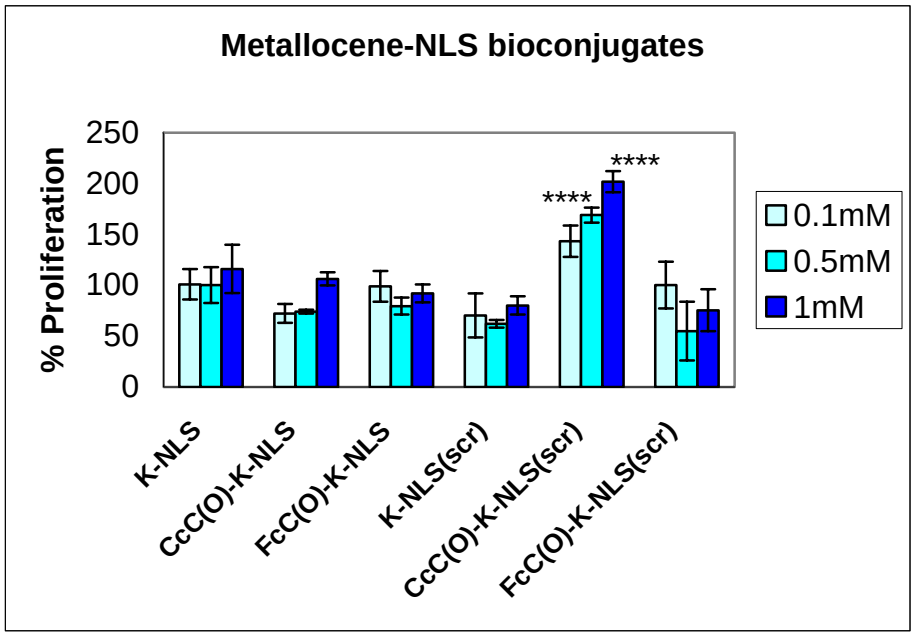

Fig. 3.3.3: Hep G2 proliferation rates after treatment with the metallocene-NLS bioconjugates (percentage of the control). Data represent the mean ±SEM. The histogram and error bars represent mean of four values and the standard error mean respectively. (****p<0.001).

Platinum-NLS Bioconjugates

The two platinum-NLS bioconjugates were also tested for their antiproliferative effects, which are presented in Figure 3.3.4. The results are presented as percentage of the control. Both compounds had no significant effect on the proliferation of Hep G2 cells in concentration of 0.1mM as compared to the control and Pt-BB-NLS had no significant effect in 0.5mM concentration as well.

Pt-DAP-NLS was found to be cytotoxic in 0.5 and 1 mM concentrations. Pt-BB-NLS also showed antiprolifertiave effect in a concentration of 1 mM as indicated by the significant difference with respect to the control.

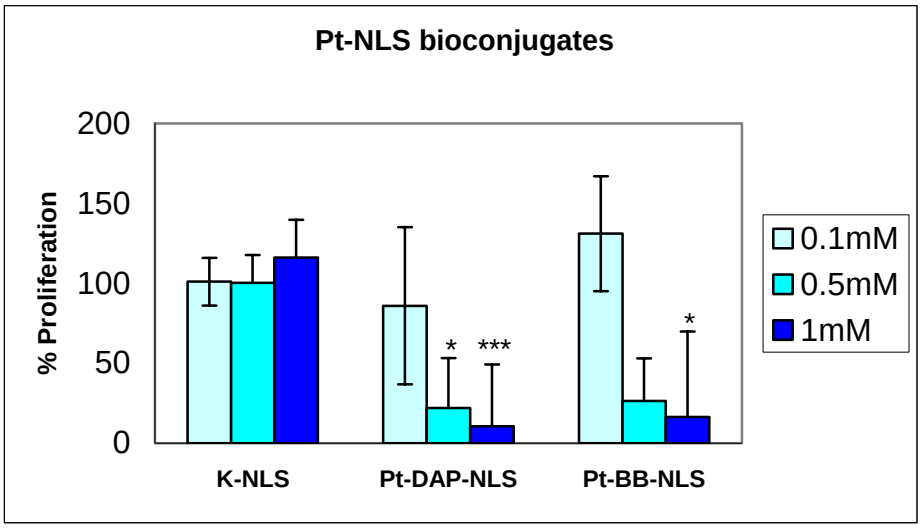

Fig. 3.3.4: Hep G2 proliferation rates after treatment with the Pt-NLS bioconjugates (percentage of the control). Data represent mean ±SEM. The histogram and error bars represent mean of four values and the standard error mean respectively. (***p<0.005, *p<0.05)

Metallocene-TAT Bioconjugates

The metallocene-TAT bioconjugates (not labelled with FITC) were tested for their cytotoxic effects (Figure 3.3.5). The results are presented as percentage of the control. K-TAT is non cytotoxic in all the tested concentrations as compared to the control. FcC(O)-K-TAT and CcC(O)-K-TAT are non toxic in 0.1 mM concentration. However, both these compounds are toxic when used at 0.5 and 1mM concentrations as indicated by the significant difference when compared to the control.

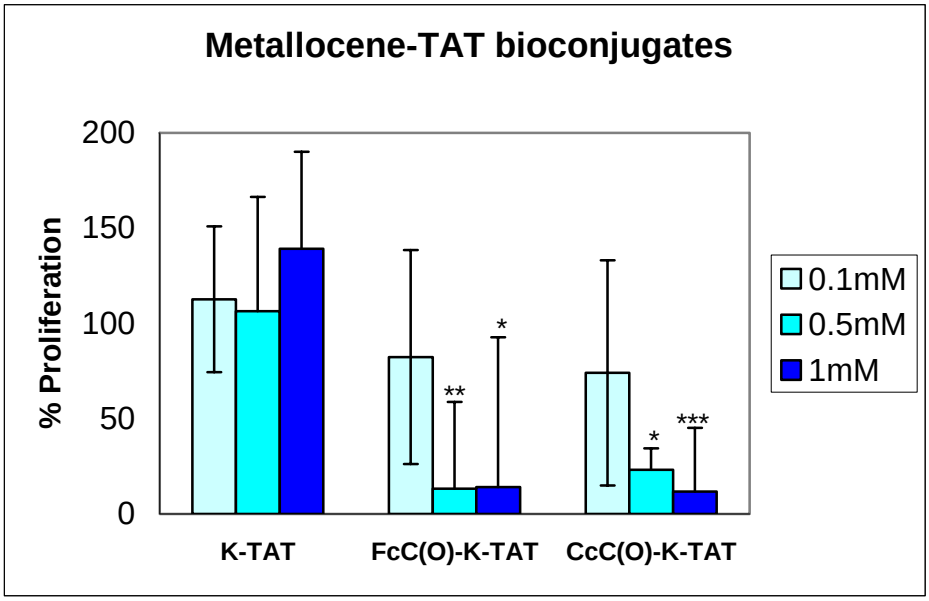

Fig. 3.3.5: Hep G2 proliferation rates after treatment with the metallocene-TAT bioconjugates (percentage of the control). Data represent ±SEM. The histogram and error bars represent mean of four values and the standard error mean respectively. (***p<0.005, **p<0.01, *p<0.05)

3.4 Receptor Binding Studies

The affinity of various neurotensin bioconjugates to NTR1 receptor subtype of the neurotensin receptor in human colon adenocarcinoma HT-29 cells was determined. These studies were carried out in collaboration with Prof. Dr. P. Bläuenstein by Dr. E. Garcia-Garayoa at the Centre for Radiopharmaceutical Science, Paul Scherrer Institute, Villingen, Switzerland.

^{99m}Tc-NT-II [retro-N^{α}-carboxymethylhistidine-NT(8-13) at a concentration of 2 kBq/ml was used as the radiotracer. ^{99m}Tc-NT-II was selected since it is based on the sturcture NT(8-13) and shows a high affinity for NT receptors (Kd 0.5 nM). The affinity was even higher than that obtained for ^{125}I-NT (Kd 1.6 nM).[297] The synthesized NT bioconjugates inhibited the binding of ^{99m}Tc-NT-II showing typical sigmoid curves (Figure 3.4.1).

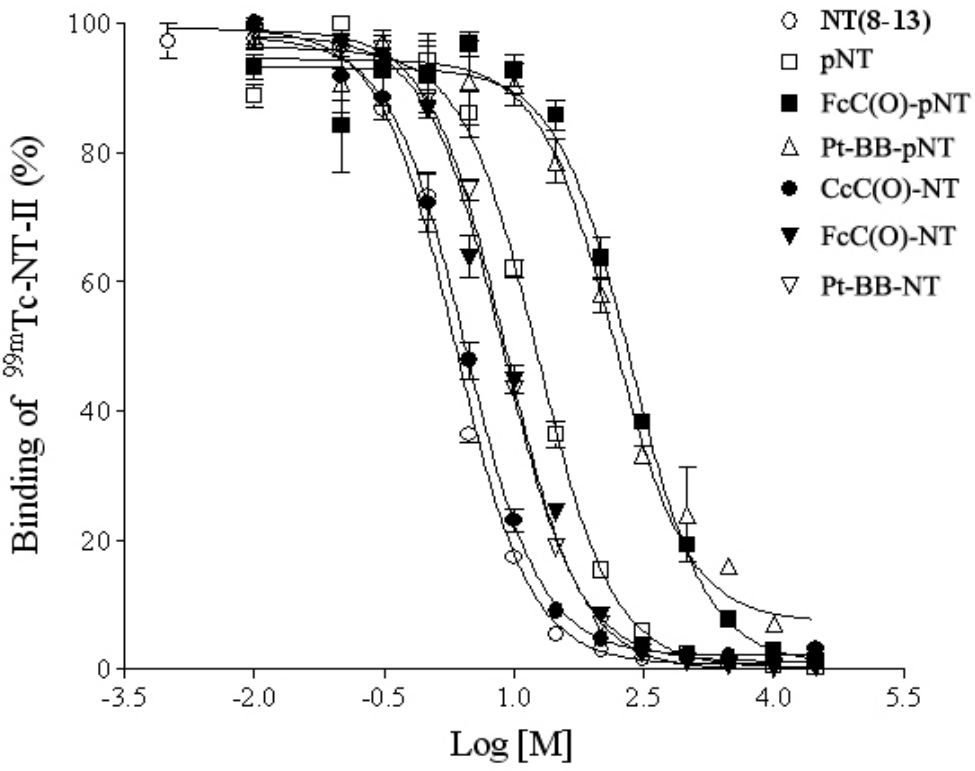

Figure 3.4.1: Log-dose competitive inhibition of binding of ^{99m}Tc-NT-II by various concentrations of different unlabeled **NT** and **pNT** bioconjugates. Each point represents the mean ± SD of triplicate determinations. (Picture kindly provided by Dr. Garcia-Garayoa)

The results of the inhibition studies yielding the respective IC_{50} of various neurotensin bioconjugates is summarized in table 3.4. The IC_{50} is the concentration needed to displace

50% of the radiotracer from the receptor. Thus a lower IC_{50} indicates a better affinity to the receptors since a lower concentration is needed to displace the radiotracer from the receptor. Higher the IC_{50} lower is the affinity. An IC_{50} similar or lower than that of the NT(8-13) is the criterion for good affinity for a given compound.

Table 3.4: Binding properties of NT and pNT neurotensin bioconjugates. Data are from atleast 3 experiments.

Comp. no.	**Sequence**	**Bioconjugate**	**IC_{50} (nM)**
	RRPYIL	NT(8-13)	1.8 ± 1.5
29	KKPYIL	pNT	27.5 ± 15.1
30	FcC(O)-KKPYIL	FcC(O)-pNT	238.1 ± 72.3*† ‡
32	Pt-BB-KKPYIL	Pt-BB-pNT	148.4 ± 19.2*† ‡
34	CcC(O)-RRPYIL	CcC(O)-NT	2.3 ± 0.4
35	FcC(O)-RRPYIL	FcC(O)-NT	21.0 ± 18.9
36	Pt-BB-RRPYIL	Pt-BB-NT	6.8 ± 2.2

All the experiments were performed using ^{99m}Tc-NT-II [NT-II= retro-N$^{\alpha}$-carboxymethyl histidine-NT(8-13)] as radiotracer (Kd = 0.5 nM).
* P<0.001 vs NT(8-13), † P<0.001 vs pNT (**29**), ‡ P<0.001vs. the corresponding metal bioconjugate, one-way ANOVA followed by Tukey's post test.

Replacement of Arg^8-Arg^9 with Lys-Lys in pNT (**29**) leads to a decrease in affinity with an IC_{50} approximately 15 times higher than that of the NT(8-13) although it was not statistically significant. A notable loss of affinity was observed in the two metal-NT bioconjugates, FcC(O)-pNT and Pt-BB-pNT, in which the arginines were replaced with lysines. The compounds showed IC_{50} of 238.1±72.3 and 148.4±19.2 respectively.

The CcC(O)-NT bioconjugate exhibited an IC_{50} (2.3±0.4 nM) comparable to the native NT(8-13) indicating a good affinity for the NTR1 receptors. Whereas, affinity for FcC(O)-NT is almost 10 times lower. The platinum bioconjugate, Pt-BB-NT, also exhibited an improved IC_{50} (6.8±2.2nM) in case when the unmodified sequence of neurotensin was used. The affinity was only 3.5 times lower that the NT(8-13) and around 21 times better than the Pt-BB-pNT bioconjugate.

Discussion

Recently, Peptide and protein-based drugs have rapidly become extensively investigated therapeutic agents. The global pharmaceutical industry is now paying great attention to the preclinical and clinical development of such drugs. In this regard, a comprehensive knowledge of the absorption and distribution properties beyond physicochemical properties, including the chemical and metabolic stability at the absorption site, passage through biomembranes and active uptake, is essential. Binding phenomenon and receptor-mediated cellular uptake are further complicating factors, in addition to generalised elimination and proteolysis as well as exsorption and receptor-mediated endocytosis at the cellular level.

Syntheses of the peptide bioconjugates

Bioorganometallic conjugates of bioactive peptides may lead to novel applications in therapy and diagnosis based on the unusual characteristics of the organometallic moieties as well as on the natural or modified biological activities of these peptides. Efficient and easy synthesis procedures are crucial for the success of such bioconjugates.

The first objective was to successfully synthesize the metal-peptide bioconjugates and to optimise the conditions for syntheses. Moreover, the characterization of these bioconjugates should be possible with normal routine techniques such as NMR, HPLC and MS. All the bioconjugates, presented in this thesis, were synthesized using the modified strategy (e.g. using Fmoc instead of Boc protecting groups) of the famous Merrifield synthesis on a solid support. The solid support is in the form of inert insoluble resin beads that are functionalised with a linker on which the peptide synthesis is carried out. The elegance of method is the incorporation of the metal moiety on the solid phase either by covalent bonding or by simple complexation. The high yields and purity of the synthesized bioconjugates indicate the efficiency of the method even in the case of fluorescence labelling on the solid support.

Purification of Cobaltocenium monocarboxylic acid

Cobaltocenium carboxylic acid was synthesized according to a reported method.[299] During this reaction, a mixture of mono and dicarboxylic acids of cobaltocenium were obtained. After purification as described in the literature, the cobaltocenium monocarboxylic acid was always contaminated with cobaltocenium dicarboxylic acid. The first synthesis of

CcC(O)-NLS (**1)** gave poor yields because of an impurity in the starting material. Therefore, for purification the soxhlet's apparatus was used. The very pure cobaltocenium monocarboxylic acid was thus collected in fractions.

Choice of Fluorescent label

The objective was to label the metallocene-peptides with a fluorescent marker. This objective had to be met within reasonable cost, ease and efficiency of synthesis and compatibility with the procedures of synthesis and technical applicability. Fluorescein isothiocyanate (FITC) was chosen as the fluorescent marker of choice. The FITC label was added to a lysine side chain manually. The synthesis procedures had to be optimised to allow this orthogonal substitution of the fluorescent label during the solid phase synthesis.

Labelling with FITC

The lysine that was to be labelled with the FITC tag was chosen with an extremely acid labile side chain protecting group that could be removed without disturbing the other protecting groups. This removal should not cleave the peptide which is also linked to an acid labile resin. Therefore, Fmoc-lysine(Mtt)-OH was used since the "Mtt" group (methyltrityl group)can be removed with 1% TFA. In the first attempt, the first lysine from the *C*-terminal was chosen for fluorescence labelling at the end of entire synthesis. The reaction gave very poor yield of the final bioconjugate. There were two reasons for this difficulty of synthesis, firstly the proximity of the target lysine with the resin and secondly the steric hindrance of the neighbouring bulky groups which protect the target lysine side chain amino group in a kind of pocket. Another simpler strategy was therefore used in which a supplementary lysine was added as the carrier of the fluorescent label at the end of the desired peptide sequence. The synthesis of various FITC labelled bioconjugates was thus achieved with success in very good yields.

Labelling with metallocenes

For both cobaltocenium and ferrocene carboxylic acids longer activation times of 10 minutes were used as compared to the normal activation time of 1 minute for the amino acids. This was especially important in the case of cobaltocenium carboxylic acid which was used as a PF_6 salt.

The sensitivity of ferrocene to oxidative conditions led to problems in the solid phase synthesis of ferrocene-peptides when TFA cleavage of the peptide was carried out. Ferrocene carboxylic acid itself was rather stable to TFA in concentrations up to 50% for several hours. However, ferrocene conjugated to a peptide sequence could not withstand even 1 % TFA. To overcome this problem, various strategies were tried namely different resins, different side chain protecting groups and different cleavage conditions and combinations of these. None of these yielded 100% satisfactory results except for one route in which Tentagel HMB resin was used and the final ferrocene-peptide was cleaved from the resin with 2% hydrazine giving a ferrocene-peptide hydrazide. Later, upon recommendation of Prof. Dr. H.-B. Kraatz, phenol was added in the acid cleavage cocktail for ferrocene compounds. The phenol seems to protect the ferrocene from oxidation during acid cleavage. Thus all the ferrocene-peptide bioconjugates were successfully synthesized with a cleavage mixture containing 85 % TFA, 10 % phenol and 5 % TIS.

Peptide Sequences

A problem with Fmoc-Arginine(Pbf)-OH, due to its poor solubility and difficult coupling was realised when an arginine was found missing in a couple of peptide sequences as indicated by mass spectrometry. Therefore, Fmoc-Arginine(Pbf)-OH was used in 6 eq. and prolonged coupling times of 45-50 minutes were used. Another point where care had to be taken during the solid phase synthesis of the peptides was the coupling of the amino acid following the proline residue which is an imine acid. Longer coupling times were used for the amino acid following proline in order to increase the efficiency of synthesis and to minimise side products.

Characterization of the bioconjugates

The synthesized bioconjugates were comprehensively characterised by nuclear magnetic resonance (NMR) spectroscopy, mass spectrometry, reverse phase HPLC and electrochemistry. Some of the physicochemical characterizing information of the bioconjugates can be used for a preliminary prediction of their behaviour in physiological conditions such as stability and solubility in aqueous media, lipophilicity and redox behaviour.

Reversed-phase liquid chromatography is one such technique that helps to determine the hydrophobic parameters of a given substance.[309] In case of peptides, the hydrophobicity of

the component amino acids is a key to the final three dimensional structure and biological activity of peptides, proteins and enzymes. The hydrophobicity or lipophilicity can be measured from the octanol/water partition co-efficient (Log P) which is one of the best predictors for the biological transport properties of peptides.[310-312] Estimation of the Log P values for some peptides has been used for the quantitative structure activity prediction or for structural parameters.[313, 314]However, the unusual properties of peptides such as the conformational flexibility, presence of ionizable species, possibility of multiple intramolecular hydrogen bonds, and active transport mechanisms should not be overlooked.

The retention times of various synthesized bioconjugates in RP-HPLC give a simple but a rough indication of the lipophilicity of these compounds although a direct correlation with the biological behaviour should not be drawn. It is only a cautious reasoning of the biological effects observed. The retention times for the fluorescently labelled/unlabelled NLS and NLS_{scr} bioconjugates with/without metal are summarised in table 4.1.

Table 4.1: Retention times of various NLS and NLS_{scr} conjugates determined by RP-HPLC.

Bioconjugate	**R_t (minutes)**	**Bioconjugate**	**R_t (minutes)**
K-NLS	6.9	K-NLS_{scr}	6.7
Cc(O)-K-NLS	8.1	CcC(O)-K-NLS_{scr}	7.4
FcC(O)-K-NLS	9.7	FcC(O)-K-NLS_{scr}	9.1
K-(FITC)-NLS	10.6	K(FITC)-NLS_{scr}	10.1
Cc(O)-K(FITC)-NLS	11.2	CcC(O)-K(FITC)-NLS_{scr}	10.7
FcC(O)-K(FITC)-NLS	12.2	FcC(O)-K(FITC)-NLS_{scr}	12.0
Pt-BB-NLS	9.4	Pt-DAP-NLS	7.8

It is obvious from this table that the ferrocene bioconjugates show higher retention times as compared to the cobaltocenium bioconjugates which bears a positive charge. In addition, the aromatic structure of the FITC imparts further lipophilicity to the bioconjugates as the retention times are higher than as for the unlabelled bioconjugates. The metal and FITC free peptides are polar due to the cationic lysine and arginine residues. The metallocenes despite imparting lipophilicity to the bioconjugates, do not abolish the solubility of these compounds in water or phosphate buffered saline. Moreover, close look at the Pt bioconjugates reveal that when the ligand is backbone (BB), an additional -CH_2- group leads to an increase in the retention time by at least 1.5 minutes as compared with the diamiopropionic acid ligand. The same tendency was observed in case of the NLS_{scr} bioconjugates. The retention time for the FITC labelled bioconjugates was approximately 3

minutes longer than the unlabelled bioconjugates. The retention times for TAT and the NT bioconjugates exhibited a similar trend (see experimental).

The redox potentials of the ferrocene bioconjugates are listed in Table 4.2. Although conflicting reports exist in literature about the effects of the redox potential on the activity of ferrocene derivatives, it is known that ferrocene is able to sense the slight changes in the structure. This is also observed in case of the synthesized bioconjugates. However it is not possible to deduce a regular pattern.

Table 4.2: E½ values of various Ferrocene bioconjugates.

Bioconjugate	**E½ (mV) FcH vs. FcH^+**
FcC(O)-NLS	247
FcC(O)-K-NLS	239
FcC(O)-K(FITC)-NLS	166
FcC(O)-NLS_{scr}	252
FcC(O)-K-NLS_{scr}	279
FcC(O)-K(FITC)-NLS_{scr}	279
FcC(O)-K-TAT	199
FcC(O)-K(FITC)-TAT	237

For the cobaltocenium bioconjugates it is interesting to note that addition of one more lysine changed the redox potential by approximately 300mV whereas the side chain substitution of FITC had almost no effect on the E½ values. The redox potentials of cobaltocenium bioconjugates are summarised in table 4.3.

Table 4.3: E½ values of various Cobaltocenium bioconjugates.

Bioconjugate	**E½ (V) FcH vs. FcH^+**
CcC(O)-NLS	-1.08
CcC(O)-K-NLS	-1.38
CcC(O)-K(FITC)-NLS	-1.37
CcC(O)-NLS_{scr}	-1.09
CcC(O)-K-NLS_{scr}	-1.38
CcC(O)-K(FITC)-NLS_{scr}	-1.35
CcC(O)-K-TAT	-1.32
CcC(O)-K(FITC)-TAT	-1.38

It is difficult to draw a parallel between the redox and the biological behaviour of the bioconjugates. Further detailed studies might lead to better insight in this phenomenon.

Biological Studies

Targeted delivery of diagnostic probes and therapeutics intracellularly is of great importance for the improvement of disease detection and treatment if one considers that the biological target is generally strictly localized, for example DNA in the nucleus. Transport of any compound into the nucleus of an intact cell is limited by at least three major membrane barriers namely the cell membrane, the endosomal membrane (in case mode of internalization is endocytosis) and the nuclear membrane.

The cellular uptake or internalisation of a given substance in intact living cells through the cell membrane into the cytoplasm can take place by either passive diffusion i.e. direct translocation in an energy-independent manner or via endocytosis. Low molecular weight compounds, including many drugs, may enter cells by passive diffusion. However, P-glycoproteins usually pump them out of the cells before they gain access to the nucleus. In case of uptake by endocytosis, the distribution of the substance in the cytoplasm and/or its delivery to the nucleus depends on its escape from the endosomes in sufficiently non-degraded form. The release from the endosomes is a complex process, which partly depends on the physicochemical properties of the endocytosed material.[315]

Cellular uptake and nuclear localisation of metallocene-TAT bioconjugates

Recently the cell penetrating peptides (CPPs) have been extensively investigated for delivery of substances across the cell membrane. The cell penetrating peptides are defined by their ability to cross the cell membrane and reach cytoplasmic and/or nuclear compartments after internalisation. These include large peptides and even proteins that can translocate through the plasma membrane as part of a physiological process. Among these CPPs, TAT peptide is the earliest discovered peptide. TAT translocates freely across the cell membrane. The shortest sequence capable of translocation is TAT(48-57). When carrying a cargo the translocation across the cell membrane and cellular distribution of the TAT peptide is highly dependent on the cargo. TAT peptide is internalised by endocytosis[316] and in many cases the inability to escape from the endosomes is observed. Moreover slight changes in the peptide sequence or charge result in impairment of the translocation across the cell membrane.[317] In a recent study, TAT was shown to effect only cytosolic delivery and no nuclear localisation was observed.[317] In addition, it was noted that the cationic charge of the peptide is not the only factor mediating cellular uptake. The distribution of the

cationic charges more amphipathically or addition of hydrophobic moieties can enhance membrane crossing. TAT peptide is characterised by low cargo efficiency as compared with other CPPs. However the advantage is that it posses less membrane permeablising effects.[318]

The cellular uptake and nuclear localisation of metallocene-TAT bioconjugates was monitored by fluorescence microscopy in live Hep G2 cells. The Hep G2 cells have relatively large nuclei, but membrane translocation in this cell line is known to be rather difficult.

We observed that the control bioconjugate, K(FITC)-TAT (0.1mM) was not internalised by the Hep G2 cells. Similarly, the cobaltocenium-TAT bioconjugate (0.1mM) was also unable to translocate across the cell membrane. It is suggested that a small cargo in the form of a fluorescence-labelled lysine bound to the TAT peptide, which results in membrane translocation impairment. The addition of a lipophilic group in the form of cobaltocenium also did not improve the transport across the membrane. This is most likely due to the positive charge on the cobaltocenium moiety, which may be indicated by our finding that the neutral ferrocene bioconjugate of TAT (0.1mM) was localised in the cytoplasm.

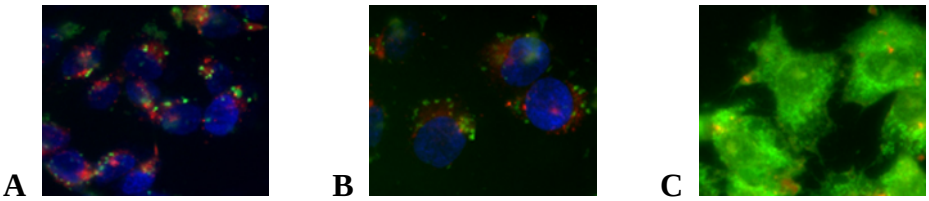

Fig. 4.1: Cellular distribution of K(FITC)-TAT (A), CcC(O)-K(FITC)-TAT (B) and FcC(O)-K(FITC)-TAT

The uptake most probably takes place by endocytosis as seen by some co-localisation with the endosomal marker (FM 4-64). This bioconjugate was not totally trapped in the endosomes, but was found to be distributed in the cytoplasm. The ferrocene moiety facilitates the escape of the bioconjugate from the endosomes and results in the cytoplasmic distribution of the bioconjugate. This is a very interesting observation because escape from the endosomes is considered to be one of the major limiting factors for the use of TAT peptide for cellular delivery.[317]

Moreover, the parallel control experiments with metallocene-TAT bioconjugates with fixation of the cells with paraformadehyde resulted in artificial redistribution of the K(FITC)-TAT and CcC(O)-K(FITC)-TAT bioconjugates in the cytoplasm. This is probably due to the cell permeablising effects of the bioconjugates. Some of the CPPs have shown to be cytotoxic in higher concentrations and indicate complex mechanisms of entry which involves pathways such as direct translocation by inducing pores in the membrane or through miscelle formation, in addition to endocytosis.[203] For this reason, the metallocene-TAT bioconjugates were tested for their effects on the proliferation of Hep G2 cells and will will be discussed later in the cytotoxicity part.

Cellular uptake and nuclear localisation of metallocene conjugates of NLS and NLS_{scr}

The transport in and out of the nucleus is a highly controlled process. Endogenously, the nuclear localisation or export signals are responsible for most of this trafficking. The transport across the nuclear membrane is mediated through the nuclear pore complexes (NPC) that form kind of aqueous channels,[231] although the docking of any substance along the pore depends on hydrophobic interactions with the NPC amino acid residues. Generally, small molecules, up to 30 kDa, can diffuse through the NPC in an energy-independent manner,[319] while larger molecules gain entry by active transport with carrier peptides such as the nuclear localisation signals (NLS). However, the actual passage of a substance, small or large is not random and it greatly depends on the physicochemical properties of that substance such as the net charge, lipophilicity, the orientation and the possibility for hydrogen bonding. As such, some small molecules like the histones are actively transported,[320] whereas some larger proteins can diffuse through the pores. Similarly, in the case of large proteins, some are more efficiently transported than others.[236] Moreover, the transport into the nuclei is also dependent on the permeability of the nuclear pore complexes at a given stage in cell cycle as well as the ratio of these pore complexes available for entry.[240]

A part of the present research focuses mainly on the metallocene-NLS conjugates. The SV 40 T antigen nuclear localisation signal was chosen to effect nuclear delivery. The NLS transports the cargo into the nucleus through the nuclear pore complexes.[234] However, inefficient entry into the cells[321] or inability to escape endosomes[252] has been reported.

Furthermore, to determine the role of the NLS peptide, upon cellular uptake and nuclear localisation the scrambled sequence of the NLS (KKVKPKR) was used. This sequence was reported by Cutrona et al.[322] and was shown to be unable to target the nuclei of the cells. It was reported that the nuclear localisation function of the NLS is essentially dependent on the presence of Lys 128.[308, 323]

Incorportion of the metallocene moiety was devised to impart the necessary lipophilicity to the NLS for crossing the cell membrane via direct translocation through the lipid bilayer. Both ferrocene and cobaltocenium were used as metal labels, because they resemble in size and other properties with the exception of one positive charge on the cobaltocenium. Another reason for choosing cobaltocenium was the fact that ferrocenes are reported to be cytotoxic and therefore the isostructural cobaltocenium that is non toxic might serve as a model to monitor the uptake. Both ferrocene and cobaltocenium bioconjugates were tested for their effects on proliferation of Hep G2 cells and the results are discussed later in the cytotoxicity part. The metallocene conjugates of the truncated peptides as well as the metal free NLS sequence were used as controls. Once distributed in the cytoplasm, the NLS in principle should carry the metallocene as well as the FITC marker into the nucleus. The fluorescence label should enable the tracking of the bioconjugate in various cellular compartments.

The internalisation of metallocene-NLS conjugates and their nuclear localization was monitored by fluorescence microscopy in live Hep G2 cells. Throughout the live cell study, the integrity of the cell membrane was checked by the ability of the cells to exclude propidium iodide. Recent investigations on other cationic peptides like Arg-rich or Tat sequences demonstrate that fixation of the cells causes artificial redistributaion of those peptides in the cytoplasm and in the nucleus, leading to false-positive results.[226] Therefore, live cell microscopic imaging was used to follow the cellular uptake and nuclear localisation of the bioconjugates. However, parallel experiments with fixation of cells were also carried out to determine whether the SV 40 NLS also gives these artifactual results upon fixation.

The metallocene-NLS bioconjugates were efficiently taken up by the cells and were also translocated in the nuclei of Hep G2 cells. A concentration-dependent uptake was observed as lessuptake was observed with lower concentrations of the bioconjugates. Co-staining with the endosomal marker, FM 4-64, was carried out to get an insight into the mode of

internalisation of these bioconjugates. In case of the cobaltocenium-NLS bioconjugate some co-localisation with the endosomal marker was observed but not extensively. The same observation was made in case of the ferrocenium-NLS bioconjugate. It is suggested that, to some extent, the bioconjugates entered the cells in an endocytosis-independent pathway. There is also the possibility that the uptake is via endocytosis but the endosomes were permeable and the bioconjugates rapidly escaped from the endosomes and were homogenously distributed in the cytoplasm or accumulated in the nuclei. Although conflicting reports exist concerning the internalisation of NLS conjugates, the majority of studies indicate an uptake by endocytosis. However, the possibility of an additional endocytosis-independent pathway has not been ruled out.

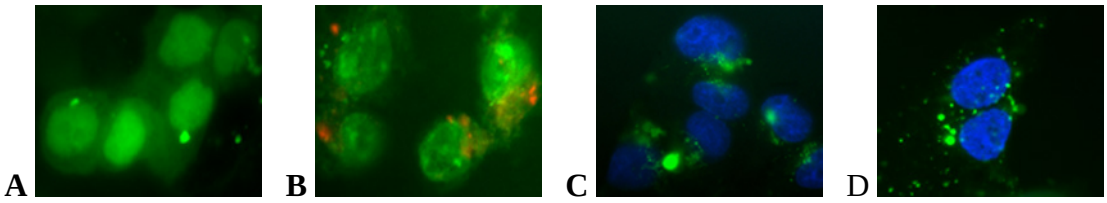

Fig.4.2: Cellular distribution and nuclear localisation of CcC(O)-K(FITC)-NLS (A), FcC(O)-K(FITC)-NLS (B) K(FITC)-NLS (C) and CcC(O)-K(FITC)-NLS_{scr}

Experiments with control compounds show that the ease of cellular uptake is a property that is particular to the presence of the metallocene moiety in the NLS conjugates. The fluorescently labelled NLS alone was unable to enter the cells. Due to its highly cationic composition, it has tendency to clump and adhere to the cell membrane as was observed in fluorescence microscopy. Similarly in case of the metallocene-dipeptides, no significant cellular uptake was observed and no nuclear localisation at all. Although small amounts may have entered the cells by passive diffusion but not in sufficient amounts to accumulate in the cytoplasm or to gain access to the nuclei. In addition, it might be efficiently eliminated from the cells by exsorption or P-glycoproteins.

Ferrocene and cobaltocenium conjugates of NLS_{scr} sequence, both labelled with FITC were studied along with a metal free, FITC labelled scrambled peptide. These conjugates not only did not gain entry into the nuclei but also were unable to enter the intact cells. These compounds had the tendency to clump together and adhere on the outer cell surface, which can be seen as bright fluorescence outside the cells.

These results suggest the correct peptide sequence is essential for the internalisation of these compounds and for nuclear distribution as well. In addition, the unique combination of metallocene and NLS seems necessary for the effects observed. The metal moiety is suggested to help the NLS to gain entry into the cells and the NLS is then responsible for shuttling into the nuclei. This seems plausible, as attempts have already been made to combine hydrophobic such as the fusion peptide of GP41 and NLS sequence in order to gain entry into the cells, escape the endosomes and to target the nucleus.[249] The positively charged cationic peptides interact with the anionic cell membrane and adhere very tightly to the surface. A hydrophobic handle would facilitate the anchoring and internalisation of the carrier. For the metallocene-NLS bioconjugates, it may be concluded that the metallocene moiety plays a role in the cellular uptake although the charge does not lead to any drastic consequences upon the uptake. This is contrast to the TAT bioconjugates where the positively charged cobaltocenium was not internalised in the cells. This shows that in case of TAT peptide changes in charge have an impact on the membrane translocation properties of this peptide.

The successful synthesis of the first metallocene conjugates to the SV 40 nuclear localization signal peptide was accomplished by SPPS. The metallocene moiety is highly stable under physiological conditions making it ideally suitable for the study of bioconjugates in cell culture media. The metallocene-NLS conjugates significantly accumulate in the nuclei of Hep G2 cells. Moreover, the organometallic moiety is essential for the uptake of the conjugates and release of the conjugate into the cytoplasm. It is known that, NLS-assisted nuclear delivery is only possible from the cytoplasm. Therefore, the escape of the compound from the endosomes is essential for subsequent translocation of any NLS bioconjugate into the nucleus. Metal-enhanced cellular uptake and peptide-mediated nuclear delivery is demonstrated herein for an organometallic species. A hydrophobic moiety seems to plays an important role in improving the uptake of the hydrophilic carrier peptide NLS. It is potentially highly useful because the metallocene moiety is relatively small, robust and easy to handle. The cyclopentadienyl rings of metallocenes although imparting enough lipophilicity, do not interfere in the biological functioning of the nuclear localisation signal.

Cytotoxicity studies

Over the years much debate has been going on the antitumour activity of ferrocene derivatives but the site or mechanism of action still remains an ambiguity. The cytotoxicity of metallocenes such as ferrocene have been postulated to be due to its direct or indirect interactions with the DNA. Although many studies have been undertaken to determine the subcellular and subnuclear target as well as the mechanism of action of these metallocene derivatives, no attempt so far has been made to monitor the cellular uptake and nuclear entry of these compounds. On the other hand, the metallocene dihalides have been extensively studied and recently the subcellular distribution of some metallocene dihalides has been reported.[324] By using the fluorescently labelled conjugates enhanced cellular uptake and nuclear localisation was observed. Once selectively delivered into the nuclei of live cells, the next question is: are these metallocene bioconjugates toxic? If DNA damage (direct or by $OH^{\cdot}$ radical generation) is the mechanism of cytotoxicity of the metallocenes, then it should be enhanced by direct delivery into the nucleus of a cell.

Therefore, the metallocene-NLS bioconjugates (not labelled with FITC) were screened in a WST-1 assay for cytotoxicity. This assay depends on the measurements of absorbance of the soluble formazan dye that is generated by the cleavage of the tetrazolium salt (WST-1) by mitochondrial dehydrogenase in metabolically active cells. In case of K-NLS, CcC(O)-K-NLS and FcC(O)-K-NLS in all the tested concentrations (0.1, 0.5 and 1mM) no statistically significant difference was observed in the proliferation rate of the Hep G2 cells, as compared with the control. Similarly, in case of K-NLS_{scr} and FcC(O)-K-NLS_{scr} no statistically significant difference was found with respect to the control in all tested concentrations. However, in case of CcC(O)-K-NLS_{scr} a slightly significant difference was found in comparison with control in concentrations of 0.5 and 1mM, indicating a stimulatory effect of this compound on the proliferation of the Hep G2 cells. This is not extraordinary since an early report by Motohashi with Ferronece mustards also demonstrated an increase in tumour growth by some of the compounds.[117]

None of the compounds were found to be cytotoxic in the tested concentrations. It may be concluded that the neutral ferrocene bioconjugate (FeII) or the cationic cobaltocenium bioconjugate are non toxic even when they are localised in the nuclei. Some reports have established the lack of activity for ferrocene derivatives.[115-118] Recently, it has been suggested that only the ferrocenium cation is responsible for reacting with dioxygen leading

to generation of $OH^{\cdot}$ radicals, which are in turn responsible for the antitumour activity of ferrocenium derivatives. This phenomenon is suggested to occur extracellularly and the cytotoxic effects observed are a result of attack of radicals on the cell membrane lipids.

The metallocene-TAT bioconjugtes were tested for cytotoxicity in the WST-1 assay for cell viability. It was observed that both the metallocene-TAT bioconjugates are cytotoxic in concentrations higher than 100μM. It was observed that the combination of metallocene and TAT peptides have the antiproliferative effects since the peptide alone is not toxic even in high concentrations. The uptake detected at higher concentration is ascribed to membrane perturbation and the toxic effects of the labelled peptides. [325] It is possible that addition of one more positive charge in case of the K-TAT results in unfavourable parameters that abolish the membrane interactions of the peptide prior to its translocation into the cell. The other problem is extensive clumping of this peptide which definitely results in less availability for uptake. It is also very likely that the toxic effects of the metallocene-TAT bioconjugates are due to disruption of the cellular membrane since almost the same toxic effects are observed in both cases of ferrocene and cobaltocenium conjugates. The former is translocated inside the cells and the later not. Therefore, an intercellular mechanism of toxicity cannot be suggested. The observed cytotoxicity may also be due to the production of membrane impermeable degradation products of the metallocene-TAT bioconjugates. It has been shown that a large portion of the internalized CPP is degraded. This mechanism is not likely to be an endosomal degradation of material taken up through classical endocytosis, as it is not sensitive to cholorquine, brefeldin-A or potassium depletion and can be competitively inhibited.[318]

A tremendous amount of research had been carried out and is still going on in the field of platinum analogues for their antitumour activity. One of the major limitations with platinum anticancer drugs is the inherent or acquired resistance of cancer cells, among many others. The major site of action of platinum compounds is DNA. In other words the target of platinum compounds is the nucleus. Therefore, a carrier like NLS that selectively carries the platinum analogue into the nucleus will most likely enhance the cytotoxicity of these compounds. Thus, in the series of metal-NLS bioconjugates, the platinum(II) complexes of the SV40 nuclear localisation signal were also synthesized on the solid phase. The solid phase synthesis of platinum analogues of small peptides and their cytotoxicity has been reported.[192, 193] These compounds did not show an improved cytotoxicity as compared with

cisplatin most probably because they are unable to reach their nuclear target that is the DNA.

The bioconjugates were stable in aqueous media so that the toxicity tests in culture media could be carried out. However, the bioconjugates were dissolved just prior to the tests. The WST-1 assay was carried out to determine the antiproliferative effects of the platinum-NLS bioconjugates. Both conjugates have a cytotoxic effect in concentrations higher than 0.1µM. It may be noted here that for proper functioning of the NLS, it has to be located in the cytoplasm. As remarked earlier, NLS does not translocate very easily through the cell membrane. Therefore, the true potential of the antitumour activity of platinum compounds can not be estimated. It may be possible that the observed effect is due to slow diffusion of the bioconjugates into the cells. It seems necessary to facilitate the cellular uptake of the bioconjugates with external means like digitonin or with the help of some carrier. Once inside the cell, it would then be possible to determine the true cytotoxicity potential of the Pt-NLS bioconjugates. It is expected that in case of resistant cell lines, despite the sequestration of platinum in the lysosomal vesicles, the NLS will result in enhanced nuclear delivery of the platinum where it can bind with the DNA.

Moreover, the Pt-NLS bioconjugates were tested in the yeast assay for cytotoxicity and genotoxicity (data not shown in this thesis, work done in collaboration). Both Pt-NLS bioconjugates were cytotoxic in both yeast strains.

Receptor binding studies on metallocene bioconjugates of NT and pNT

The metallocene moieties can impart lipophilicity to the peptides they are attached to without extensively compromising their biological function. This lipophilicity may in turn enable the peptide to cross various biological membranes such as the blood brain barrier. The blood brain barrier presents a major limitation in the therapeutic application of compounds intended for a central effect such as pain management and various neurological pathologies. Certain small regulatory peptides such as the neurotensin play important functions in the central nervous system as well as in the periphery. In certain diseases like cancer where the neurotensin receptors are overepressed, it can indirectly induce proliferation. Active research is going on to exploit the various biological activities of neurotensin for therapeutic purposes. In addition the neurotensin receptors that are

specifically overexpressed in certain cancers might also be exploited for tumour detection by radio-imaging as well as for the selective delivery of anticancer agents to tumour sites.[289-291]

During the course of present research the metal conjugates of neurotensin were synthesised and tested for their binding efficiency to the NTR1 receptors in an adenocarcinoma cell line. In addition to the wild type NT sequence (RRPWIL) another slightly modified sequence, the pseudo neurotensin in which the arginines were replaced by lysines, were also synthesized and tested. The metal-free peptides were also tested for their affinity to the receptors in order to determine the effect of the amino acid residue mutation.

Replacement of Arg^8-Arg^9 with Lys-Lys in pseudo neurotensin resulted in a decrease in the affinity with an IC_{50} approximately 15 times higher than the wild type NT(8-13) sequence. This decrease was, however, not statistically significant. The cobaltocenium bioconjugate of NT showed almost comparable affinity to the receptors, while in case of the platinum bioconjugate there was only a slight effect on the affinity. However, in case of the ferrocene bioconjugate the affinity was 12 times lower compared with the wild type NT(8-13) but this decrease was not statistically significant. The pseudo neurotensin bioconjugates all showed statistically significant drop in the affinities as compared to the two metal-free peptides as well as the respective metal-NT bioconjugates. This is understandable because the guanidino groups of arginines are involved in specific interactions with the receptors. The metals were placed at the *N*-terminal since a free *N*-terminal is not a prerequisite for binding whereas a free *C*-terminal is important.

The comparative binding of some of these bioconjugates like the cobaltocenium-NT bioconjugate shows that further exploitation such as determination of the agonist or antagonistic effects of these bioconjugates at the NTR1 receptors could be imagined. Moreover, the metallocene bioconjugates especially the cobaltocenium-NT bioconjugate may facilitate the crossing of the blood brain barrier (BBB) membranes while retaining the binding affinity. One major limitation for NT analogues is their inability to cross the BBB[264] in therapy as antipsychotics and analgesics. Lastly, cytotoxic metals derivatives such as the platinum can be specifically delivered to the tumour tissues that overexpress NT receptors ensuring selectivity. The bioconjugates were also tested for their cytotoxic effects in a yeast assay (data not shown in this thesis, work done in collaboration).

Conclusion

A multitude of challenges is associated with satisfactory cellular uptake and nuclear targeting. Practically all macromolecules and small molecules whose physicochemical properties do not allow passive diffusion are impermeable to cell membrane. Application of peptide vectors capable of transporting such molecules into the cells or even into the nucleus in the form of covalent conjugates is proving to be a useful way to circumvent this problem.

During the course of the present research, various metal bioconjugates of bioactive peptides namely NLS, TAT and NT were successfully synthesized by solid phase peptide synthesis. All the bioconjugates were comprehensively characterised. This is the first reported SPP Synthesis of metallocene-NLS, -TAT and -NT bioconjugates.

The metallocene-NLS bioconjugates show enhanced cellular uptake and nuclear localisation. This seems to be a property conferred only due to the presence of the metallocene moiety. The bioconjugates did not inhibit proliferation of Hep G2 cells even in high concentration. The results indicate a good potential for these compounds to be used as vectors for directed nuclear delivery.

The results with the TAT peptide conjugates indicate that the ferrocene moiety facilitates endosomal escape of the conjugate. Whereas positively charged cobaltocenium-TAT bioconjugate is not translocated into the cells. Toxicity of these bioconjugates is observed at higher concentrations as indicated by the inhibition of proliferation of Hep G2 cells. The study may impart a further understanding of the behaviour of TAT peptide in cell membrane translocation.

The metal conjugates of NT may be used to facilitate the crossing of the BBB and in the case of toxic metals may be used for selectively targeting the tumours that overexpress the neurotensin receptors.

Based on these results an insight into the biological behaviour of bioorganometallic peptide conjugates has been gained. The metal conjugates show a potential for the improvement of cellular uptake of the carrier peptides. They may as well be further investigated for the selective delivery to targets as in case of NT conjugates.

References

[1] R. H. Fish, G. Jaouen, *Organometallics* **2003**, *22*, 2166-2177.
[2] N. Metzler-Nolte, *Angew. Chem. Int. Ed.* **2001**, *40*, 1040-1043.
[3] R. Dagani, *Chem. Eng. News* **2002**, *80*, 23-29.
[4] G. Jaouen, S. Top, A. Vessieres, R. Alberto, *J. Organomet. Chem.* **2000**, *600*, 23-26.
[5] W. Beck, K. Severin, *Chem. unserer Zeit* **2002**, *6*, 356-365.
[6] *J. Organomet. Chem.* **2003**, *668*, special issue.
[7] H. Chen, J. A. Parkinson, R. E. Morris, P. J. Sadler, *J. Am. Chem. Soc.* **2003**, *125*, 173-186.
[8] C. S. Allardyce, P. J. Dyson, D. J. Ellis, S. L. Heath, *Chem. Commun.* **2001**, 1396-1397.
[9] S. Top, A. Vessieres, G. Leclerq, J. Quivy, J. Tang, J. Vaissermann, M. Huche, G. Jaouen, *Chem. Eur. J.* **2003**, *9*, 5223-5236.
[10] G. Jaouen, A. Vessieres, I. S. Butler, *Acc. Chem. Res.* **1993**, *26*, 361-369.
[11] P. C. Bull, G. R. Thomas, J. M. Rommens, J. R. Forbes, D. W. Cox, *Nature Genet.* **1993**, *5*, 327-337.
[12] C. Vulpe, B. Levinson, S. Whitney, S. Packman, J. Gitschier, *Nature Genet.* **1993**, *3*, 7-13.
[13] J. F. Mercer, J. Livingston, H. B., J. A. Paynter, C. Bergy, S. Chandrasekharappa, *Nature Genet.* **1993**, *3*, 20-25.
[14] D. R. Rosen, *Nature* **1993**, *362*, 59-62.
[15] G. H. Petsko, *Methods Enzymol.* **1985**, *114*, 147-156.
[16] K. Severin, R. Bergs, W. Beck, *Angew. Chem. Int. Ed.* **1998**, *37*, 1634-1654.
[17] B. E. Moutassim, H. Elamouri, J. Vaissermann, G. Jaouen, *Organometallics* **1995**, *14*, 3296-3302.
[18] A. Gorfti, M. Salmain, G. Jaouen, M. J. McGlinchey, A. Bennouna, A. Mousser, *Organometallics* **1996**, *15*, 142-151.
[19] S. Top, J. Tang, A. Vessieres, D. Carrez, C. Provot, G. Jaouen, *Chem. Commun.* **1996**, 955-956.
[20] B. Rudolf, J. Zakrewski, M. Salmain, G. Jaouen, *Tetrahedron Lett.* **1998**, *39*, 4281-4282.
[21] S. Srinivasan, Y. A. Chizmadzhev, J. O. M. Bockris, B. E. Conway, E. Yeager, *Comprehensive Treatise of Electrochemistry, Vol. 10, Bioelectrochemistry*, Plenum Press, New York, **1985**.
[22] Y. Degani, A. Heller, *J. Phy. Chem.* **1987**, *91*, 1285-1289.
[23] Y. Degani, A. Heller, *J. Am. Chem. Soc.* **1988**, *110*, 2615-2620.
[24] A. D. Ryabov, V. N. Goral, L. Gorton, E. Csoregi, *Chem. Eur. J.* **1999**, *5*, 961-967.
[25] A. D. Ryabov, *Angew. Chem. Int. Ed.* **1991**, *30*, 931-941.
[26] R. Kramer, *Angew.Chem. Int. Ed.* **1996**, *35*, 1197-1199.
[27] C. Sergheraert, J.-C. Brunet, A. Tartar, *J. Chem. Soc., Chem. Commun.* **1982**, 1417-1418.
[28] W. S. Sheldrick, A. J. Gleishmann, *J. Organomet. Chem.* **1994**, *470*, 183-187.
[29] A. J. Gleishmann, J. M. Wolff, W. S. Sheldrick, *J. Chem. Soc., Dalton Trans.* **1995**, 1549-1554.
[30] R. S. Herrick, R. M. Jarret, T. P. Curran, D. R. Dragoli, M. B. Flaherty, S. E. Lindyberg, R. A. Slate, L. C. Thornton, *Tetrahedron Lett.* **1996**, *30*, 5289-5292.
[31] H.-B. Kraatz, J. Lusztyk, G. D. Enright, *Inorg. Chem.* **1997**, *36*, 2400-2405.
[32] B. Kayser, K. Polborn, W. Steglich, W. Beck, *Chem. Ber.* **1997**, *130*, 171-177.
[33] S. S. Wong, *Chemistry of protein conjugation and cross linking*, CRC press, Boca Raton (Fl) USA, **1991**.
[34] D. E. Metzler, *Biochemistry*, Academic Press, New York, **1977**.
[35] M. Salmain, A. Vessieres, P. Brossier, I. S. Butler, G. Jaouen, *J. Immunol. Methods* **1992**, *148*, 65-75.
[36] J. D. Schmitt, M. S. P. Sansom, I. D. Kerr, G. G. Lunt, R. Eisenthal, *Biochem.* **1997**, *36*, 1115-1122.
[37] E. C. Constable, *Angew.Chem. Int. Ed.* **1991**, *30*, 407.
[38] P. Cheret, P. Brossier, *Res. Commun. Pathol. Pharmacol.* **1986**, *54*, 237-253.
[39] F. Mariet, P. Brossier, *Res. Commun. Pathol. Pharmacol.* **1990**, *68*, 251-262.
[40] S. G. Weber, W. C. Purdy, *Anal. Lett.* **1979**, *12*, 1-9.
[41] K. DiGleria, H. Allen, O. Hill, J. McNeil, M. J. Green, *Anal. Chem.* **1986**, *58*, 1203-1205.
[42] A. E. G. Cass, G. Davis, G. D. Francis, H. A. O. Hill, W. J. Aston, I. J. Higgins, E. V. Plotkin, L. D. L. Scott, A. P. F. Turner, *Anal. Chem.* **1984**, *56*, 667-671.
[43] P. D. Hale, L. I. Boguslavsky, T. Inagaki, H. I. Karan, H. S. Lee, T. A. Skotheim, Y. Okamoto, *Anal. Chem.* **1991**, *63*, 677-682.
[44] I. Willner, S. Rubin, *Angew. Chem. Int. Ed.* **1996**, *35*, 367-385.
[45] R. Schibli, P. A. Schubiger, *Eur. J. Nucl. Med.* **2002**, *29*, 1529-1542.
[46] G. Wilkinson, M. Rosenblum, M. C. Whiting, R. Woodward, *J. Am. Chem. Soc.* **1952**, *74*, 2125-2126.
[47] D. R. van Staveren, N. Metzler-Nolte, *Chem. Rev.* **2004**, *104*, 5931-5985.
[48] K. E. Dombrowski, W. Baldwin, J. E. Sheats, *J. Organomet. Chem.* **1986**, *302*, 281-306.
[49] H. G. Alt, *J. Am. Chem. Soc., Dalton Trans.* **1999**, 1703-1709.

[50] H. G. Alt, A. Koppl, *Chem. Rev.* **2000**, *100*, 1205-1221.
[51] D. M. J. Foo, P. Sinnema, B. Twamley, P. J. Shapiro, *Organometallics* **2002**, *21*, 1005-1007.
[52] H. Schwemlein, L. Zsolnai, G. Huttner, H. H. Brintzinger, *J. Organomet. Chem.* **1983**, *256*, 285-289.
[53] A. J. Taylor, M. Wenzel, *Xenobiotica* **1978**, *8*, 107-112.
[54] M. Schneider, M. Wenzel, G. Schachschneider, *Z. Naturforsch. C* **1982**, *37 (1-2)*, 136-138.
[55] D. Langheim, M. Wenzel, *J. Label Compds.* **1973**, *9(2)*, 291-292.
[56] M. Wenzel, *J. Label Compd Radiopharm.* **1992**, *31*, 641-605.
[57] J. Wald, R. Alberto, K. Ortner, L. Candreia, *Angew. Chem. Int. Ed.* **2001**, *40*, 3062-3066.
[58] H. J. Pietzsch, B. Johannsen, *Eur. J. Nucl. Med.* **2002**, *29*, 263-275.
[59] H. F. Kung, H. J. Kim, M. P. Kung, S. K. Meegalla, K. Plossl, H. K. Lee, *Eur. J. Nucl. Med.* **1996**, *23*, 1527-1530.
[60] M. P. Kung, D. A. Stevenson, K. Plossl, S. K. Meegalla, A. Beckwith, W. D. Essman, M. Mu, I. Lucki, H. F. Kung, *Eur. J. Nucl. Med.* **1997**, *24*, 372-380.
[61] R. R. Cesati, G. Tamagnan, R. M. Baldwin, S. S. Zoghbi, R. B. Innis, N. S. Kula, R. J. Baldessarini, A. J. Katzenellenbogen, *Bioconjug. Chem.* **2002**, *13*, 29-39.
[62] R. Alberto, R. Schibli, A. P. Schubiger, U. Abram, H. J. Pietzsch, B. Johannsen, *J. Am. Chem. Soc.* **1999**, *121*, 6076-6077.
[63] G. Jaouen, S. Top, A. Vessieres, P. Pigeon, G. Leclerq, I. Laios, *Chem. Commun.* **2001**, 383-384.
[64] T. W. Spradau, J. A. Katzenellenbogen, *Bioorg. Med. Chem. Lett.* **1998**, *8*, 3235-3240.
[65] M. Wenzel, C. Klinge, *J. Label Compd Radiopharm.* **1994**, *34*, 981-987.
[66] S. Top, H. Elhafa, A. Vessieres, J. Quivy, J. Vaissermann, D. W. Huges, M. J. McGlinchey, J. P. Mornon, E. Thoreau, G. Jaouen, *J. Am. Chem. Soc.* **1995**, *117*, 8372-8380.
[67] F. L. Bideau, A. Luna-Perez, J. Marrot, M.-N. Rager, E. Stephan, S. Top, G. Jaouen, *Tetrahedron* **2001**, *57*, 3939-3944.
[68] J. Tang, S. Top, A. Vessieres, N. Sellier, J. Vaissermann, G. Jaouen, *Appl. Organomet. Chem.* **1997**, *11*, 771-781.
[69] F. Wust, K. E. Carlson, J. A. Katzenellenbogen, H. Spies, B. Johannsen, *Steroids* **1998**, *63*, 665-671.
[70] F. Wust, M. B. Skaddon, P. Leibnitz, H. Spies, J. A. Katzenellenbogen, B. Johannsen, *Bioorg. Med. Chem.* **1999**, *7*, 1827-1835.
[71] M. B. Skaddan, F. R. Wust, J. A. Katzenellenbogen, *J. Org. Chem.* **1999**, *64*, 8108-8121.
[72] M. Wenzel, H. Meinhold, G. Schachschneider, *Eur. J. Nucl. Med.* **1985**, *10*, 138-142.
[73] P. D. Beer, *Acc. Chem. Res.* **1998**, *31*, 71.
[74] P. D. Beer, Z. Chen, M. G. B. Drew, A. O. M. Johnson, D. K. Smith, P. Spencer, *Inorg. Chim. Acta* **1996**, *246*, 143.
[75] P. D. Beer, A. R. Graydon, A. O. M. Johnson, D. K. Smith, *Inorg. Chem.* **1997**, *36*, 2112.
[76] W. Schuhmann, T. J. Ohara, H.-L. Schmidt, A. Heller, *J. Am. Chem. Soc.* **1991**, *113*, 1394.
[77] I. Willner, A.Riklin, B. Shoham, D.Rivenzon, E.Katz, *Adv. Mater.* **1993**, *5*, 912.
[78] M. I. Pividori, A.Merkoci, S. Alegret, *Biosens. Bioelectron* **2000**, *15*, 291-303.
[79] E. Palecek, M. Fojta, M. Tomschik, J. Wang, *Biosensors & Bioelectronics* **1998**, *13 (6)*, 621-628.
[80] E. Palecek, M. Fojta, *Anal. Chem.* **2001**, *73 (3)*, 75A-83A.
[81] R. C. McGlennen, *Clin. Chem.* **2001**, *47*, 393-402.
[82] N. A. Lacher, K. E. Garrison, M. R. S., S. M. Lunte, *Electrophoresis* **2001**, *22 (12)*, 2526-2536.
[83] A. Vessieres, K. Kowalski, J. Zakrzewski, A. Stepien, M. Grabowski, G. Jaouen, *Bioconjug. Chem.* **1999**, *10*, 379-385.
[84] A. Vessieres, M. Salmain, P. Brossier, G. Jaouen, *J. Pham. Biomed. Anal.* **1999**, *21*, 625-633.
[85] N. F.-Durand, M. Salmain, R. Bogna, A. Vessieres, J. Zakrewski, G. Jaouen, *Chem. Bio. Chem.* **2004**, *5*, 519-525.
[86] P. Köpf-Maier, H. Köpf, *Struct. Bonding* **1988**, *70*, 103-185.
[87] P. Kopf-Maier, H. Kopf, *Metal compounds in cancer therapy*, Chapman and Hall, London, **1994**.
[88] L. Y. Kuo, A. H. Liu, T. J. Marks, *Metal inos in bilogical systems, Vol. 33*, Marcel Dekker, New York, **1996**.
[89] M. M. Harding, G. Mokdsi, *Curr. Med. Chem.* **2000**, *7*, 1289-1303.
[90] W. E. Berdel, H. J. Schmoll, M. E.Scheulen, A. Korfel, M. F. Knoche, A. Harstrci, F. Bach, J. Baumgart, G. Sass, *J. Cancer Res. Clin. Oncol.* **1994**, *120 (suppl.)*, R172.
[91] C. V. Christodoulou, D. R. Ferry, D. W. Fyfe, A. Young, J. Doran, T. M. T. Sheehan, A. Eliopoulos, K. Hale, J. Baumgart, G. Sass, D. J. Kerr, *J. Clin. Oncol.* **1998**, *16*, 2761-2769.
[92] A. Korfel, M. E. Scheulen, H. J. Schmoll, O. Grundel, A. Harstrick, M. F. Knoche, L. M. Fels, M. Skorzec, F. Bach, J. Baumgart, G. Sab, S. Seeber, E. Thiel, W. E. Berdel, *Clin. Cancer. Res.* **1998**, *4*, 2701-2708.
[93] M. Tacke, L. P. Cuffe, W. M. Gallagher, Y. Lou, O.Mendoza, H. Muller-Benz, F.-J. K. Rehmann, N. Sweeney, *J. Inorg. Biochem.* **2004**, *98*, 1987-1994.
[94] M. M. Harding, G. J. Harden, L. D. Field, *FEBS Lett.* **1993**, *322*, 291-294.

[95] L. Y. Kuo, M. S. Kanatzides, M. Sabat, L. Tipton, T. J. Marks, *J. Am. Chem. Soc.* **1991**, *113*, 9027-9045.
[96] M. L. McLaughlin, J. M. Cronan, T. R. Schaller, R. D. Snelling, *J. Am. Chem. Soc.* **1990**, *112*, 8949-8952.
[97] J. H. Murray, M. M. Harding, *J. Med. Chem.* **1994**, *37*, 1936-1941.
[98] J. H. Toney, C. P. Brock, T. J. Marks, *J. Am. Chem. Soc.* **1986**, *108*, 7263-7274.
[99] J. H. Toney, T. J. Marks, *J. Am. Chem. Soc.* **1985**, *107*, 947-953.
[100] L. Y. Kuo, G. Mercouri, M. S. Kanatzides, T. J. Marks, *J. Am. Chem. Soc.* **1987**, *109*, 7207-7209.
[101] M. M. Harding, M. Prodigalidad, M. J. Lynch, *J. Med. Chem.* **1996**, *39*, 5012-5016.
[102] M. Guo, H. Sun, H. J. McArdle, L. Gambling, P. J. Sadler, *Biochemistry* **2000**, *39*, 10023-10033.
[103] L. Messori, P. Orioli, V. Banholzer, I. Pais, P. Zatta, *FEBS Lett.* **1999**, *442*, 157-161.
[104] G. Mokdsi, PhD thesis, University of Sidney **2001**.
[105] G. Mokdsi, M. M. Harding, *J. Inorg. Biochem.* **2001**, *83*, 205-209.
[106] G. Mokdsi, M. M. Harding, *J. Inorg. Biochem.* **2001**, *86*, 611-616.
[107] P. Köpf-Maier, H. Köpf, E. W. Neuse, *Angew. Chem. Int. Ed.* **1984**, *6*, 446-447.
[108] V. J. Fiorina, R. J. Dubois, S. Brynes, *J. Med. Chem.* **1978**, *21 (4)*, 393-395.
[109] G. N. Yashchenko, A. A. Shashmurina, G. M. Anoshina, L. A. Gorelova, N. G. Evstigneeva, L. V. Alekseeva, L. B. Radina, *Khim. Farm. Zh.* **1978**, *12*, 68.
[110] M. Wenzel, M. Schneider, E. Liss, *Z. Naturforsch.* **1979**, *34c*, 670-671.
[111] H. Tamura, M. Miwa, *Chem. Lett.* **1997**, 1177-1178.
[112] Y. N. V. Gopal, D. Jayaraju, A. K. Kondapi, *Arch. Biochem. Biophys.* **2000**, *376 (1)*, 229-235.
[113] E. W. Neuse, *Macromolecules containing Metal and Metal like Elements* **2004**, *3*, 89-117.
[114] M. Wenzel, Y. Wu, E. Liss, E. W. Neuse, *Z. Naturforsch.* **1988**, *43c*, 963-966.
[115] P. Köpf-Maier, H. Köpf, *Chem. Rev.* **1987**, *87*, 1137-1152.
[116] P. Köpf-Maier, H. Köpf, E. W. Neuse, *Cancer Res. Clin. Oncol.* **1984**, *108*, 336-340.
[117] N. Motohashi, R. Meyer, S. R. Gollapudi, K. R. Bhattiprolu, *J. Organomet. Chem.* **1990**, *398*, 205-217.
[118] G. Tabbi, C. Cassino, G. Cavigiolio, D. Colangelo, A. Ghiglia, I. Viano, D. Osella, *J. Med. Chem.* **2002**, *45*, 5786-5796.
[119] B. Weber, A. Serafin, J. Michie, C. v. Rensburg, J. C. Swarts, L. Bohm, *Anticancer Res.* **2004**, *24(2B)*, 763-770.
[120] R. Kovjazin, T. Eldar, M. Patya, A. Vanichkin, H. M. Lander, A. Novogrodsky, *FASEB J.* **2003**, 467-469.
[121] W. C. M. Duivenvoorden, Y. Liu, G. Schatte, H.-B. Kraatz, *Inorg. Chim. Acta* **2005**, *358*, 3183-3189.
[122] K. Schlögl, *Monatsh. Chem.* **1957**, *88*, 601-621.
[123] E. Cuignet, C. Sergheraert, A. Tartar, M. J. Dautrevaux, *J. Organomet. Chem.* **1980**, *195*, 325-329.
[124] E. Cuignet, M. Dautrevaux, C. Sergheraert, A. Tartar, B.Attali, J. Cross, *Eur. J. Med. Chem.* **1982**, *203-206*.
[125] J. C. Brunet, E. Cuignet, M. Dautrevaux, A. Demarly, H. Gras, P. Marcincal, C. Sergheraert, A. Tartar, J. C. Vanvoorde, M. Vanpoucke, *Proceedings of the sixteenth European Peptide Symposium* **1980**, 603-607.
[126] P. Maes, A. Ricouart, E. Escher, A. Tartar, C. Sergheraert, *Collect. Czech. Chem. Commun.* **1988**, *53*, 2914-2919.
[127] A. Tartar, A. Demarly, C. Sergheraert, E. Escher, **1983**, *In proceedings of the eighth American Peptide Symposium*, 377-380.
[128] D. E. Robertson, R. S. Farid, C. C. Moser, J. L. Urbauer, S. E. Mulholland, R. Pidikiti, J. D. Lear, A. J. Wand, W. F. DeGrado, P. L. Dutton, *Nature* **1994**, *368 (6470)*, 425-432.
[129] C. C. Moser, J. M. Keske, K. Warncke, R. S. Farid, P. L. Dutton, *Nature* **1992**, *355*, 796-802.
[130] D. N. Beratan, J. N. Betts, J. N. Onuchic, *Science* **1991**, *252*, 1285-1288.
[131] R. Langen, J.L.Colon, D. R. Casimiro, T. B. Karpishin, J. R. Winkler, H. B. Gray, *J. Biol. Inorg. Chem.* **1996**, *1*, 221-225.
[132] P. D. Beer, J. Cadman, *Coord. Chem. Rev.* **2000**, *20*, 131-155.
[133] H.-B. Kraatz, M. Galka, *Metal Ions Biol. Syst.* **2001**, *38*, 385-409.
[134] D. P. Fairlie, M. L. West, A. K. Wong, *Curr. Med. Chem.* **1998**, *1998*, 29-62.
[135] L. Stryer, *Biochemistry*, W. H. Freeman and Company, San Francisco, **1994**.
[136] W. Bauer, K. Polborn, W. Beck, *J. Organomet. Chem.* **1999**, *579*, 269-297.
[137] T. Moriuchi, A. Nomoto, K. Yoshida, T. Hirao, *J. Organomet. Chem.* **1999**, *589*, 50-58.
[138] Heinz-Bernhard Kraatz, Donald M. Leek, Abdelaziz Houmam, Gary D. Enright, Janusz Lusztyk, D. D. M. Wayner, *J. Organometal. Chem.* **1999**, *589*, 38-49.
[139] D. Obrecht, M. Altorfer, J. A. Robinson, *Adv. Med. Chem.* **1999**, *4*, 1-68.
[140] A. Nomoto, T. Moriuchi, S. Yamazaki, A. Ogawa, T. Hirao, *Chem. Commun.* **1998**, *1998*, 1963-1964.

[141] T. Moriuchi, A. Nomoto, K. Yoshida, A. Ogawa, T. Hirao, *J. Am. Chem. Soc.* **2000**, *123*, 68-75.
[142] T. Moriuchi, A. Nomoto, K. Yoshida, T. Hirao, *Organometallics* **2001**, *20*, 1008-1013.
[143] G. Holzemann, *Kontakte (Darmstadt)* **1991**, *2*, 55-64.
[144] G. Holzemann, *Kontakte (Darmstadt)* **1991**, *1*, 3-13.
[145] Pete Saweczko, Gary D. Enright, H.-B. Kraatz, *Inorg. Chem.* **2001**, *40*, 4409-4419.
[146] D. R. van Staveren, T. Weyhermuller, N. Metzler-Nolte, *Dalton Transc.* **2003**, 210-220.
[147] L. Barisic, M. Dropucic, V. Rapic, H. Pritzkow, S. Kirin, N. Metzler-Nolte, *Chem. Commun.* **2004**, 2004-2005.
[148] J. L. Madinaveitia, *Brit. J. Pharmacol.* **1965**, *24*, 352-359.
[149] A. F. Dratz, J. C. Coberly, J. H. Goldstein, *J. Nucl. Med.* **1964**, *5*, 40-47.
[150] R. A. Yeary, *Toxicol. Appl. Pharmacol.* **1969**, *15*, 666-676.
[151] A. Turnbull, F. Cleton, C. A. Finch, *J. Clin. Invest.* **1962**, *41*, 1897-1907.
[152] J. T. Yarrington, K. W. Huffman, G. A. Leeson, D. J. Syrinkle, D. E. Loudy, C. Hampton, G. J. Wright, J. P. Gibson, *Fund. Appl. Toxicol.* **1983**, *3*, 86-94.
[153] W. H. Soine, PhD Thesis, University of Kansas (Lawrence. Kansas), **1978**.
[154] R. P. Hanzlik, P. Soine, W. H. Soine, *J. Med. Chem.* **1979**, *22*, 424-428.
[155] W. H. Kim, PhD Thesis, Temple University (Phila. PA), **1977**.
[156] D. Drenckhahn, U. Groschel-Stewart, *J. Cell Biol.* **1980**, *86*, 475-482.
[157] M. Cais, S. Dani, Y. Eden, Y. Gandolfi, M. Horn, E. E. Isaacs, Y. Josephy, Y. Saar, E. Slovin, L. Snarshy, *Nature* **1977**, *270*, 534-535.
[158] M. Cais, E. Slovin, L. Snarshy, *J. Organomet. Chem.* **1978**, *160*, 223-230.
[159] E. I. Edwards, R. Epton, G. Marr, *J. Organomet. Chem.* **1976**, *122*, C49-C53.
[160] E. I. Edwards, R. Epton, G. Marr, G. K. Rogers, K. J. Thompson, *Spec. Publ. Chem. Soc.* **1977**, *28*, 92-100.
[161] J. T. Chantson, M. V. V. Falzacappa, S. Crovella, N. Metzler-Nolte, *J. Organomet. Chem.* **2005**, *690*, 4564-4572.
[162] N. J. Long, *Metallocenes*, Blackwell Science, Oxford, **1998**.
[163] G. R. Newkome, C. N. Moorfield, *Dendritic Molecules: Concepts, Syntheses, Perspectives*, VCH, Weinheim, **1996**.
[164] M. Hearshaw, J. R. Moss, *Chem. Commun.* **1999**, 1-8.
[165] I. Cuadrado, M. Moran, C. M. Casado, B. Alonso, J. Losada, *Coord. Chem. Rev.* **1999**, *193-195*, 395-445.
[166] F. J. Stoddart, T. Welton, *Polyhedron* **1999**, *18*, 3575-3591.
[167] S. Achar, C. E. Immoos, M. G. Hill, V. J. Catalano, *Inorg. Chem.* **1997**, *36*, 2314-2320.
[168] Y. Wang, C. M. Cardona, A. E. Kaifer, *J. Am. Chem. Soc.* **1999**, *121*, 9756-9757.
[169] K. Takada, D. J. Diaz, H. Abruna, I. Cuadrado, B. Gonzalez, C. M. Casado, B. Alonso, M. Moran, J. Losada, *Chemistry* **2001**, *7 (5)*, 1109-1117.
[170] C. M. Casado, B. Gonzalez, I. Cuadrado, B. Alonso, M. Moran, J. Losada, *Angew.Chem. Int. Ed.* **2000**, *39*, 2135-2138.
[171] R. Castro, I. Cuadrado, B. Alonso, C. M. Casado, M. Moran, A. Kaifer, *J. Am. Chem. Soc.* **1997**, *119*, 5760.
[172] C. M. Casado, I. Cuadrado, B. Alonso, M. Moran, J. Losada, *Electroanal. Chem.* **1999**, *463*, 87-92.
[173] B. Gonzalez, C. M. Casado, B. Alonso, I. Cuadrado, M. Moran, Y. Wang, A. E. Kaifer, *Chem. Commun.* **1998**, 2569-2570.
[174] E. O. Fisher, G. E. Herberich, *Chem. Ber.* **1961**, *94*, 1517.
[175] T. J. Gill, L. T. M. Jr., *J. Immunology* **1966**, *96*, 906-912.
[176] P. D. Beer, M. G. B. Drew, A. R. Graydon, *J. Chem. Soc. Dalton Trans.* **1996**, *21*, 4129-4134.
[177] V. M. Hultgren, A. W. A. Mariotti, A. M. Bond, A. G. Wedd, *Anal. Chem.* **2002**, *74 (13)*, 3151-3156.
[178] B. Rosenberg, L. V. Camp, J. E. Trosko, V. H. Mansour, *Nature* **1969**, 385-386.
[179] B. Rosenberg, L. v. Camp, T. Krigas, *Nature* **1965**, 698-699.
[180] J. Lokich, *Cancer Invest.* **2001**, *19*, 756-760.
[181] J. Lokich, N. Anderson, *Ann.Oncol.* **1998**, *9*, 13-21.
[182] S. M. Cohen, S. J. Lippard, *Prog. Nucleic Acid Res. Mol. Biol.* **2001**, *67*, 93-1030.
[183] V. Brabec, *Prog. Nucleic Acid Res. Mol. Biol.* **2002**, *71*, 1-68.
[184] M. D.Hall, S. Amjadi, M. Zhang, P. J. Beale, T. W. Hambley, *J. Inorg. Biochem.* **2004**, *98*, 1614-1624.
[185] M. A. Fuertes, C. Alonso, J. M. Perez, *Chem. Rev.* **2003**, *103*, 645-662.
[186] R. P. Perez, *Eur. J. Cancer* **1998**, *34*, 1535-1542.
[187] L. R. Kelland, *Eur. J. Cancer* **1994**, *30A*, 725-727.
[188] O. Aronov, A. T. Horowitz, A. Gabizon, M. A. Fuertes, J. M. Perez, D. Gibson, *Bioconjug. Chem.* **2004**, *15*, 814-823.
[189] D. Wang, S. J. Lippard, *Nature reviews (Drug Discovery)* **2005**, *4*, 307-320.

[190] M. S. Robillard, A. Rob, P. M. Valentijn, N. J. Meeuwenoord, G. A. van d. Marcel, J. H. van Boom, J. Reedijk, *Angew. Chem. Int. Ed.* **2000**, *112*, 3226-3226.
[191] G. Guillena, G. Rodriguez, M. Albrecht, G. van Koten, *Chem. Eur. J.* **2002**, *8 (23)*, 5368-5376.
[192] M. S. Robillard, M. Bacac, H. van d. Elst, A. Flamigni, G. A. v.an d. Marcel, J. H. van Boom, J. Reedijk, *J. Comb. Chem.* **2003**, *5*, 821-825.
[193] M. S. Robillard, N. P. Davies, G. A. van d. Marcel, J. H. van Boom, J. Reedijk, V. Murray, *J. Inorg. Biochem.* **2003**, *96*, 331-338.
[194] K. S. Schmidt, M. Boudvillain, A. Schwartz, G. A. van d. Marcel, J. H. van Boom, J. Reedijk, B. Lippert, *Chem. Eur. J.* **2002**, *8 (24)*, 5566-5570.
[195] S. Liu, D. S. Edwards, J. A. Barrett, *Bioconjug. Chem.* **1997**, *8*, 621-636.
[196] M. Langer, R. La Bella, E. Garcia-Garayoa, A. G. Beck-Sickinger, *Bioconjug. Chem.* **2001**, *2001*, 1028-1034.
[197] M. Henze, J. Schuhmacher, A. Dimitrakopoulou-Strauss, L. G. Strauss, H. R. Macke, M. Eisenhut, U. Haberkorn, *Eur. J. Nucl. Med.Molecular Imaging* **2004**, *31*, 466-.
[198] K. E. Bullok, M. Dyszlewski, J. L. Prior, C. M. Pica, V. Sharma, D. Piwnica-Worms, *Bioconju. Chem.* **2002**, *13*, 1226-1237.
[199] J. P. Leonetti, N. Mechti, G. Degols, C. Gagnor, B. Lebleu, *P. N. A. S. US A* **1991**, *88*, 2702-2706.
[200] M. W. Reed, D. Fraga, D. E. Schwartz, J. Scholler, R. D. Hinrichsen, *Bioconjug. Chem.* **1995**, *6*, 101-108.
[201] M. M. Takahashi, S. Kagiwada, S. A. Suzuki, S. Ohnishi, *Biochemistry* **1992**, *31*, 1986-1992.
[202] O. Zelphati, G. Zon, L. Leserman, *Antisense Res. Dev.* **1993**, *3*, 323-338.
[203] P. M. Fischer, E. Krausz, D. P. Lane, *Bioconjug. Chem.* **2001**, *12*, 825-841.
[204] M. Lindgren, M. Hällbrink, M. A. Prochiantz, Ü. Langel, *Trends Pharmacol. Sci.* **2000**, *21*, 99-103.
[205] A. Scheller, B. Wiesner, M. Melzig, M. Bienert, J. Oehlke, *Eur. J. Biochem.* **2000**, *267*, 6043-6049.
[206] M. A. Prochiantz, *Curr. Opin. Cell Biol.* **2000**, *12*, 400-406.
[207] D. Derossi, A. H. Joliot, G. Chassaing, M. A. Prochiantz, *J. Biol. Chem.* **1994**, *269*, 10444-10450.
[208] E. Vives, P. Brodin, B. Lebleu, *J. Biol. Chem.* **1997**, *272*, 16010-16077.
[209] S. Futaki, S. Suzuki, W. Ohashi, T. Yagami, S. Tanaka, K. Ueda, Y. Sugiura, *J. Biol. Chem.* **2001**, *276*, 5836-5840.
[210] M. Pooga, M. Hällbrink, M. Zorko, Ü. Langel, *FASEB J.* **1998**, *12*, 67-77.
[211] J. Oehlke, A. Scheller, B. Wiesner, E. Krause, M. Beyerman, E. Klauschenz, M. Melzig, M. Bienert, *Biochim. Biophys. Acta* **1998**, *1414*, 127-139.
[212] L. Chaloin, P. Vidal, A. Heitz, N. V. Mau, J. Mery, G. Divita, F. Heitz, *Biochemistry* **1997**, *36*, 11179-11187.
[213] P. Vidal, L. Chaloin, A. Heitz, N. V. Mau, J. Mery, G. Divita, H. F., *J. Membr. Biol.* **1998**, *162*, 259-264.
[214] S. Fawell, J. Seery, Y. Daikh, C. Moore, L. L. Chen, B. Pepinsky, J. Barsoum, *PNAS* **1994**, *91*, 664-668.
[215] H. Nagahara, A. M. Vocero-Akbani, E. L. Snyder, A. Ho, D. G. Latham, N. A. Lissy, M. Becker-Hapak, S. A. Ezhevsky, S. F. Dowdy, *Nat. Med.* **1998**, *4*, 1449-1452.
[216] S. R. Schwarze, A. Ho, A. M. Vocero-Akbani, S. F. Dowdy, *Science* **1999**, *285*, 1569-1572.
[217] A. Astriab-Fisher, D. Sergueev, M. Fisher, B. R. Shaw, R. L. Juliano, *Pharm. Res.* **2002**, *19*, 744-754.
[218] R. D. Palmiter, T. B. Cole, S. D. Findly, *EMBO J.* **1996**, *15*, 1784-1791.
[219] M. Lewin, N. Carlesso, C. H. Tung, X. W. Tang, D. Cory, D. T. Scadden, R. Weissleer, *Nat. Biotechnol.* **2000**, *18*, 410-414.
[220] A. D. Frankel, C. O. Pabo, *Cell* **1988**, *55*, 1189-1193.
[221] M. Green, P. M. Loewenstein, *Cell* **1988**, *55*, 1179-1188.
[222] P. A. Wender, D. J. Mitchell, K. Pattabiraman, E. T. Pelky, L. Steinman, J. B. Rothbard, *PNAS* **2000**, *97*, 13003.
[223] D. J. Mitchell, D. T. Kim, L. Steinman, C. G. Fathman, J. B. Rothbard, *Pept. Res.* **2000**, *56*, 318-325.
[224] Ü. Langel, *Cell-Penetrating Peptides: Processes and Application*, CRC Press, Boca Raton Fl., **2002**.
[225] M. M. Fretz, G. A. Koning, E. Mastrobattista, W. Jiskoot, G. Storm, *Biochim. Biophys. Acta* **2004**, *1665*, 48-56.
[226] J. P. Richard, K. Melikov, E. Vives, C. Ramos, B. Verbeure, M. J. Gait, L. V. Chernomordik, B. Lebleu, *J. Biol. Chem.* **2003**, *278*, 585-590.
[227] T. B. Potocky, A. K. Menon, S. H. Gellman, *J. Biol. Chem.* **2003**, *278*, 50188-50194.
[228] J. A. Leifert, J. L. Whittion, *Mol. Ther.* **2003**, *8*, 13-20.
[229] P. E. G. Thoren, D. Persson, P. I. Goksör, A. Onfelt, B. Norden, *Biochem. Biophys. Res. Comm.* **2003**, *307*, 100-107.
[230] J. L. Zaro, W. Shen, *Biochem. Biophys. Res. Comm.* **2003**, *307*, 241-247.
[231] D. Görlich, U. Kutay, *Annu. Rev. Cell Dev. Biol.* **1999**, *15*, 607-660.
[232] I. W. Mattaj, L. Englmeier, *Annu. Rev. Biochem.* **1998**, *67*, 265-306.

[233] E. Pennisi, *Science* **1998**, *279*, 1129-1131.
[234] Y. Yoneda, M. Hieda, E. Nagoshi, Y. Miyamoto, *Cell Struc. Funct.* **1999**, *24*, 425-433.
[235] D. A. Jans, C. K. Chan, S. Huebner, *Med. Res. Rev.* **1998**, *18*, 189-223.
[236] D. Görlich, I. W. Mattaj, *Science* **1996**, *271*, 1513-1518.
[237] K. Ribbeck, D. Görlich, *EMBO J.* **2001**, *20*, 1320-1330.
[238] K. Helen Bremner, Leonard W. Seymour, Ann Logan, M. L. Read, *Bioconjug. Chem.* **2004**, *15*, 152-161.
[239] D. Kalderon, W. D. Richardson, A. T. Markham, A. E. Smith, *Nature* **1984**, *311*, 33-38.
[240] C. M. Feldherr, D. Akin, *J. Cell Biol.* **1990**, *111*, 1-8.
[241] J. Robbins, S. M. Dilworth, R. A. Laskey, C. Dingwall, *Cell* **1991**, *64*, 615-623.
[242] A. Pokorska, C. Drevet, C. Scazzocchio, *J. Mol. Biol.* **2000**, *298*, 585-596.
[243] S. Nakielny, G. Dreyfuss, *Cell* **1999**, *99*, 677-690.
[244] E. Conti, M. Uy, L. Leighton, G. Blobel, J. Kuriyan, *Cell* **1998**, *94*, 193-204.
[245] D. Görlich, F. Vogel, A. D. Mills, E. Hartmann, R. A. Laskey, *Nature* **1995**, *377*, 246-247.
[246] W. D. Richardson, A. D. Mills, S. M. Dilworth, R. A. Laskey, C. Dingwall, *Cell* **1988**, *52*, 655.
[247] M. A. Zanta, P. Belguise-Valladier, J.-P. Behr, *P.N. A. S. USA* **1999**, *96*, 91-96.
[248] G. Cutrona, E. M. Carpaneto, M. Ulivi, S. Roncella, O. Landt, M. Ferrarini, L. Boffa, *Nature* **2000**, *18*, 300-303.
[249] L. Chaloin, P. Vidal, P. Lory, J. Méry, N. Lautredou, G. Divita, F. Heitz, *Biochem. Biophys. Res. Commun.* **1998**, *243*, 601-608.
[250] B. G. delaTorre, F. Albericio, E. S. -Behmoaras, A. Bachi, R. Eritja, *Bioconjug. Chem.* **1999**, *10*, 1005-1012.
[251] T. V. Akhlynina, D. A. Jans, A. A. Rosenkranz, N. V. Statsyuk, I. Y. Balashova, G. Toth, I. Pavo, A. B. Rubin, A. S. Sobolev, *J. Biol. Chem.* **1997**, *272*, 20328-20331.
[252] A. G. Tkachenko, H. Xie, D. Coleman, W. Glomm, J. Ryan, M. F. Anderson, S. Franzen, D. L. Feldheim, *J. Am. Chem. Soc.* **2003**, *125*, 4700-4701.
[253] A. G. Tkachenko, H. Xie, Y. Liu, D. Coleman, J. Ryan, W. Glomm, M. K. Shipton, S. Franzen, D. L. Feldheim, *Bioconjug. Chem.* **2004**, *15*, 482-490.
[254] P. Haefliger, N. Agorastos, A. Renard, G. G. -Brugnoli, C. Marty, R. Alberto, *Bioconjug. Chem.* **2005**, *16*, 582-587.
[255] J. J. Ludtke, G. Zhang, M. G. Sebestyén, J. A. Wolff, *J. Cell Sci* **1999**, *112*, 2033-2041.
[256] J. C. Reubi, H. R. Helmut, E. P. Krenning, *J. Nucl. Med.* **2005**, *46 (suppl. 1)*, 67S-75S.
[257] J. G. McAfee, R. D. Neumann, *Nucl. Med. Biol.* **1996**, *23*, 673-676.
[258] E. P. Krenning, D. J. Kwekkeboom, S. Pauwels, L. K. Kvols, J. C. Reubi, *Nucl. Med. Annual*, Raven Press, New York, **1995**.
[259] I. Virgolini, M. Raderer, A. Kurtaran, P. Angelberger, S. Banyai, Q. Yang, S. Li, M. Banyai, J. Pidlich, N. Niederle, W. Scheithauer, P. Valent, *New Eng. J. Med.* **1994**, *331*, 1116-1121.
[260] W. A. Breeman, L. J. Hofland, M. d. Jong, B. F. Bernard, A. Sirinivasan, D. J. Kwekkeboom, T. J. Visser, E. P. Krenning, *Int. J. Cancer* **1999**, *81*, 658-665.
[261] S. R. Karra, R. Schibli, H. Gali, K. V. Katti, T. J. Hoffman, C. Higginbotham, G. L. Sieckman, W. A. Volkert, *Bioconjug. Chem.* **1999**, *10*, 254-260.
[262] A. Safavy, M. B. Khazaeli, H. Qin, D. J. Buchsbaum, *Cancer* **1997**, *80*, 2354-2359.
[263] C. M. Townsend, R. J. Bold, J. Ishizuka, *Surgery Today* **1994**, *24 (9)*, 772-777.
[264] J.-P. Vincent, *Cell. Mol. Neurobiol.* **1995**, *15 (5)*, 501-512.
[265] K. D. Adachi, P. W. Kalivas, J. O. Schenk, *J. Neurochem.* **1990**, *54 (4)*, 1321-1328.
[266] C. B. Nemeroff, D. Luttinger, A. J. J. Prange, *Trends Neurosci.* **1980**, *3*, 212-215.
[267] J.-P. Vincent, *Cell Mol. Neurobiol.* **1995**, *15*, 501-512.
[268] P. Kitabgi, *Ann. NY Acad. Sci* **1982**, *400*, 37-44.
[269] R. C. Scarpa, R. E. Carraway, D. E. Cochrane, *Peptides* **2004**, *25 (7)*, 1159-1169.
[270] J.-P. Vincent, J. Mazella, P. Kitabgi, *TIPS* **1999**, *20*, 302-309.
[271] P. Chalon, *FEBS Lett.* **1996**, *386*, 91-94.
[272] J. Mazella, *J. Neurosci.* **1996**, *16*, 5613-5620.
[273] N. Vita, *Eur. J. Pharmacol.* **1998**, *360*, 265-272.
[274] J. Mazella, *J. Biol. Chem.* **1998**, *273*, 26273-26276.
[275] W. Rostene, P. Kitabgi, D. Pelaprat, *Encyclopedia of Biological Chemistry, Vol. 3*, Elsevier Ltd., Oxford, **2004**.
[276] M. Goedert, *Meth. Enzymol.* **1989**, *168*, 462-481.
[277] C. Labbe-Jullie, I. Dubuc, A. Brouard, S. Doulut, E. Bourdel, D. Pelaprat, J. Mazella, J. Martinez, W. Rostene, J. Constentin, P. Kitabgi, *J. Pharmcol. Exp. Ther.* **1994**, *268*, 328-336.
[278] B. M. Tyler, B. Cusack, C. L. Douglas, T. Souder, E. Richelson, *Brain Res.* **1998**, *792*, 246-252.
[279] K. S. Kanba, S. Kanba, A. Nelson, H. Okazaki, E. Richelson, *J. Neurochem.* **1988**, *50*, 131.
[280] F. Hong, B. Cusack, A. Fauq, E. Richelson, *Curr. Med. Chem.* **1997**, *4*.

[281] Y.-P. Pang, B. Cusack, K. Groshan, E. Richelson, *J. Biol. Chem.* **1996**, *271 (25)*, 15060-15068.
[282] J. C. Bozou, N. Robert, I. Magnaldo, J.-P. Vincent, P. Kitabgi, *Biochem. J.* **1989**, *264*, 871-878.
[283] T. W. Moody, C. A. Mayr, T. J. Gillespie, T. P. Davis, *Peptides* **1998**, *19 (2)*, 253-258.
[284] P. Kitabgi, F. DeNadai, C. Rovere, J. N. Bidard, *Ann. NY Acad. Sci* **1992**, *662*, 30-42.
[285] T. P. Davies, P. N. M. Konings, *Crit. rev. Neurobiol.* **1993**, *7*, 163-174.
[286] E. G. Garayoa, L. A. Tannahill, P. Blauenstein, *Nucl. Med. Biol.* **2001**, *28*, 75.
[287] L. D. Wise, D. J. Wustrow, USA, **1995**, p. 19.
[288] P. R. Dobner, *Cell. Mol. Life. Sci.* **2005**, *62*, 1946-1963.
[289] J. C. Reubi, patent; USA, **1998**, p. 33.
[290] A. Sirinivasan, J. L. Erion, M. A. Schmidt, patent; USA, **2000**, p. 38.
[291] N. Berthold, A. Nikolopoulou, E. Chiotellis, T. Maina, A. Galanis, P. Sotiriou, G. Pairas, P. Cordopatis, in *Proc. 27th Eur. Peptide Symp.*, Z. Edizioni, Sorrento, Italy, **2002**, pp. 996-997.
[292] D. Tourwe, K. Iterbeke, P. Conrath, P. A. Schubiger, L. Allemann, A. Egli, R. Alberto, N. Carrell-Remy, M. Willmann, P. Blauenstein, in *Proc. 16th Amer. Peptide Symp.*, Kluwern Academic Publishers, Minneapolis, **1999**, pp. 792-793.
[293] E. G. Garayoa, L. A. Tannahill, P. Blauenstein, M. Willmann, N. Carrell-Remy, D. Tourwe, K. Iterbeke, P. Conrath, P. A. Schubiger, *Nucl. Med. Biol.* **2001**, *28*, 75-84.
[294] F. Hong, J. Zaidi, B. Cusack, E. Richelson, *Bioorg. Med. Chem.* **2002**, *10*, 3849-3858.
[295] P. Blauenstein, E. G. Garayoa, R. Dominique, A. Blanc, D. Tourwe, A. B.-Sickinger, P. A. Schubiger, *Cancer Biother. Radiopharm.* **2004**, *19 (2)*, 181-188.
[296] D. Tourwe, J. Mertens, M. Ceusters, L. Jeannin, K. Iterbeke, D. Terriere, C. Chavatte, R. Boumon, *Tumour Targetting* **1998**, *3 (1)*, 41-45.
[297] E. G. Garayoa, P. Blauenstein, M. Bruehlmeier, A. Blanc, K. Iterbeke, P. Conrath, D. Tourwe, P. A. Schubiger, *J. Nucl. Med.* **2002**, *43 (3)*, 374-383.
[298] P. A. Schubiger, L. Allemann-Tannahill, A. Egli, R. Schibli, R. Alberto, N. Carrell-Remy, M. Willmann, P. Blauenstein, D. Tourwe, *Q. J. Nucl. Med.* **1999**, *43 (2)*, 155-158.
[299] John E. Sheats, M. D. Rausch, *J. Org. Chem.* **1970**, *35*, 3245-3249.
[300] J. Gariepy, *Bioconj. Chem.* **2002**, *13*, 679-684.
[301] W. C. Still, M. Kahn, A. Mitra, *J. Org. Chem.* **1978**, *43*, 2923-2925.
[302] D. P. Aden, A. Fogel, S. Plotkin, I. damjanov, B. B. Knowles, *Nature* **1979**, *282*, 615-616.
[303] B. B. Knowles, C. C. Howe, D. P. Aden, *Science* **1980**, *209*, 497-499.
[304] M. Ishiyama, H. Tominaga, M. Shiga, K. Sasamoto, Y. Ohkura, K. Uneo, *Biol. Pharm. Bull.* **1996**, *19 (11)*, 1518-1520.
[305] H. H. Versteeg, E. Nijhuis, G. R. van der Brink, M. Evertzen, G. N. Pynaert, S. J. H. van Deventer, P. J. Coffer, M. P. P. Peppelenbosch, *Biochem. J.* **2000**, *350*, 717-722.
[306] A. G. Tkachenko, H. Xie, D. Coleman, W. Glomm, J. Ryan, M. F. Anderson, S. Franzen, D. L. Feldheim, *J. Am. Chem. Soc.* **2003**, *125*, 4700-4701.
[307] M. Lundberg, M. Johansson, *Biochem. Biophys. Res. Commun.* **2002**, *291*, 367-371.
[308] D. Kalderon, B. L. R. D. Richardson, E. A. Smith, *Cell* **1984**, *39*, 499-509.
[309] T. Braumann, *J. Chromatogr.* **1986**, *373*, 191-225.
[310] R. A.Conradi, A. R. Hilgers, N. F. H. Ho, P. S. Burton, *Pharm. Res.* **1992**, *9*, 435-439.
[311] W. A. Banks, A. J. Kastin, *Brain Res. Bull.* **1985**, *15*, 287-292.
[312] P. Buchwald, N. Bodor, *Proteins : Structure, Function and Genetics* **1998**, *30*, 86-99.
[313] I. B. Golovanov, I. G. Tsygankova, *Russ. J. Gen. Chem.* **2002**, *72 (1)*, 137-143.
[314] M. Akamatsu, T. Fujita, *J. Pharm. Sci.* **1992**, *81 2*, 164-174.
[315] C. M. Varga, T. J. Wickham, D. A. Lauffenburger, *Biotechnol. Bioeng.* **2000**, *70*, 593-605.
[316] D. A. Mann, A. D. Frankel, *EMBO J.* **1991**, *10*, 1733-1739.
[317] J. J. Turner, A. A. Arzumanov, M. J. Gait, *Nucl. Acids Res.* **2005**, *33 (1)*, 27-42.
[318] M. Hällbrink, A. Floren, A. Elmquist, M. Pooga, T. Bartfai, Ü. Langel, *Biochim. Biophys. Acta* **2001**, *1515*, 101-109.
[319] Y. Yoneda, A. Kametaka, T. Sekimoto, *Acto Histochem. Cytochem.* **2002**, *35*, 435-440.
[320] S. Jäkel, W. Albig, U. Kutay, F. R. Bishoff, K. Schwamborn, *EMBO J.* **1999**, *18*, 2411-2423.
[321] J. J. Ludtke, G. Zhang, M. G. Sebestyen, J. A. Wolff, *J. Cell Sci.* **1999**, *112*, 2033-2041.
[322] G. Cutrona, E. M. Carpaneto, M. Ulivi, S. Roncella, O. Landt, M. ferrarini, L. C. Boffa, *Nature Biotech.* **2000**, *18*, 300-303.
[323] W. H. Colledge, B. L. Richardson, W. D. Edge, E. A. Smith, *Mol. Cell. Biol.* **1986**, *6*, 4136-4138.
[324] J. B. Waern, H. H. Harris, B. Lai, Z. Cai, M. M. Harding, C. T. Dillon, *J. Biol. Inorg. Chem.* **2005**, *10 (5)*, 443-452.
[325] Pille Saalik, Anna Elmquist, Mats Hansen, Kart Padari, Kulliki Saar, Kaido Viht, Ulo Langel, M. Pooga, *Bioconjug. Chem.* **2004**, *15*, 1246-1253.

APPENDIX

List of supplementary figures

1) Cellular distribution of compound **11** at a concentration of 0.1mM, CY2 & CY3 filters, green and red fluorescence, merged image.

2) Cellular distribution of compound **11** at a concentration of 0.1mM, CY2, CY3 and UV filters; green, red and blue fluorescence, merged image.

3) Cellular distribution of compound **11** at a concentration of 0.1mM, CY3 & UV filters; red and blue fluorescence, merged image.

4) Cellular distribution of compound **13** at a concentration of 0.1mM, CY2 filter, green fluorescence.

5) Cellular distribution of compound **13** at a concentration of 0.1mM, CY2 & CY3 filter, green and red fluorescence, merged image.

6) Cellular distribution of compound **13** at a concentration of 0.1mM, CY3 filter, red fluorescence.

7) Cellular distribution of compound **18** at a concentration of 0.1mM, CY2 & CY3 filters, green and red fluorescence, merged image.

8) Cellular distribution of compound **18** at a concentration of 0.1mM, CY2, CY3 and UV filters; green, red and blue fluorescence, merged image.

9) Cellular distribution of compound **18** at a concentration of 0.1mM, CY3 & UV filters; red and blue fluorescence, merged image.

10) Cellular distribution of compound **21** at a concentration of 0.1mM, CY2 & DAPI filters, green and blue fluorescence, merged image.

11) Cellular distribution of compound **21** at a concentration of 0.1mM, CY2, CY3 and UV filters; green, red and blue fluorescence, merged image.

12) Cellular distribution of compound **21** at a concentration of 0.1mM, CY3 & UV filters; red and blue fluorescence, merged image.

13) Cellular distribution of compound **22** at a concentration of 0.1mM, CY2 & CY3 filters, green and red fluorescence, merged image.

14) Cellular distribution of compound **22** at a concentration of 0.1mM, CY2, CY3 and UV filters; green, red and blue fluorescence, merged image.

15) Cellular distribution of compound **22** at a concentration of 0.1mM, CY3 & UV filters; red and blue fluorescence, merged image.

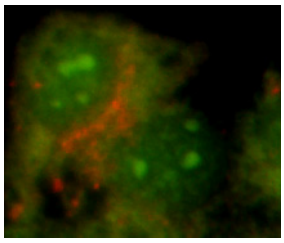

1

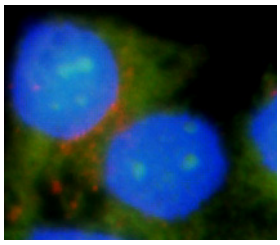

2

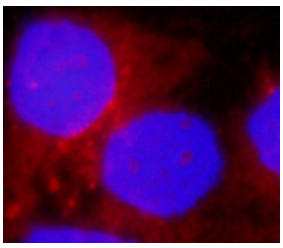

3

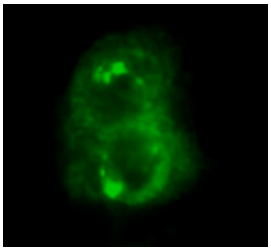

4

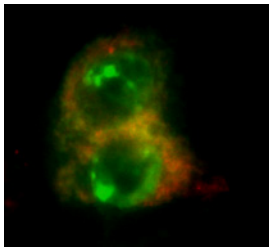

5

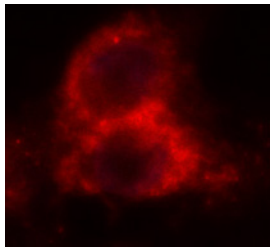

6

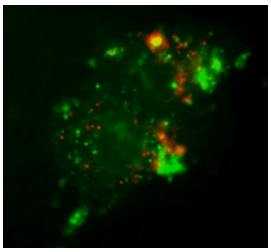

7

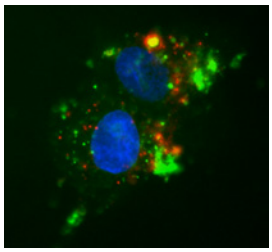

8

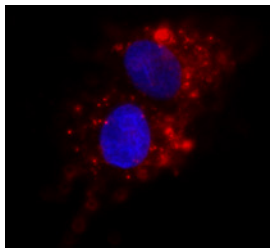

9

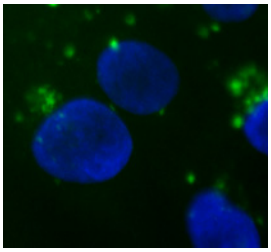

10

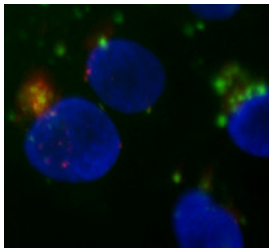

11

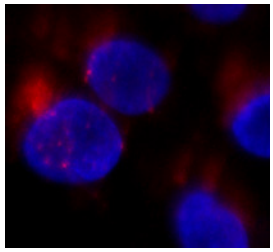

12

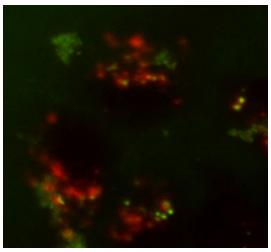

13

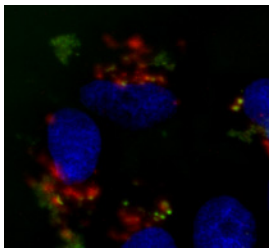

14

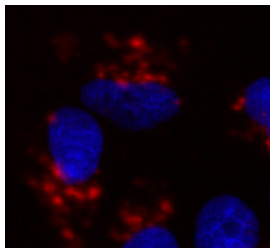

15

16) Cellular distribution of compound **24** at a concentration of 50µM, CY2 & CY3 filters, green and red fluorescence, merged image.

17) Cellular distribution of compound **24** at a concentration of 50µM, CY2, CY3 and UV filters; green, red and blue fluorescence, merged image.

18) Cellular distribution of compound **24** at a concentration of 50µM, CY3 & UV filters; red and blue fluorescence, merged image.

19) Cellular distribution of compound **27** at a concentration of 50µM, CY2 & CY3 filters, green and red fluorescence, merged image.

20) Cellular distribution of compound **27** at a concentration of 50µM, CY2, CY3 and UV filters; green, red and blue fluorescence, merged image.

21) Cellular distribution of compound **27** at a concentration of 50µM, CY3 & UV filters; red and blue fluorescence, merged image.

22) Cellular distribution of compound **28** at a concentration of 50µM, CY2 & CY3 filters, green and red fluorescence, merged image.

23) Cellular distribution of compound **28** at a concentration of 50µM, CY2, CY3 and UV filters; green, red and blue fluorescence, merged image.

24) Cellular distribution of compound **28** at a concentration of 50µM, CY3 & UV filters; red and blue fluorescence, merged image.

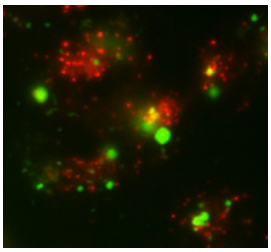

16

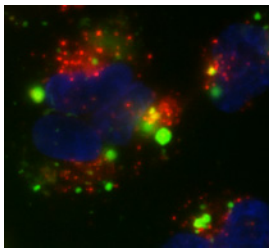

17

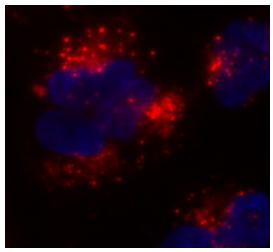

18

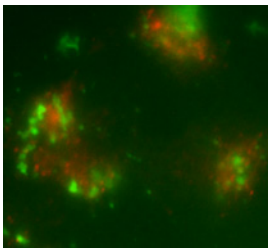

19

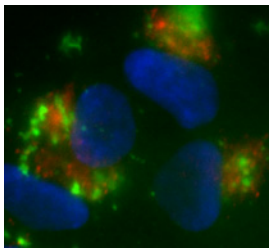

20

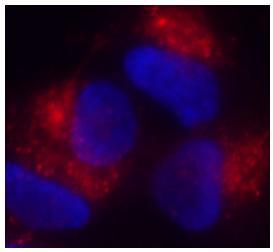

21

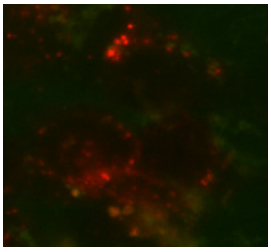

22

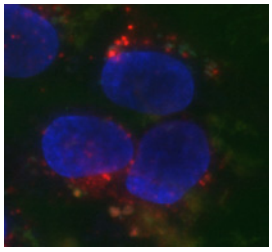

23

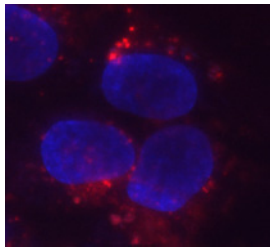

24

List of synthesized bioconjugates

Comp. No.	Abbreviation	Sequence
1	CcC(O)-NLS	CcC(O)-PKKKRKV
2	FcC(O)-NLS	FcC(O)-KPKKKRKV
3	CcC(O)-NLS_{mca}	CcC(O)-$PKKKRK_{mca}V$
4	Pt-BB-NLS	Pt-BB-PKKKRKV
5	Pt-DAP-NLS	Pt-BB-PKKKRKV
6	K-NLS	KPKKKRKV
7	K(FITC)-NLS	K(FITC)-PKKKRKV
8	CcC(O)-K-NLS	CcC(O)-KPKKKRKV
9	FcC(O)-K-NLS	FcC(O)-KPKKKRKV
10	CcC(O)-K(FITC)-NLS	CcC(O)-K(FITC)-PKKKRKV
11	FcC(O)-K(FITC)-NLS	FcC(O)-K(FITC)-PKKKRKV
12	CcC(O)-K(FITC)-V	CcC(O)-K(FITC)-V
13	FcC(O)-K(FITC)-V	FcC(O)-K(FITC)-V
14	NLS_{src}	KKVKPKR
15	CcC(O)-NLS_{src}	CcC(O)-KKVKPKR
16	FcC(O)-NLS_{src}	FcC(O)-KKVKPKR
17	K-NLS_{src}	KKKVKPKR
18	K(FITC)-NLS_{src}	K(FITC)-KKVKPKR
19	CcC(O)-K-NLS_{src}	CcC(O)-KKKVKPKR
20	FcC(O)-K-NLS_{src}	FcC(O)-KKKVKPKR
21	CcC(O)-K (FITC)-NLS_{src}	CcC(O)-K(FITC)-KKVKPKR
22	FcC(O)-K(FITC)-NLS_{src}	FcC(O)-K(FITC)-KKVKPKR
23	K-TAT	KGRKKRRQRRR
24	K(FITC)-TAT	K(FITC)-GRKKRRQRRR
25	CcC(O)-K-TAT	CcC(O)-KGRKKRRQRRR
26	FcC(O)-K-TAT	FcC(O)-KGRKKRRQRRR
27	CcC(O)-K(FITC)-TAT	CcC(O)-K(FITC)-GRKKRRQRRR
28	FcC(O)-K(FITC)-TAT	FcC(O)-K(FITC)-GRKKRRQRRR
29	pNT	KKPYIL
30	FcC(O)-pNT	FcC(O)-KKPYIL
31	CcC(O)-pNT	CcC(O)-KKPYIL
32	Pt-BB-pNT	Pt-BB-KKPYIL
33	NT	RRPYIL
34	CcC(O)-NT	CcC(O)-RRPYIL
35	FcC(O)-NT	FcC(O)-RRPYIL
36	Pt-BB-NT	Pt-BB-RRPYIL